2022

The Use of Vesgen for Analysis of Retinal Vasculature in Pulmonary Arterial Hypertension

Mariana Desiree DuPont
University of Alabama at Birmingham

THE USE OF VESGEN FOR ANALYSIS OF RETINAL VASCULATURE IN PULMONARY ARTERIAL HYPERTENSION

by

MARIANA DESIREE` DUPONT

MARIA GRANT, COMMITTEE CHAIR
JARROD BARNES
TIMOTHY KRAFT
STEFANIE KRICK
TIM LAHM

A DISSERTATION

Submitted to the graduate faculty of The University of Alabama at Birmingham,
in partial fulfillment of the requirements for the degree of
Doctor of Philosophy

BIRMINGHAM, ALABAMA

2022

THE USE OF VESGEN FOR ANALYSIS OF RETINAL VASCULATURE IN PULMONARY ARTERIAL HYPERTENSION

MARIANA DESIREE` DUPONT

VISION SCIENCE

ABSTRACT

Pulmonary artery hypertension is a chronic and progressive disease leading to right heart failure and, ultimately, death if untreated. The goal of the studies in this dissertation was to determine if fluorescein angiography (FA), and color fundus angiography (CF) imaging could be used to garner critical information about retinal changes in individuals with pulmonary artery hypertension (PAH). VESsel GENerational Analysis (VESGEN) is a noninvasive computer program that assigns branching generation to large and small vessels. VESGEN was utilized to investigate vascular alterations in FA, and CF imaging investigating disease progression in PAH. This dissertation demonstrated that PAH patients had aberrant retinal vasculature in FA imaging when compared to controls, and that these abnormalities may correspond with standard clinical outcome metrics in PAH. Using CF in conjunction with VESGEN analysis as a retinal imaging modality in PAH patients rather than FA with manual in-put service as a safer way for retinal change monitoring. VESGEN, combined with deep learning processing, shows potential in identifying vascular pathology earlier and in more subtle vascular alterations. Based on our results, VESGEN with FA and CF imaging may serve as an additional research tool for monitoring small changes in the progression of PAH and other systemic vascular diseases.

Keywords: VESGEN, retinal imaging, image processing, vascular segmentation, PAH

DEDICATION

To my mother (Nina DuPont), brothers (Tyson Smith and Michael DuPont, Jr), and my late father (Michael DuPont Sr.)

My biggest support system!

ACKNOWLEDGMENTS

I would like to thank my parents, Nina and Michael, Sr., for never allowing me to give up on my dreams and always being there for me during my most challenging times. I would like to thank my brothers, Tyson and Michael Jr., for listening to me vent when things did not go my way. I want to thank my best friend, Kelsey Gates, for never leaving my side, even on my most challenging days. With most profound appreciation, I thank my Ph.D. mentor Dr. Maria Grant. Thank you for accepting me into your lab, pushing me to become greater, and providing me with the tools I need to excel in science. Thank you for being patient with me during countless editing and revising of my manuscripts. Thank you to my committee members, Doctors Timothy Kraft, Timothy Lahm, Jarrod Barnes, and Stefanie Krick, for helping me throughout my five years at the University of Alabama at Birmingham. Thank you for all the sacrificed time to ensure I would achieve above and beyond. I thank the University of Alabama at Birmingham, the Vision Sciences Graduate Program, and the Vision Science faculty for accepting me into the program and providing me the opportunity to obtain this doctorate. Lastly, I would like to thank all my current and past lab mates for making to experience worth remembering.

TABLE OF CONTENTS

Page

LIST OF TABLES

LIST OF FIGURES

Figures *Page*

INTRODUCTION

RETINAL VESSEL CHANGES IN PULMONARY ARTERIAL HYPERTENSION

OPTIMIZING RETINAL VASCULAR IMAGING FOR DETECTING CHANGES IN PULMONARY ARTERY HYPERTENSION

LIST OF ABBREVIATIONS

6MWD	6-minute walk distance
AI	artificial Intelligence
A_v	vessel area density
CF	color fundus
CI	cardiac index
CO	cardiac output
CTD	connective tissue disease
D_f	fractal dimension
DL	deep learning
DM	diabetes mellitus
DME	diabetic macular edema
DR	diabetic retinopathy
FA	fluorescein angiography
GLMM	generalized linear mixed modeling
HF	heart failure
IGF-1	insulin-like growth factor-1
LIF	leukemia inhibitory factor
mPAP	mean pulmonary arterial pressure
NASA	National Aeronautics and Space Administration

PAH	pulmonary arterial hypertension
PAP	Pulmonary artery pressure
PCWP	pulmonary capillary wedge pressure
p_{FDR}	Benjamini-Hochberg false discovery rate
PH	pulmonary hypertension
PVR	pulmonary vascular resistance
RAP	right atrial pressure
RHC	right heart catheterization
ROI	region of interest
SANS	Spaceflight associated neuro-ocular syndrome
$ScvO_2$	superior vena cava oxygen saturation
SvO_2	pulmonary arterial oxygen saturation
T_v	tortuosity
VEGF	vascular endothelial growth factor
VESGEN	VESsel GENeration

CHAPTER 1

INTRODUCTION

The structure of the retina

A window into the body is through the pupil and then directly to the retina. The inside of the eye is separated into two sections: anterior and posterior. The anterior segment consists of the cornea, iris, ciliary body, lens, and anterior and posterior chamber spaces filled with aqueous fluid. The retina, choroid, and optic nerve head are all part of the posterior segment, as is the vitreous compartment, which is filled with vitreous fluid (1).The retina is a spherical anatomic structure on the inner side of the back of the eye. The

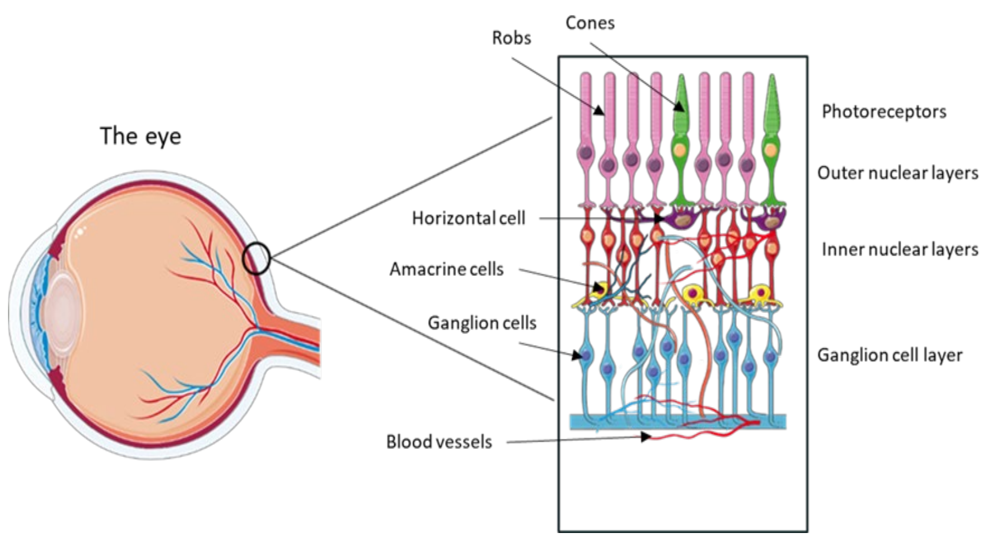

Figure 1: **Representative image of the retina**
Representative image of the retina identifying the layers of the retina and blood vessels. Cells within the retina layers are identified on the left and major layers on the right. Due to the limitations of the image not all layers were identified or visible.

retina is thinnest at the foveal floor (0.10, 0.150-0.200 mm) and thickest at the foveal rim (0.23, 0.320 mm)(2). It is the only part of the central nervous system (CNS) that can be directly visualized non-invasively. The retina is composed of 10 layers: The inner limiting membrane, nerve fiber layer, ganglion cell layer, inner plexiform layer, inner nuclear layer, middle limiting membrane, outer plexiform layer, outer nuclear layer, and the external limiting membrane (3). Among these layers, blood vessels are found from the inner limiting membrane to the outer plexiform layer (Figure 1).

Blood Vessels of the Retina

The peripheral vascular system (PVS) comprises all blood vessels located outside the heart. Each segment of the peripheral vascular system has a different function and structure depending on the organ it serves (4). All tissues rely on a blood supply, which relies on endothelial cells. Endothelial cells can alter their quantity and configuration. Tissue development and healing would be impossible without endothelial cells` expansion and reconstruction of the blood vessel network (5,6).

Arteries are vital in providing blood and nutrients to organs. Arteries are constantly under stress the presence of elastin in large arteries allows them to expand in size and adjust their diameter (7). The aorta, the primary high-pressure conduit connecting the heart's left ventricle, then divides into the internal and external carotid arteries (3). The aorta divides into smaller arteries known as arterioles and ~~finally~~ capillaries that go throughout the body. The pulmonary arteries transport oxygen-depleted blood from the heart to the lungs at low pressure (8).

Arteries have three main layers: the adventitia, the tunica media, and the tunica intima. The adventitia, or outside layer, contains connective tissue, which allows for anchoring arteries to nearby tissues and provides structural support and form to the vessel (9). The tunica media, or middle layer, is composed of elastic and muscular tissue that allows arteries to handle high pressure and controls the internal diameter of the vessel. The last layer is the tunica intima, or inner layer, lined by endothelium and offers a frictionless passage for blood flow (4,10).

When an artery reaches a target organ, it divides into smaller arteries. Arterioles are smooth muscular blood vessels that carry blood to the organs. The autonomic nervous system influences the diameter and shape of arterioles. Arterioles respond to a tissue's demand for extra nutrients and oxygen. Because they have less elastic tissue in their walls, arterioles play an essential role in systemic vascular resistance. Capillaries have thin-walled vessels with a single endothelial layer. Because of the capillary's thin walls, nutrients and metabolites are predominantly exchanged by diffusion. The arteriolar lumen controls blood flow through capillaries (4).

The ratio of artery width to related vein width is 2:3. Blood passes from venules into larger veins. Venules are the tiniest veins that collect blood from capillaries and are prone to rupture due to their thin walls. Venules also participate in the exchange of oxygen and nutrients. Unlike the arteries, the venous pressure is modest. Veins are less elastic compared to arteries; having thin walls allowing them to hold higher percentage of the blood in the circulation than arteries (4,10). In addition, veins have one-way valves inside them that allow blood to flow in a forward direction toward the heart. Respiratory alterations that impact pressure gradients in the abdomen and chest cavity similarly influence forward blood flow from the lower extremities to the heart. This pressure disparity is most significant during deep inspiration but is present throughout the respiratory cycle (4).

The retina requires a continual supply of highly oxygenated blood to keep it nourished. To accommodate these high needs, the retina has a dual blood supply system; it is supplied by the choroid and branches of the ophthalmic artery. The ophthalmic artery gives rise to the central retinal and posterior ciliary arteries, which nourish the inner and outer structural layers (3). The central retinal artery goes out the optic nerve through the dura mater right beneath the optic nerve, allowing the retinal and macular cells to be nourished (3,11). The first branch of the ophthalmic artery is the central retinal artery which emerges at the optic disk and provides 20-30% of all blood flow to the retina. Retinal arteries are distinguished from arteries of comparable size in other organs by a highly developed smooth muscle layer and the absence of an interior elastic lamina. The artery wall has five to seven layers of smooth muscle cells at the optic disk, dropping to one or two at the periphery (3). The posterior ciliary artery's second branch of the ophthalmic artery divides into the short and long posterior ciliary arteries, which enter the sclera and supply blood to the outer and middle retina (3). The long and short posterior ciliary arteries also supply blood to the choroid. Many smaller vessels branch off the superficial retina outer layers and penetrate deeper into the retina's inner layers (12). The vortex veins and the central retinal vein, which join the superior and inferior ophthalmic veins, are the primary venous outflow routes from the eye (13). Upon leaving the retina, the central retinal veins leave the eye via the optic nerve and drain into the cavernous sinus (11).

Vasculature Structure

Early detection of alterations in retinal vessels allows for inferences about the overall health of blood vessels, potentially allowing for early treatment of retinal diseases that can prevent long-term damage, including blindness. Diabetes and hypertension, for example, can cause alterations in the retinal arteries, such as vascular narrowing, arteriovenous, and occlusion, leading to retinal pathology(14–17).

Tortuosity

Tortuosity (**Figure 2A**) is defined as the degree of the twistedness of a curved structure and is quantified as the ratio of vessel curve length over the linear distance between two ends. Tortuosity can damage any arterial bed, from subungual capillaries and retinal arteries to medium and major arteries like the coronary, cerebrovascular, or iliac vessels, as well as the aorta itself (18). This vascular aberration can affect a broad spectrum of vessels throughout the body, from big arteries and veins to small arterioles and veins, including the retina (18). Vessel tortuosity may be limited to a single vessel or widespread, can be diagnosed at different ages, and typically processes over time. The first known depiction of vascular tortuosity in the body was in a drawing by Leonardo da Vinci (19). Leonardo da Vinci linked the aging process by showing that superficial arteries of the arm become twisted in the elderly compared to straight in the young (19). Various terms have been used to describe different types of tortuosity, including s-curve, kinking, looping, and coiling (20,21). Clinical studies have associated alterations, such as tortuosity changes, in arteries and veins with aging as well as various diseases, including atherosclerosis, hypertension, carotid artery, genetic conditions, and type 2 diabetes (18,22–25).

Vascular Density

The production of new blood vessels (angiogenesis) is crucial for development, but aberrant blood vessel growth has been linked to various diseases. Vascular density (**Figure 2B**) changes are often a result of hypoxia. In return, a reduction in oxygen results in increased angiogenesis (growth of new blood vessels) in the retina and other organs throughout the body (26). Vascular endothelial growth factors (VEGF) and their receptors are the fundamental signaling mechanism that controls endothelial cell proliferation and migration, resulting in angiogenesis (27).

Vascular density of the retina is defined as a ratio or percentage of total vessel area to the entire region of interest (ROI). Changes of the vascular density can occur in macro-and micro-vessels. Often microvascular changes such as capillary remodeling have been linked to changes in diabetic retinopathy and other diseases associated with hypertension (28,29). Imaging technologies such as the ones used in this dissertation can reveal the architectural organization of capillaries, which may be the first signs of ischemia/hypoxia, occurring before arteriolar and venular changes (30,31). Vascular density can be measured in a range of parameters. This dissertation examines vascular density based on vessel area density, vessel curvature based on tortuosity, structural changes based on fractal dimensions, and total vessel numbers. These parameters were measured via vessel generation (VESGEN) analysis software, which is discussed in detail later in the introduction.

Fractal Dimension

Fractal dimension (**Figure 2C**) is a ratio that provides a statistical measurement of complexity by comparing details in a pattern. The goal of fractal analysis as it applies to branching structures in tissues, vasculature, and organs is to calculate the fractal dimension of the objects and structures then utilize this number as a classifier to differentiate between normal, aberrant and diseased structures (32,33). Most retinal microvascular abnormalities arise early in the disease process, are localized in capillaries, and result in permeability changes. The fractal analysis does not identify these early vascular changes. The fractal analysis of blood vessels in the retinal circulation is a global assessment of blood vessel pattern; as such, it is not sensitive to tiny changes in a small section of the entire pattern (33–35).

The fractal dimension measures how well a fractal item fills space. Nonetheless, there is some correlation between a pattern's observed complexity or roughness and its fractal dimension. The fractal dimension grows in proportion to the intricacy of how the item fills space. The fractal dimension in a plane is “two” if the item fills the space. Several designs that fill space similarly share the same fractal dimension and exhibit comparable scaling relations. Nonetheless, the single number may be crucial in defining the process that led to the pattern's creation as a feature descriptor (33).

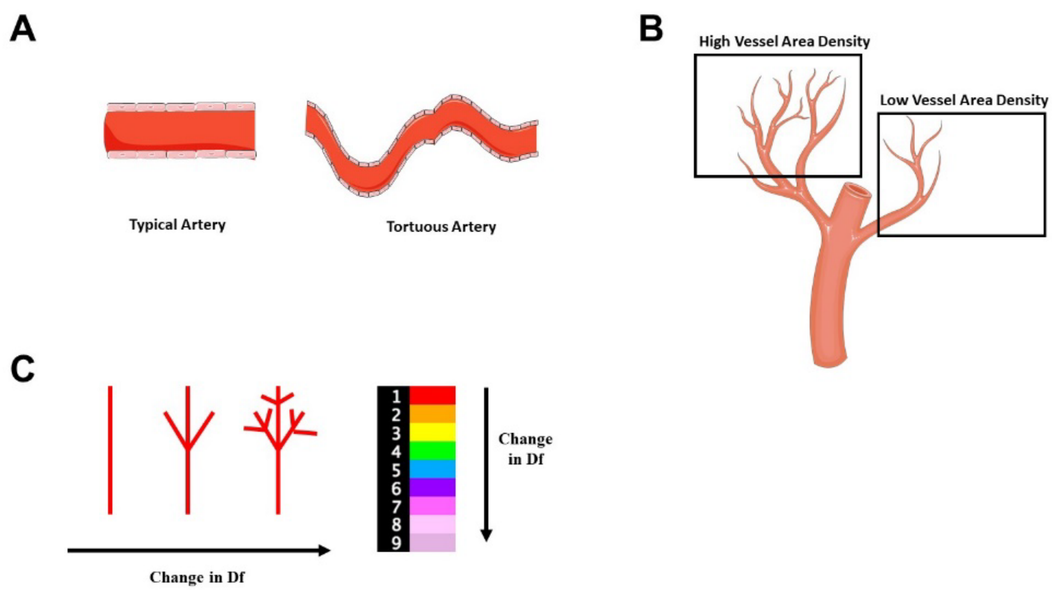

Figure 2: Simplified representation of key VESGEN outputs
Representative output examples of, tortuosity (A), vessel area density (B), and fractal dimension (C), key output parameters.

History of Retinal Imaging

Due to its structure, the retina provides a direct view into the body without an invasive procedure. During the early 1800s, a French physician, Jean Mery, performed the first documented attempt at retinal imaging. This was achieved by submerging a live cat in water, revealing the visible retinal vessels. It led to the invention of the ophthalmoscope in 1823 by Jan Evangelista Purkyně, later reinvented in 1845 by Charles Babbage (36). Lastly, the concept of the ophthalmoscope was further improved to what we know today by Helmholtz in 1851(37,38).

The first retinal image was completed in 1885 by Messrs Jackman and Webster by exposing the retina to light for over 20 minutes (39). Imaging the retina is important, since it allows assessing vascular complications such as diabetes, hypertension, retinopathy of prematurity, and other known diseases allowing for earlier detection (38,40,41). Today retinal imaging is used to detect retinal diseases and progression. This dissertation will focus on both invasive and non-invasive imaging techniques:

Color Fundus

Ocular fundus imaging is essential for monitoring the health of the human eye. Fundus imaging dates back to the early 1900s when discovered by Allvar Gullstrand and is still used today as a safe and cost-effective way to image vascular changes in the retina (38). Color Fundus (CF) provides color, or red-free, images via a specialized low-power microscope with an attached camera to capture the retina's color images to document the abnormalities' presence. CF imaging is typically provided between 30 and 55 degrees; CF imaging is often used in clinical trials and provides excellent insight into understanding retinal diseases such as diabetic retinopathy (42).

While commonly used today for large-scale detect of retinal diseases. CF imaging has many limitations, including its ability to obtain only 2-D imaging of 3D objects, its inability to accurately establish the presence of macular edema, and coexisting media opacities such as cataracts and the vitreous hemorrhage; the field of view can be restricted (42).

Fluorescein Angiography

Discovered in the early 1960s, fluorescein angiography uses a fluorescent agent during the diagnostic procedure. Fluorescence is a form of photoluminescence that happens when fluorophores absorb electromagnetic radiation and are momentarily excited to a higher energy state (43). Fluorescein molecules are stimulated by blue light (465-490 nm) and emitted by green-yellow light (520-530 nm). The blue light and green-yellow light are separated by a barrier filter, which enables only the green-yellow fluorescent light to pass through while blocking the blue reflected light (44). This concept results in a narrow wavelength band allowing the ability to image and capture fluorescent dye injected into the arteries and veins and the dye binding to circulating leukocytes. Unlike conventional fundus pictures, fluorescein angiography produces remarkable contrast and documents leakage, neovascularization, dilatation, and capillary dropout in vascular diseases such as diabetic retinopathy and macular degeneration (45). These clinical diagnoses are used to identify the amount of damage, design a treatment plan, or monitor therapy progress (38,43). Furthermore, angiography can determine the existence, location, and characteristics of choroidal neovascularization, allowing treatment with laser photocoagulation, photodynamic therapy, or antiangiogenic medicines (43).

While safe and well-tolerated by most patients, these dyes pose a risk of allergic reactions and nausea. Adverse reactions often occur in 5%-10% of patients and range from mild to severe (43). The incidence of fatal reactions is 1:49,557 angiographies, and of severe but non-fatal accidents, 1:18,020 angiographies (46). Among those incidents, individuals with a history of diabetes or systemic arterial hypertension have a 9.72% greater chance of adverse reactions (46).

While the gold standard approach for seeing retinal arteries and veins has been fluorescein angiography, it has a limited resolution to identify deeper plexus and choroids, which look hazy and shadowy and lack the ability to provide sufficient detail of the deep retinal capillary plexus (43).

Vessel Generations Analysis

Vessel generation (VESGEN) 2D analysis is a NASA-based application, user-interactive image J plugin. Previously VESGEN has been used in several studies (14,47–49), including a preliminary methodological study, where VESGEN 2D was used to investigate the progression of diabetic retinopathy (DR). This study showed oscillation of angiogenesis of the microvessels of diabetics during the progression of DR, with vessel density decreasing significantly in severe Non- Proliferative (NP) DR (14,47).

VESGEN 2D input is a user-supplied vascular binary image, which is based on the input image provided by the user, for which one of three analysis approaches can be chosen: (1) Vascular Tree, (2) Vascular Network, or (3) Tree-Network Composite. Images converted into different vascular maps are among the output data with measurements of vascular parameters that are specified for individual vascular branching and overall imaging measurements (48,50).

Generations of vessels are determined by a set of rules where a decrease in vessel diameter is 71% of the primary determinant of a new branching generation. This is based on the idea that blood flow velocity is conserved at an asymmetric vessel bifurcation. VESGEN contains a user-adjustable 15% default tolerance factor (71% ± 15% at a relatively symmetric offspring vessel bifurcation) (VESGEN 2D User guide version 1.10 Parsons-Wingerter et.al. 2011) (48). Each analysis approach will generate a color image in addition to the output data, used to indicate the generational branching and an optional grouped color map of the generational branching. There, VESGEN allows the ability to produce meaningful results by grouping into 3 or 4 generations, also known as small, medium, and large vessels (48,50). This dissertation utilized one of the three vascular morphology known as vascular trees (**Figure 3**), a formation of tapering vessels that are very branched, asymmetric, and nonhomogeneous. In addition, the vascular tree pattern can be separated into arterial and venous trees using basic concepts of vessel connectivity and shape in a relatively quick and straightforward approach. The morphology of arterial and venous characteristics and the connectivity, branching, and tapering aspects of vascular trees are the two variables that make up these principles (VESGEN 2D User

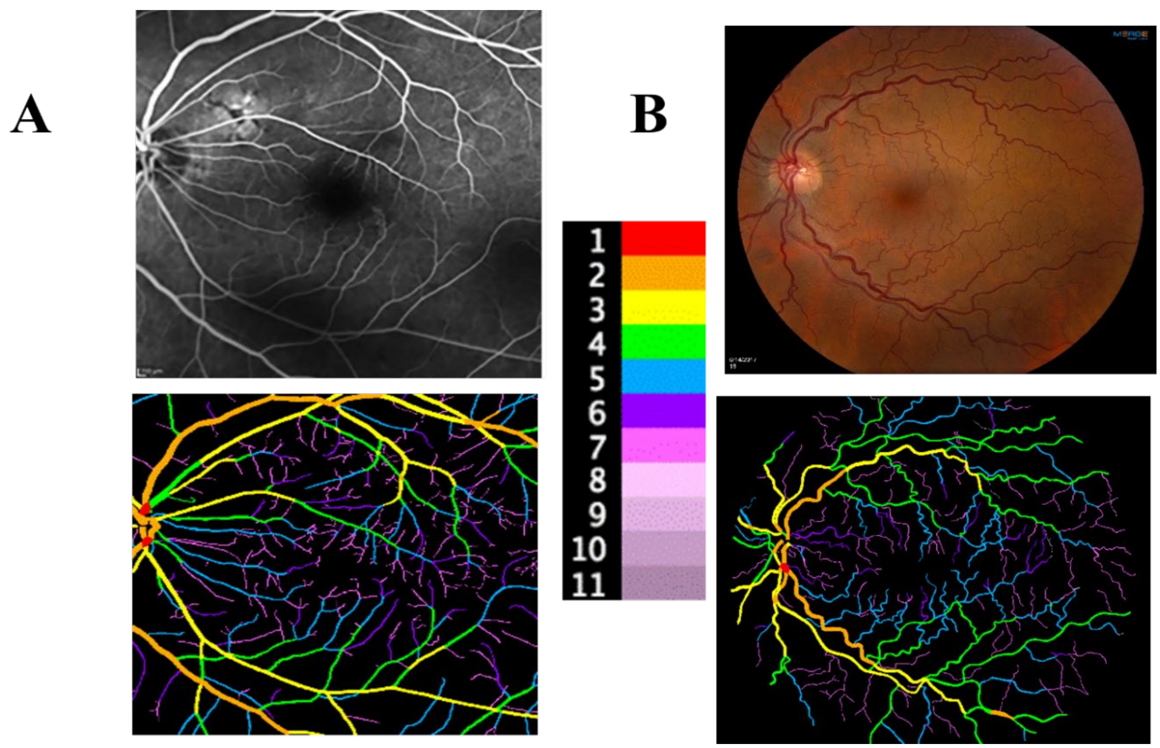

Figure 3: Vascular morphology examples of VESGEN
Vascular images and VESGEN maps from an fluorescein angiography image from a subjects with type 2 diabetes and mild diabetic retinopathy (DR) (a) and color fundus from a subject with pulmonary arterial hypertension (b). Macrovascular vessels defined as results from generation 1-3 plus results of generation 4-5. Microvascular vessels defined as generation 6-11. Branching generation generated by VESGEN. Legend (center) identifies branching generations.

guide version 1.10, Parsons-Wingerter et. al. 2011). VESGEN output parameters used in this dissertation include vessel tortuosity (length of vessel divided by the distance between endpoints of the vessel), fractal dimension (ratio providing a statistical index of complexity), vessel area density (density of total vascular area, Av = vascular area/ROI), and the number of vessels (Number of vessels) (VESGEN 2D User guide version 1.10, Parsons-Wingerter et. al. 2011).

Deep Learning

Deep learning is a subset of a larger class of machine learning approaches that combine artificial neural networks and representation learning. Deep learning has made significant progress in tackling challenges that have long withstood the best efforts of the field of artificial intelligence (AI). Deep learning mimics how people acquire specific types of knowledge and it is a critical component of data science, which also covers statistics and predictive modeling. Compared to traditional machine-learning techniques, which are limited in their ability to process natural data in their raw form, AI is supervised and the programmer must be precise (51).

Artificial intelligence's ability to automate retinal vessel segmentation is an ongoing task. Deep learning segmentation uses a trainable neural network that learns from manually segmented samples before applying to a batch of images used in these studies. In this case of deep learning, the computer works to find ways to transition from an input picture to vessel segmentation. In this dissertation, the deep learning training approach used was STARE(52) (STructured Analysis of the Retina) dataset (training images) and RVGANs (53) (retinal vessel generative adversarial network (GAN) (automated segmentation).

Michael Goldbaum, MD, of the University of California, San Diego, launched the STARE (STructured Analysis of the Retina) Project in 1975. The STARE database contains 400 raw photographs with over 40 hand-labeled images used to compare blood vessel segmentation work. The STARE data was used for deep learning due to its higher specificity than other programs. It was later applied to fundus images and scaled down to match the STARE dataset resolution for correct segmentation by RVGAN (52,53).

Diseases with Retinal Involvement

The retina is affected by several systemic illnesses; therefore, imaging the retina aids in understanding eye disorders as a consequences of diabetes, hypertension, and other cardiovascular diseases to be recognized, diagnosed, and managed (38). The structure of the retinal microvasculature has been discovered as an independent predictor of hypertension, diabetes, cardiovascular disease, coronary heart disease, stroke, and other retinal factors such as the thickness of the retinal nerve fiber layer macular volume (34,54–56). VESGEN has been previously used in a cross-sectional study to examine the oscillation of vessel density during the progression of diabetic retinopathy, suggesting alternating phases of angiogenesis and vascular dropout, resulting of remodeling of the vessels (14).

Diabetes Mellitus

Diabetes mellitus (DM) is defined as the body's inability to properly process food for use as energy resulting in an abundance of sugar in the blood (57). DM affects approximately 420 million people worldwide, with an expected 578 million by 2030 (58). DM is categorized into two types. Type 1 results from the body's inability to produce insulin and is often presented in children or adolescents. While type 2 is defined as the body's failure to respond or produce enough insulin (59) and often affects older adults who have presented long-term hyperglycemia, often resulting from poor dietary choices and lifestyles (57). DR is the leading cause of vision loss among working-age adults and is caused by damage to the blood vessels. DR contributes to over 12,000 new cases of blindness each year (60). DR falls into two main classes: non-proliferative (absent of neovascularization and typically earlier in stage) and proliferative (presence of neovascularization and later in stage). Each stage can be accompanied by macular edema or the buildup of fluid in the macula, the primary cause of vision loss (61). DR is often diagnostic using secondary vascular changes such as microaneurysms and hemorrhages. Although, previous studies have shown that 10% of individuals 40 years of age and older without diabetes may develop these secondary vascular changes making these more common in people without diabetes than previously known (62).

Visibility of primary vascular changes such as vascular dropout and angiogenesis, two known hallmarks for identifying the progression of DR, are visible as early as mild DR (63,64). These changes are vital for understanding the progression and severity of DR. Some of the vital changes include narrowing of the retinal artery, which suggests increased risk of diabetes, and retinal vein widening, which has suggested progression of DR and higher risk of a stroke (62). Another disease, while not systemic, that has known to have an association with retinal vascular changes is pulmonary arterial hypertension.

Pulmonary Arterial Hypertension

Pulmonary hypertension (PH) is defined as increased mean pulmonary arterial pressure ≥20 mmHg at rest as determined by right heart catheterization. PH is characterized by progressive loss and remodeling of the pulmonary arteries and small vessels. PH is divided into four subgroups: Pulmonary arterial hypertension (PAH, group 1), PH due to left heart diseases (group 2), PH due to respiratory diseases or hypoxia (group 3), PH due to chronic thromboembolic (group 4), and PH with unclear and/or multifactorial mechanisms (group 5) (65). For this dissertation, we focused only on PAH (group 1). The inclusion of pulmonary hypertension (PH) subjects irrespective of subgroup (such as Group 2 and 3 PH) would have resulted in additional confounders (age, smoking, obstructive sleep apnea, diabetes mellitus, cardiovascular disease), which can be associated with retinal abnormalities and difficult to control.

PAH is a chronic and progressive disease characterized by vascular obstruction leading to an increase in vascular resistance. Untreated, PAH can ultimately result in death. The effective diameter of the blood arteries diminishes as the severity of PAH worsens, resulting in a cumulative and permanent increase in pulmonary vascular resistance (PVR). While the right heart maintains its systolic function, cardiac output (CO) and mean pulmonary artery pressure (mPAP) rise gradually. As the PVR rises, the right heart begins to fail, in addition to CO. During severe right heart failure decompensation (reduction in CO), the mPAP reduces according to Ohm's law (66).

PAH is relatively rare, affecting about 15 to 50 persons per million (66–68). Right heart catheterization (RHC) is essential to diagnose PH abnormalities and conclusively diagnose PAH. RHC provides useful information on the degree of hemodynamic impairment, assesses responsiveness to PAH medication, and defines prognosis, consequently aiding clinical decision-making in managing PAH (69). In addition, the cardiopulmonary exercise test (CPET) is a noninvasive approach for assessing the integrative cardiopulmonary response to exercise. It provides data on the circulatory, respiratory, metabolic, and muscle responses to physical exertion (70,71). Previously, some CPET parameters have shown to have association with 6 minute walk test and has shown suggested pattern of vascular disease which has resulted in suggestions of diseases progression (70).

PAH is divided into subgroups based on various underlying diseases or pathophysiological causes. PAH is characterized as a state with a mean PAP >20 mmHg, normal left atrial pressure, and pulmonary vascular resistance of 3 Wood units or greater. Patients with a family history of PAH or a known germline mutation are considered heritable PAH (HPAH). In addition, the mutation bone morphogenetic protein receptor type II (BMPR2) gene, has over 300 distinct mutations that have been linked, with a more than 75% among PAH families (72) and 11% (73) of all sporadic IPAH cases. BMPR2 causes function loss and results in signaling changes downstream of the receptor (74).

APAH (associated PAH) refers to PAH caused by congenital heart disease (CHD), PAH caused by liver disease (porto-pulmonary PAH), HIV-related PAH, and schistosomiasis. PAH is also linked to auto-immune illnesses such as systemic sclerosis, mixed connective tissue diseases (MCTD), and systemic lupus erythematosus (SLE). In addition, no cause or related illness has been discovered in the biggest category of PAH, idiopathic PAH (IPAH) (75).

The right ventricle is thin-walled and crescent-shaped, making it prone to any sudden increase in wall stress for example, a rapid rise in PVR, may cause right ventricular dilatation and quick pump failure. However, when the left ventricle faces a sustained rise in systemic vascular resistance, a steady increase in PVR allows for RV adaptation and remodeling. In PAH angio-proliferative vasculopathy affects the pre-capillary arterioles, increasing pulmonary vascular resistance, increasing the right ventricular afterload, and ultimately leading to right heart failure, which is the leading cause of death (76).

Female patients accounted for 63 percent of all IPAH patients in the 1980s NIH registry, but this percentage has climbed to 80 percent in the more recently Registry to Evaluate Early and Long term PAH Disease Management (REVEAL) registry (77) . Several variables impact the female/male ratio, including geography, age, and etiology. PAH can, however, occur in men and is frequently linked with worse clinical results (68)

Patients with onset of PAH symptoms before 36 years of age showed the highest likelihood of delayed diagnosis. According to a 2011 study, 2967 individuals with PAH were enrolled in the Registry to Evaluate Early and Long-term PAH Disease Management (REVEAL Registry), about 21.1% had greater than two years between the onset of symptoms and diagnosis with PAH, resulting in the delay of treatment, which potentially worsens clinical outcomes or survival (78,79).

Histologic and pathophysiology aspects of PAH

PAH can be idiopathic or related to a variety of diseases. The fundamental causes of PAH subtypes vary; however, all are distinguished by excessive pulmonary vasoconstriction and aberrant vascular remodeling processes. Which typically impacts all artery layers (intima, medium, and adventitia) resulting in substantial loss of cross-sectional area and, as a result, increased right ventricular afterload. Pulmonary artery compliance is also reduced, adding to the load on the right ventricle (80,81). PAH formation is complex and diverse, with a wide range of cell types inside the PA vascular walls implicated in the disease process. These cells include pulmonary artery endothelial cells (PAECs), pulmonary artery smooth muscle cells (PASMCs), fibroblasts, inflammatory cells, and platelets. Initial pulmonary vasoconstriction causes muscularization of peripheral arteries and medial enlargement of muscular arteries (82). PAEC damage and malfunction as a result of environmental stressors is also considered an early insult in PAH, and the healing process can result in neointimal development, vascular blockage, and later formation of plexiform lesions, which increases PVR (82).

The physiological result of these changes is partial obstruction of small pulmonary arteries, which also results in increased PVR, right ventricular failure, and mortality. The disruption of four critical signaling pathways causes pulmonary vascular defects: nitric oxide (NO), prostacyclin (PGI2), thromboxane A2 (TXA2), and endothelin-1 (ET-1). PAH is generated by decreased PGI2 synthesis (cyclooxygenase-2 dysregulation) and NO synthase (eNOS) function, with concomitant vasoconstrictive and the mitogenic consequences of an elevated ET-1 signaling pathway (83).

Through its strategic position in the arterial wall, the endothelium responds to changes in blood oxygen and nutrient content by sending signals that vary vascular tone, barrier permeability, and circulating cell recruitment. Endothelial dysfunction in PAH has been widely characterized, as evidenced by diminished angiogenic responses, metabolic abnormalities, and inappropriate activation of inflammatory pathways (84,85).

Nitric oxide (NO) is generated in endothelial cells by endothelial-derived nitric oxide, which catalyzes the oxidation of l-arginine to l-citrulline in the presence of oxygen and nicotinamide adenine dinucleotide phosphate (NADPH). NO diffuses into the underlying pulmonary vascular smooth muscle cells (PVSMC) and binds to soluble guanylate cyclase (sGC), which converts GTP to cyclic guanosine monophosphate (cGMP). Following activation of downstream cGMP-dependent protein kinases (PKG), pulmonary vasodilation occurs. Furthermore, NO reduces PVSMC proliferation, platelet aggregation, and thrombosis, all of which contribute to a healthy pulmonary vasculature. The reduction of bioavailability of NO results in vasoconstriction and increased smooth muscle cell proliferation, inflammation, and thrombosis in PAH (83,86).

Reduced nitric oxide generation causes an increase in arginase activity, which has been linked to the development of pulmonary hypertension in numerous illnesses. In a trial of ten individuals with idiopathic pulmonary hypertension, a 30-minute infusion of 500 mg/kg L-arginine lowered pulmonary artery pressure comparable to a prostacyclin infusion (87). Other studies have shown that inhalation of nitrite, a byproduct of NO oxidation that can be converted back to NO in the lung, reverses established PAH. Both nitrite and nitrate, which can be converted to nitrite by oral commensal bacteria, were demonstrated to reduce PAH via NO-dependent signaling (66,88–90).

The antagonistic eicosanoids prostacyclin (PGI2) and thromboxane (TX) are produced by the action of cyclooxygenase on phosphomembrane arachidonic acid. Endothelial cells synthesize prostacyclins from arachidonic acid via cyclooxygenase and prostacyclin synthase. PGI2 binds to particular I-prostanoid (IP) receptors in smooth muscle cells, causing adenylate cyclase to be activated. This enzyme converts ATP to cyclic adenosine monophosphate (cAMP), which results in smooth muscle relaxation and subsequent vasodilation. Prostacyclin reduces platelet aggregation, slows smooth muscle proliferation, and has anti-inflammatory and antithrombotic properties (83,86). In PAH, the pathway changes to produce thromboxane A2, which causes platelet aggregation, vasoconstriction, and proliferation (91). Furthermore, individuals with PAH have decreased prostacyclin synthesis as well as prostacyclin receptor and prostacyclin expression (86).

Endothelin-1 (ET-1) is a 21-amino acid peptide potent vasoconstrictor and mitogen generated by endothelial cells that has powerful vasoactive capabilities by binding to receptors on vascular endothelium and smooth muscle cells, ET-A and ET-B. When activated, ETA is present on vascular smooth muscle cells and promotes vasoconstriction, hypertrophy, proliferation, cell migration, and fibrosis. Activating the ET-A receptor produces vasoconstriction in the pulmonary circulation under normal circumstances.

On the other hand, activating the ET-B receptor promotes clearance of ET-1 and activation of NO and prostacyclin release. ET-B can be found on the surfaces of vascular smooth muscle and endothelial cells. ET-B activation promotes vasoconstriction on smooth muscle, but on endothelial surfaces, ET-B activation causes vasodilation and anti-proliferation (66,86,92). ET-A and smooth muscle ET-B expression increases during PAH, while endothelium ET-B expression decreases. In addition, PAH patients have higher ET-1 levels in their plasma and pulmonary vascular endothelial cells (93,94).

PAH and the Retina

The bulk of PAH research focuses on endothelial dysfunction in the pulmonary circulation, with little focus on whether comparative pathology might be seen in the rest of the circulatory system. In PAH, blood arteries in the lungs are restricted, obstructed, or damaged, resulting in injuries that reduce blood flow through the lungs and raise blood pressure in the lung arteries (95). This causes the heart to work harder, ultimately resulting in heart failure (HF).

HF is a condition that serves as the last standard route for various disease processes. The heart cannot provide enough blood at normal filling pressures to meet the body's metabolic demands. “Forward heart failure” (left sided) is defined largely by reduced cardiac output and concomitant hypoperfusion symptoms such as tiredness, weakness, lightheadedness, disorientation, and lack of appetite. “Backward heart failure” (right sided) causes "congestive" pulmonary edema symptoms such as dyspnea, orthopnea, PND, cough, and peripheral edema. The differentiation between left sided and right sided failure is mainly based on physical examination symptoms and signs, although these findings can be insensitive and vague. In PAH, right heart failure is a major cause of morbidity and mortality (96).

Although there are significant differences between the heart and the eye, the vasculature of the eye shares many characteristics with the systemic vasculature and is frequently subject to the same inherent and environmental factors. The development of many eye disorders is linked to cardiovascular functioning and risk factors (97,98). In particular, arterial pinching, constriction of retinal arteries, and dilatation of retinal veins are major indicators of increased cardiovascular risk. Because of a malfunction in the venous outflow from the eye, pressure in the dilated veins is frequently considerably elevated. Because retinal blood flow is self-regulated, it is independent of perfusion pressure (PP) (98,99). The primary regulators include vascular endothelial cells and neuronal and glial cells. When flashing light is transmitted onto the retina, the arteries and veins expand, a process mediated mainly by nitric oxide (NO). The visual stimulation of the retina dilates capillaries and arterioles, followed by flow-mediated dilatation of the larger retinal arteries. This provides information on the function of the vascular endothelium and may be of particular interest, as endothelial dysfunction is linked to the majority, if not all, cardiovascular risk factors (98,100). In line with this, there is growing evidence that PAH patients have different morphological alterations in other regions of the body besides the lungs and heart (79,98,101,102).

Aberrant episcleral arteries have been observed in individuals with familial PAH who have BMPR2 mutations (103). Additionally, abnormally dilated episcleral arteries were discovered in unaffected carriers before the onset of PAH (103). In addition to the eye, significant morphological alterations in nailfold capillaries (104,105) and sublingual (106) vasculature have also been reported. Two studies using nailfold capillaroscopy independently found altered capillary density in patients with IPAH compared to healthy people (104,105). Another team measured the blood flow, tortuosity, and curvature of sublingual arteries in 14 healthy controls and 26 PAH patients. Patients with PAH showed a lower sublingual blood flow index and increased tortuosity and curvature compared to healthy sex-matched control participants (106). After adjusting for age, gender, and comorbidities, including diabetes and systemic hypertension, these disparities remained substantial. In individuals with PAH, there was no association between treatment status, disease severity, and the severity of sublingual vascular parameters (79,102,106).

Changes in the retina associated with PAH were first mentioned in a 2012 case report (101). In this case study, a 28-year-old female (younger than average onset age) with Idiopathic PAH showed ocular findings of bilateral dilated episcleral vessels, small intraretinal hemorrhages, mild capillary leakage, and macular detachment. The medical record noted that this person had no history of diabetes or hypertension, two known diseases commonly associated with vascular changes (62). These findings were paralleled by elevated systemic venous pressure suggesting a possible worsening of PAH. Upon a right heart catheterization, mean pulmonary artery pressure had increased by 27%, and the right atrium and right ventricle pressures increased by 20% and 33%, respectively (101). In another study, adaptive optics scanning light ophthalmoscopy (AOSLO) was performed on two female patients with Group 1 PH: one was a 32-year-old functional class 2 patient with IPAH, and the other was a 41-year-old functional class 3 patient with Eisenmenger syndrome. Tortuosity was identified in a substantial proportion of imaging arteries in both individuals. Surprisingly, these findings are similar to those reported in patients with systemic hypertension and diabetes, despite the fact that none of the individuals had these conditions or any other cardiac risk factors (107). This dissertation examines the associations between the retina and systemic diseases using fluorescein angiography, color fundus imaging, and VESGEN to facilitate the detection and progression of PAH while examining and comparing known imaging techniques for safer diagnosis.

Closing Remarks

Unique alterations in blood vessels accompany a variety of systemic diseases. During an ophthalmoscopic examination, retinal vascular alterations and their immediate morphological repercussions are detectable. These discoveries can aid in better understanding serious systemic or localized disorders. Alterations in retinal vessels allow for making inferences about the overall health of unseen blood vessels. Diabetes and hypertension, for example, can cause pathological alterations in the retinal arteries, leading to retinal damage (108). Early detection and treatment of such disorders can frequently avert long-term damage, including blindness and death. As a result, assessing retinal arteries and veins should be an important aspect of every eye checkup. Healthy retinal vessels are uniform in diameter and travel with a slightly typical pattern (108,109).

In closing, PAH patients should be monitored for ocular pathology and retinal abnormalities. Retinal abnormalities of PAH could serve as a screening tool to better understand progression of diseases.

RETINAL VESSEL CHANGES IN PULMONARY ARTERIAL HYPERTENSION

By

MARIANA DUPONT, SAVANNA LAMBERT, ANTONIO RODRIGUEZ-MARTIN, OKAERI HERNANDEZ, MARK LAGATUZ, TAYGAN YILMAZ, ANDREW FODERARO, GRAYSON L. BAIRD, PATRICIA PARSONS-WINGERTER, TIM LAHM, MARIA B. GRANT, COREY E. VENTETUOLO

Pulmonary Circulation 12:e12035. https://doi.org/10.1002/pul2.12035, 2022

Format adapted for dissertation

ABSTRACT

Pulmonary arterial hypertension (PAH) is classically considered an isolated small vessel vasculopathy of the lungs with peripheral pulmonary vascular obliteration. Systemic manifestations of PAH are increasingly acknowledged, but data remain limited. We hypothesized that retinal vascular changes occur in PAH. PAH subjects underwent retinal fluorescein angiography (FA) and routine disease severity measures were collected from the medical record. FA studies were analyzed using VESsel GENerational Analysis (VESGEN), a noninvasive, user-interactive computer software that assigns branching generation to large and small vessels. FAs from controls ($n = 8$) and PAH subjects ($n = 9$) were compared. The tortuosity of retinal arteries was higher in PAH subjects compared to unmatched controls (1.17, 95% confidence interval: [1.14, 1.20] in PAH vs. 1.13, 95% CI: [1.12, 1.14] in controls, $p = 0.01$). Venous tortuosity was higher and more variable in PAH (1.17, 95% CI: [1.14, 1.20]) compared to controls (1.13, 95% CI: [1.12, 1.15]), $p = 0.02$. PAH subjects without connective tissue disease had the highest degree of retinal tortuosity relative to controls (arterial, $p = 0.01$; venous, $p = 0.03$). Younger PAH subjects had greater retinal arterial tortuosity, which attenuated with age and was not observed in controls. Retinal vascular parameters correlated with some clinical measures of disease in PAH subjects. In conclusion, PAH subjects exhibit higher retinal vascular tortuosity. Retinal vascular changes may track with pulmonary vascular disease progression. Use of FA and VESGEN may facilitate early, noninvasive detection of PAH.

INTRODUCTION

Pulmonary arterial hypertension (PAH), the most aggressive type of pulmonary hypertension (PH), is a progressive pulmonary vasculopathy without a cure. The hallmark of PAH is profound pulmonary vascular remodeling that leads to narrowed and ultimately obliterated blood vessels.[1–3] A growing body of literature suggests that PAH is a systemic disease that involves vascular beds in other organ systems, including the kidneys, the systemic musculature, and the coronary circulation.[2,4] Ocular manifestations have been reported in a handful of PAH cases,[5–7] but it is not known whether these abnormalities are due to primary retinal vascular changes, adverse effects of PAH medications, or are reflective of PAH-related changes in systemic blood flow or oxygen content.

As the presenting symptoms of PAH are nonspecific, the diagnosis and treatment of PAH are frequently delayed, resulting in an unacceptably high mortality rate. Right heart catheterization (RHC) is the gold standard for diagnosing PAH which includes increased pulmonary artery pressure (PAP) and pulmonary vascular resistance (PVR) in the absence of elevated pulmonary artery occlusion pressure.[8–10] However, while this method is the most direct measure of pulmonary vascular burden, it is invasive. In addition, central hemodynamics may be relatively insensitive measures of early or subclinical pulmonary vascular and microvascular changes. To date, noninvasive techniques for monitoring PAH lack sensitivity and specificity.[11] Identifying additional noninvasive techniques for earlier detection or serial monitoring of PAH is a critical unmet need. Such markers may prove especially valuable in systemic conditions known to be associated with an increased risk of PAH development, such as connective tissue disease (CTD) or bone morphogenetic protein receptor 2 gene mutation carrier status.

The retinal vasculature can be delineated by fluorescein angiography (FA), a minimally invasive technique that images the retina following systemic injection of solubilized fluorescein.[12] Pathological changes seen on FA have been identified as a marker of vascular damage in systemic diseases such as diabetes.[13] To map and quantify vascular morphology in PAH, we analyzed FA images using VESsel GENeration (VESGEN), a novel, automated software developed by the US National Aeronautics and Space Administration (NASA).[14–18] We hypothesized that PAH subjects would exhibit retinal vessel abnormalities compared with controls and that the degree of retinal vascular pathology would correlate with markers of PAH severity, including hemodynamics.

METHODS

Subjects with a clinical diagnosis of World Symposium on Pulmonary Hypertension Group 1 PH (PAH) and meeting traditional hemodynamic criteria at diagnosis[19,20] were recruited. For this pilot study, stable prevalent patients on PAH medications were enrolled. Exclusion criteria included age younger than 18 years, non-Group 1 PH, diabetes mellitus (Hgb A1C ≥ 6.5 or being treated for diabetes mellitus), malignancy, imprisonment, pregnancy, or a known history of any retinal disease. The most recent hemodynamic parameters, performed within 1 year of study enrollment (but not necessarily meeting strict hemodynamic definitions for PAH), were extracted from the medical record and included: right atrial pressure (RAP), mean PAP (mPAP), pulmonary capillary wedge pressure (PCWP), superior vena cava oxygen saturation ($ScvO_2$), pulmonary arterial oxygen saturation (SvO_2), cardiac output and index (CO and CI, respectively), and PVR. Clinical data, including 6-min walk distance (6MWD) and functional class were extracted from clinic records as close as possible to study visit.

Inclusion criteria for healthy controls included any male or female of 21 years of age and older who were eligible to participate and able to cooperate with the eye exam protocol. Exclusion criteria included age-related macular degeneration, glaucoma, uveitis, known hereditary retinal degenerations, diabetic retinopathy, or other significant ocular complications, and systemic conditions such as systemic hypertension, peripheral vascular disease, active malignancy, myocardial infarction, diabetes, cerebral vascular accident, or cerebral vascular procedure, current pregnancy, history of organ transplantation, presence of a graft, evidence of ongoing acute or chronic infection, and anemia. Both PAH and healthy control subjects provided written informed consent. Enrollment for PAH cases and healthy controls was coterminous and therefore not matched.

Image acquisition

All subjects had imaging performed by experienced retinal photographers with color fundus photographs and FA. Photographers were blinded to the severity of PAH or control status of the subjects. FA images from three eyes from three different PAH subjects could not be used due to poor quality. For this pilot study, we took a pragmatic approach and leveraged available control images that were acquired at a higher imaging resolution (35°) than the PAH images (55°), thus capturing more small vessels per unit area. Comparisons were therefore limited to vessel tortuosity, which is independent of magnification (i.e., scale-invariant).[18]

Image processing

Original FA images (2392 × 2048 pixel) were processed, traced into binary (black/white) images, and analyzed at various zoom levels using 2019 Photoshop Adobe Creative Cloud on a 15.6-inch HP laptop at a resolution of 1366 × 768 pixel. A color fundus image was used to define the difference between arteries and veins that were separated from each other according to physiological vascular branching rules.[14–16]

Vascular quantification

Automated algorithms for the VESGEN analysis are based on physiological rules of vertebrate vascular branching that include vessel bifurcational branch points and tapering, and characteristics of laminar blood flow. The VESGEN software is a user-interactive JAVA-based computer interactive vascular analysis that is globally available from NASA (https://software.nasa.gov/search/ software/vesgen) and operates as a complex plug-in to ImageJ software (National Institutes of Health).[16] Binary arterial, venous and combined arterio-venous images with the enclosing region of interest (ROI) obtained by the image processing were imported into VESGEN to automatically map to quantify the vascular parameters of interest. These included: (a) tortuosity (Tv), which is calculated by the length of the centerline of a single vessel divided by the distance between the two endpoints of that single vessel, and (b) vessel area density (Av), defined as the density of the total vascular area.[14–18] Macrovascular vessels were defined as vessels identified as generations 1–5. Microvascular vessels were defined as vessels identified as generation 6 and greater.

Statistical analysis

Data were summarized as median (range) or N (percentage). Arterial and venous Tv were modeled between cases and controls using generalized linear mixed modeling (GLMM) assuming a normal distribution with sandwich estimation, where observations (for each eye) were nested within subjects. Age was modeled as a moderator between cases and controls. We also conducted a sensitivity analysis in which cases were separated into CTD and non-CTD and compared to controls. GLMM was also used to examine functional class (binomial distribution), 6MWD, RAP, mPAP, CO, CI, PVR, ScvO2 and SvO2 with predictors total artery Tv, total artery Av, microartery Av, and microvein Tv (normal distribution), respectively, as exploratory analyses. All analyses were conducted using SAS Software 9.4 (SAS Inc.) with the GLIMMIX procedure. Alpha was established a priori at the 0.05 level, and all interval estimates were calculated for 95% confidence. Exploratory analyses that examined the relationship between retinal parameters and PAH severity were adjusted using a Benjamini-Hochberg false discovery rate (pFDR) of 0.20,21 where this value (and below) denotes significance.

RESULTS

Characteristics of subjects

Nine PAH patients and eight control subjects were compared. Characteristics of PAH subjects and controls are summarized in Table 1. PAH subjects were predominantly female (88%). The most common PAH etiology was CTD-associated (n = 4; 44%) followed by idiopathic PAH (n = 3; 33%).

VESGEN characterizes retinal vascular phenotype in PAH

Illustrative examples of tortuosity (T_v) and vessel area density (A_v) are displayed in Figure 1, which includes images of three representative cases from PAH subjects: a more extreme vascular pathology (Figure 1a), a case closest to the mean value of the quantified vascular results (Figure 1b), and a milder case (Figure 1c). After processing from a retinal FA image (Figure 2; first column), the binary image of arteries, veins, or of overlapping arteries and veins (Figure 2; second column), served as the input image to the VESGEN software, together with the ROI image. Vessel generations were then mapped and quantified by VESGEN (Figure 2; third and fourth columns). A control retina with the higher imaging resolution (35°) compared to the PAH images (55°) is included in Figure 2d. These analyses demonstrate the feasibility of retinal phenotyping and vascular quantification with VESGEN for PAH.

Retinas of PAH patients exhibit higher vessel tortuosity than controls

First, the retinal vascular T_v of PAH subjects compared to that of control subjects was assessed. The T_v of the retinal arteries was both greater and more variable in PAH (1.17, 95% confidence interval: [1.14, 1.20]) compared to controls (1.13, 95% CI: [1.12, 1.14]), $p = 0.01$ (Figure 3a). As seen in Figure 4a, when PAH subjects were separated into those with and without CTD, this difference persisted. Subjects with CTD tended to have arterial T_v which was closer to controls (1.15, 95% CI: [1.12, 1.18] vs. 1.13, 95% CI: [1.12, 1.14], $p = 0.13$) whereas non-CTD PAH subjects had the highest degree of T_v (1.19, 95% CI: [1.15, 1.23] relative to controls, $p = 0.01$). However, the difference between arterial T_v in PAH subjects with and without CTD was not significantly different ($p = 0.15$). The greater variability in PAH was accounted for, in part, by a significant interaction with age ($p = 0.002$). Specifically, in PAH, arterial T_v decreased −0.002 (95% CI: [−0.003, −0.0009], $p = 0.0001$) for every 1-year increase in age, a relationship which was not observed with controls ($p = 0.80$; Figure 5a). Similarly, venous T_v was both higher and more variable in PAH (1.17, 95% CI: [1.14, 1.20]) compared to controls (1.13, 95% CI: [1.12, 1.15]), $p = 0.02$ (Figure 3b). As seen in Figure 4b, when cases were separated by CTD, similar relationships were observed in venous T_v as with arterial T_v ($p = 0.03$). However, there was no significant interaction between age and the association between PAH cases and controls and venous T_v ($p = 0.22$; Figure 5b).

Retinal vascular measures and associations with disease severity in PAH patients

A number of retinal parameters were associated with markers of disease severity in PAH (Table 2). Higher retinal arterial density was associated with greater 6MWD ($p_{FDR} = 0.19$), lower RAP ($p_{FDR} = 0.12$), and higher CI ($p_{FDR} = 0.14$) and higher microartery density was associated with higher $ScvO_2$ and SvO_2 ($p_{FDR} = 0.10$ and $p_{FDR} = 0.01$, respectively). Some of the observed associations were either discordant or directionally inconsistent. For example, higher arterial T_v was associated with higher RAP ($p_{FDR} = 0.15$) but higher $ScvO_2$ and SvO_2 ($p_{FDR} = 0.06$ and $p_{FDR} = 0.04$, respectively); similar discordance was observed with macroarterial T_v. Additional significant associations were noted between microvein tortuosity and PAH parameters (Table 2), but not for macrovein tortuosity and PAH endpoints (data not shown).

DISCUSSION

The salient features of this small pilot study demonstrate that vessel tortuosity was increased in PAH subjects as compared to controls. This observation held true irrespective of PAH subtype (CTD and non-CTD). Age modified this relationship in PAH, such that younger PAH patients had more evidence of arterial tortuosity. While retinal tortuosity and density tracked with more severe PAH in some instances, some findings were inconsistent.

Results of our study suggest that the major retinal vascular adaptations during PAH are increased retinal T_v and decreased A_v. Abnormalities in T_v, the twisting and curving of a particular vessel, have previously been associated with severe systemic hypertension, ischemic heart disease, and retinopathy.[22–25] Changes in A_v provide information on vascular integrity.[14–18] Retinal vascular density changes as a possible biomarker have been reported in several other diseases such Alzheimer diseases, mild cognitive impairment, Fabry disease and diabetes mellitus.[26–28] Our control subjects T_v ranged from approximately 1.11 to 1.15 pixel/pixel. Higher T_v was observed in arteries (1.17 ± 0.04) and veins (1.17 ± 0.04) of PAH subjects, indicating that retinal T_v in treated PAH patients may be abnormally increased. We interpret this finding to indicate that either sustained elevations in PVR lead to retinal vascular remodeling or that retinal changes occur concurrently with pulmonary vascular disease, although our findings need to be validated in additional studies.

Most of the individuals experienced similar bilateral vascular changes; however, unique cases existed where each retina displayed a distinct vascular pattern. In these unique cases, differences in T_v and vascular density ranged from 0.02 to 0.05 pixel/pixel and 0.01–0.03 $pixel^2/pixel^2$, respectively, between the eyes of a single individual.

Studies have previously shown that increased retinal arterial T_v is linked with severe systemic hypertension, female sex and aging.[22,29] However, our results show that PAH T_v appears to decrease with age, and that the differences in T_v between cases and controls was greatest in those with predominantly idiopathic disease. This is unexpected, since CTD-associated PAH tends to occur in older patients and concurrent with systemic vascular disease.[30] It is also known that older PAH patients may have more risk factors for mixed disease (non-Group 1 PH) and similarly experience less hemodynamic impairment.[31] For these reasons, we enrolled only PAH patients. While these findings need to replicated, our results suggest that retinal abnormalities may be even more substantial in "pure" PAH than captured here. One potential explanation for the decreased T_v in older subjects could be that vessels from older subjects are stiffer and therefore less prone to becoming tortuous.

Patients with PAH may exhibit systemic vascular dysfunction due to decreased systemic cardiac output[32] that when chronic can lead to structural changes in systemic blood vessels, including those in the eye.[32–35] Ocular abnormalities have been reported in several small case series in PAH. In a 2012 report, a 28-year-old female with PAH for 3 years had blurred vision and metamorphopsia in the right eye. The subject had no prior ocular or medical history. Images of the vessels showed normal choroidal and retinal perfusion, scattered microaneurysms, and areas of mild capillary leakage in the temporal periphery of both eyes, findings consistent with elevated systemic venous pressure and that suggested PAH progression. After 7 months of PAH treatment, visual symptoms resolved. This study was the first to report ocular findings preceded PAH exacerbation.[5] Nickel et al. demonstrated that murine retinas exposed to hypoxia have increased vessel area and vessel branching which correlates directly with right ventricular systolic pressure[7] and that pathological retinal vascular changes were present in two female subjects with PAH, although no quantification of the vasculature was provided.[7] Our study adds to these previous findings by demonstrating in a well characterized PAH cohort that retinal arterial T_v and density correlate with disease metrics. Discordant directions for arterial T_v and microarterial density particularly with $ScVO_2$ and SvO_2 are puzzling and deserve further study. It is conceivable that fluctuations in $ScVO_2$ or SvO_2 stimulate angiogenesis via activation of hypoxiainducible factors, thus leading to a higher density of retinal vessels. However, these newly formed vessels may exhibit a tortuous appearance. This hypothesis remains to be tested in future studies.

This cross-sectional study has limitations. PAH subjects and controls were not matched. PAH subjects and controls for this study were drawn from different sampling populations and the imaging approach varied slightly, which may have created bias. We included only prevalent PAH subjects who were treated and had generally well-controlled disease. We are unable to assess the impact of certain PAH therapies that can cause ocular complications (e.g., phosphodiesterase type 5 inhibitors) on retinal health due to the small sample size. Clinical measures of PAH were taken from the medical record as close as possible to retinal imaging but were not measured as part of the study and were not concurrent. This may have contributed to some of the directionally inconsistent observations. Longitudinal changes over time should be assessed in future studies. The performance characteristics (sensitivity and specificity) of retinal imaging and VESGEN versus standard screening echocardiography need to be established in future studies; differences in cost would also need to be considered.

In conclusion, we found that PAH patients exhibit abnormal retinal vasculature as compared to controls and that retinal abnormalities may correlate with traditional clinical outcome measures in PAH. These results suggest that PAH patients should be monitored for ocular pathology, and that retinal abnormalities may track with pulmonary vascular disease burden. Whether retinal abnormalities may precede PAH and whether retinal imaging could serve as a screening tool should be clarified in future studies.

ACKNOWLEDGMENTS

The authors acknowledge and thank the subjects that participated in this study and their families. The research was supported by the Department of Veterans Affairs Merit Review Award 1I01BX002042 (TL), NIH 1R01HL144727-01A1 (TL); NIH R01 HL141268 (CEV), NASA Vascularized Tissue Centennial Challenge (PPW, ML), Space Radiation Program (PPW, ML), Human Research Program (PPW, ML); and NIH EY028038; EY028861; EY028858; EY012601 (MBG).

CONFLICT OF INTERESTS

Corey E. Ventetuolo has served as a consultant to Altavant Sciences, Acceleron Pharma and United Therapeutics and received support from Altavant Sciences to her institution for the conduct of a clinical trial. The remainder of the authors have no conflicts to declare.

ETHICS STATEMENT

This study was approved by the Institutional Review Boards at Rhode Island Hospital (Study #411516), University of Florida (Study #535–2011), and Indiana University (Study #1402550709).

AUTHOR CONTRIBUTIONS

Mariana DuPont prepared images, analyzed the data, interpreted results, and wrote the manuscript. Savanna Lambert, Antonio Rodriguez-Martin, and Okaeri Hernandez prepared images. Mark Lagatuz aided in support for all VESGEN software-related issues. Taygan Yilmaz and Andrew Foderaro recruited study subjects and performed retinal angiography. Tim Lahm, Maria B. Grant, and Corey E. Ventetuolo designed the experiments, interpreted the data, discussed the results and wrote the manuscript. Patricia Parsons-Wingerter and Grayson L. Baird helped to analyze data, write the manuscript, and discussed the results.

REFERENCES

1. Brown LM, Chen H, Halpern S, Taichman D, McGoon MD, Farber HW, Frost AE, Liou TG, Turner M, Feldkircher K, Miller DP, Elliott CG. Delay in recognition of pulmonary ar- terial hypertension: factors identified from the REVEAL Registry. Chest. 2011;140(1):19–26.

2. Rosenkranz S, Howard LS, Gomberg-Maitland M, Hoeper MM. Systemic consequences of pulmonary hypertension and right- sided heart failure. Circulation. 2020;141(8):678–93.

3. Bitker L, Sens F, Payet C, Turquier S, Duclos A, Cottin V, Juillard L. Presence of kidney disease as an outcome predictor in patients with pulmonary arterial hypertension. Am J Nephrol. 2018;47(2):134–43.

4. Sise ME, Courtwright AM, Channick RN. Pulmonary hy- pertension in patients with chronic and end-stage kidney disease. Kidney Int. 2013;84(4):682–92.

5. Skondra D, Chang GC, Farber HW, Eliott D. Ophthalmologic diagnosis of exacerbation of idiopathic pulmonary arterial hypertension. Arch Ophthalmol. 2012;130(12):1619–21.

6. Lewczuk N, Zdebik A, Bogusławska J, Turno-Krecicka A, Misiuk-Hojło M. Ocular manifestations of pulmonary hy- pertension. Surv Ophthalmol. 2019;64(5):694–9.

7. Nickel NP, Shamskhou EA, Razeen MA, Condon DF, Messentier Louro LA, Dubra A, Liao YJ, Zamanian RT, Yuan K, Perez VAJ. Anatomic, genetic and functional prop- erties of the retinal circulation in pulmonary hypertension. Pulm Circ. 2020;10(2):2045894020905508–4.

8. D'Alto M, Romeo E, Argiento P, D'Andrea A, Vanderpool R, Correra A, Bossone E, Sarubbi B, Calabro R, Russo MG, Naeije R. Accuracy and precision of echocardiography versus right heart catheterization for the assessment of pulmonary hypertension. Int J Cardiol. 2013;168(4):4058–62.

9. Shimada YJ, Shiota M, Siegel RJ, Shiota T. Accuracy of right ventricular volumes and function determined by three- dimensional echocardiography in comparison with magnetic resonance imaging: a meta-analysis study. J Am Soc Echocardiogr. 2010;23(9):943–53.

10. Badesch DB, Champion HC, Gomez Sanchez MA, Hoeper MM, Loyd JE, Manes A, McGoon M, Naeije R, Olschewski H, Oudiz RJ, Torbicki A. Diagnosis and assess- ment of pulmonary arterial hypertension. J Am Coll Cardiol. 2009;54(1 Suppl):S55–66.

11. Casserly B. Brain natriuretic peptide in pulmonary arterial hypertension: biomarker and potential therapeutic agent. Drug Des Devel Ther. 2009;3:269–87.

12. Schmitz-Valckenberg S, Holz FG, Bird AC, SPAIDE RF. Fundus autofluorescence imaging: review and perspectives. Retina. 2008;28(3):385–409.

13. Salz DA, Witkin AJ. Imaging in diabetic retinopathy. Middle East Afr J Ophthalmol. 2015;22(2):145–50.

14. Vyas RJ, Young M, Murray MC, Predovic M, Lim S, Jacobs NM, Mason SS, Zanello SB, Taibbi G, Vizzeri G, Parsons-Wingerter P. Decreased vascular patterning in the retinas of astronaut crew members as new measure of ocular damage in spaceflight-associated neuro-ocular syndrome. Invest Ophthalmol Vis Sci. 2020;61(14):34.

15. Parsons-Wingerter P, Radhakrishnan K, Vickerman MB, Kaiser PK. Oscillation of angiogenesis with vascular dropout in diabetic retinopathy by VESsel GENeration analysis (VES- GEN). Invest Ophthalmol Vis Sci. 2010;51(1):498–507.

16. Vickerman MB, Keith PA, McKay TL, Gedeon DJ, Watanabe M, Montano M, Karunamuni G, Kaiser PK, Sears JE, Ebrahem Q, Ribita D, Hylton AG, Parsons-Wingerter P. VESGEN 2D: automated, user-interactive software for quantification and mapping of angiogenic and lymphangio- genic trees and networks. Anat Rec. 2009;292(3):320–32.

17. Zamanian-Daryoush M, Lindner D, Tallant TC, Wang Z, Buffa J, Klipfell E, Parker Y, Hatala D, Parsons-Wingerter P, Rayman P, Yusufishaq MSS, Fisher EA, Smith JD, Finke J, DiDonato JA, Hazen SL. The cardioprotective protein apoli- poprotein A1 promotes potent anti-tumorigenic effects. J Biol Chem. 2013;288(29):21237–52.

18. Lagatuz M, Vyas RJ, Predovic M, Lim S, Jacobs N, Martinho M, Valizadegan H, Kao D, Oza N, Theriot CA, Zanello SB, Taibbi G, Vizzeri G, Dupont M, Grant MB, Lindner DJ, Reinecker HC, Pinhas A, Chui TY, Rosen RB, Moldovan N, Vickerman MB, Radhakrishnan K, Parsons- Wingerter P. Vascular patterning as integrative readout of complex molecular and physiological signaling by vessel generation analysis. J Vasc Res. 2021;58(4):207–30.

19. Badesch DB, Raskob GE, Elliott CG, Krichman AM, Farber HW, Frost AE, Barst RJ, Benza RL, Liou TG, Turner M, Giles S, Feldkircher K, Miller DP, McGoon MD. Pulmonary arterial hypertension: baseline characteristics from the RE- VEAL Registry. Chest. 2010;137(2):376–87.

20. Dong L, He JG, Liu ZH, Lu XL, Zeng WJ, Sun YJ, Ni XH, Gu Q, Zhao ZH, Cheng XS, Xiong CM. Multicenter study of disease attributes in adult patients with pulmonary hy- pertension. Zhonghua Yi Xue Za Zhi. 2012;92(16):1087–90.

21. McDonald JH. Handbook of biological statistics. biostathandbook.com; 2009.

22. Han H-C. Twisted blood vessels: symptoms, etiology and biomechanical mechanisms. J Vasc Res. 2012;49(3):185–97.

23. Hayreh SS, Servais GE, Virdi PS. Retinal arteriolar changes in malignant arterial hypertension. Ophthalmologica. 1989; 198(4):178–96.

24. Owen CG, Newsom RSB, Rudnicka AR, Barman SA, Woodward EG, Ellis TJ. Diabetes and the tortuosity of vessels of the bulbar conjunctiva. Ophthalmology. 2008;115(6): e27–32.

25. Taarnhøj NC, Munch IC, Sander B, Kessel L, Hougaard J, Kyvik K, Sørensen T, Larsen M. Straight versus tortuous ret- inal arteries in relation to blood pressure and genetics. Br J Ophthalmol. 2008;92(8):1055–60.

26. Cennamo G, Montorio D, Santoro C, Cocozza S, Spinelli L, Di Risi T, Riccio E, Russo C, Pontillo G, Esposito R, Imbriaco M, Pisani A. The retinal vessel density as a new vascular biomarker in multisystem involvement in fabry dis- ease: an optical coherence tomography angiography study. J Clin Med. 2020;9(12):4087.

27. Wang X, Zhao Q, Tao R, Lu H, Xiao Z, Zheng L, Ding D, Ding S, Ma Y, Lu Z, Xiao Y. Decreased retinal vascular density in alzheimer's disease (AD) and mild cognitive impairment (MCI): an optical coherence tomography angiography (OCTA) study. Front Aging Neurosci. 2020;12:572484.

28. Saif PS, Salman AE-RG, Omran NAH, Farweez YAT. Assess- ment of diabetic retinopathy vascular density maps. Clin Ophthalmol. 2020;14:3941–53.

29. Wenn CM, Newman DL. Arterial tortuosity. Australas Phys Eng Sci Med. 1990;13(2):67–70.

30. Mathai SC, Bueso M, Hummers LK, Boyce D, Lechtzin N, Le Pavec J, Campo A, Champion HC, Housten T, Forfia PR, Zaiman AL, Wigley FM, Girgis RE, Hassoun PM. Dispropor- tionate elevation of N-terminal pro-brain natriuretic peptide in scleroderma-related pulmonary hypertension. Eur Respir J. 2010;35(1):95–104.

31. Ventetuolo CE, Praestgaard A, Palevsky HI, Klinger JR, Halpern SD, Kawut SM. Sex and haemodynamics in pul- monary arterial hypertension. Eur Respir J. 2014;43(2):523–30.

32. Nickel NP, Yuan K, Dorfmuller P, Provencher S, Lai YC, Bonnet S, Austin ED, Koch CD, Morris A, Perros F, Montani D, Zamanian RT, de Jesus Perez VA. Beyond the lungs: systemic manifestations of pulmonary arterial hy- pertension. Am J Respir Crit Care Med. 2020;201(2):148–57.

33. Abraham AS, Cole RB, Bishop JM. Reversal of pulmonary hypertension by prolonged oxygen administration to patients with chronic bronchitis. Circ Res. 1968;23(1):147–57.

34. Zimmer HG, Zierhut W, Seesko RC, Varekamp AE. Right heart catheterization in rats with pulmonary hypertension and right ventricular hypertrophy. Basic Res Cardiol. 1988;83(1): 48–57.

35. Grodins FS. Integrative cardiovascular physiology: a mathematical synthesis of cardiac and blood vessel hemodynamics. Q Rev Biol. 1959;34(2):93–1

Table 1. Baseline characteristics of PAH cases and controls		
Variables	**Controls**	**PAH**
Number	8	9
Age (years)	36 (25-52)	50 (26 – 72)
Sex		
Male	2 (25)	1 (11)
Female	6 (75)	8 (88)
Race, n (%)		
White	5 (62)	7 (77)
Black	1 (12)	2 (22)
Other	2 (25)	0
BMI, kg/m^2	.	34 (24 – 46)
PAH etiology, n (%)		
Idiopathic PAH	.	3 (33)
Heritable PAH		1 (11)
Connective tissue disease-associated PAH	.	4 (44)
Human immunodeficiency virus-associated PAH		1 (11)
Hemodynamics		
Right atrial pressure, mm Hg	.	9 (5 – 17)
Mean pulmonary artery pressure, mm Hg	.	40 (20 – 67)
Cardiac output, L/min	.	6.0 (5.5 - 7.7)
Pulmonary capillary wedge pressure, mm Hg	.	10 (5 – 15)
Pulmonary vascular resistance, Dynes-sec/cm^{-5}	.	449 (186 – 775)
Functional class, n (%)		
Class 1		0
Class 2		4 (44)
Class 3		5 (55)
Class 4		0
Six minute walk distance, meters		357 (150 – 446)
PAH therapies*, n (%)		
Calcium channel blockers	.	2 (22)
Phosphodiesterase type 5 inhibitors	.	5 (55)
Endothelin receptor antagonists	.	3 (33)
Prostacyclin analogues	.	3 (33)

Note: Data are shown as median (range) or n (percentage). Abbreviations: BMI, body mass index; PAH, pulmonary arterial hypertension. a Subjects were represented individually even when taking combination therapy

Predictor (bold)	Coefficient	95% CI		p value	Adjusted P value
Outcome					
Total artery tortuosity					
Functional class	8.80	2.20	15.39	0.017	0.13*
Six minute walk distance	0.31	-1.07	1.68	0.61	0.74
Right atrial pressure	-12.97	-37.63	11.67	0.24	0.36
Mean pulmonary artery pressure	-76.94	-218.58	64.69	0.23	0.36
Cardiac output	1.07	1.01	6.49	0.02	0.10*
Cardiac Index	1.32	-11.43	-4.63	<0.01	<0.05*
Pulmonary vascular resistance	-815.91	-1412.90	-815.91	0.02	0.09*
Superior vena cava oxygen saturation	-98.53	-184.71	-12.35	0.03	0.10*
Pulmonary arterial oxygen saturation	-64.32	-171.86	43.20	0.19	0.33
Total artery vessel area density					
Functional class	3.20	-41.47	47.87	0.87	0.95
Six minute walk distance	5.11	0.65	9.58	0.03	0.09*
Right atrial pressure	-61.70	-142.13	18.72	0.10	0.24
Mean pulmonary artery pressure	-71.10	-345.17	202.96	0.54	0.68
Cardiac output	-1.69	-15.99	12.59	0.77	0.87
Cardiac Index	12.78	-2.97	28.54	0.09	0.23
Pulmonary vascular resistance	88.12	-2203.20	2379.46	0.92	0.99
Superior vena cava oxygen saturation	-2.85	-120.40	114.68	0.95	0.95
Pulmonary arterial oxygen saturation	-6.50	-196.91	183.91	0.93	0.97
Macro artery tortuosity					
Functional class	7.25	1.05	13.44	0.028	0.10*
Six minute walk distance	0.34	-0.93	1.62	0.53	0.68
Right atrial pressure	-11.94	-28.23	4.34	0.12	0.26
Mean pulmonary artery pressure	-72.61	-171.70	26.46	0.12	0.25
Cardiac output	2.94	1.04	4.83	0.01	0.11*
Cardiac Index	-5.90	-8.66	-3.15	<0.01	0.02*

Pulmonary vascular resistance	-630.02	-1031.12	-228.93	<0.01	0.02*
Superior vena cava oxygen saturation	-74.67	-137.14	-12.21	0.02	0.08*
Pulmonary arterial oxygen saturation	-59.90	-136.19	16.38	0.10	0.23
Micro artery vessel area density					
Functional class	6.93	-175.92	189.77	0.93	0.95
Six minute walk distance	24.08	-58.48	106.64	0.50	0.66
Right atrial pressure	609.03	-938.95	2157.01	0.37	0.50
Mean pulmonary artery pressure	1325.78	-1285.86	5202.29	0.19	0.32
Cardiac output	74.41	-57.59	206.42	0.20	0.32
Cardiac Index	24.86	-126.05	175.78	0.68	0.81
Pulmonary vascular resistance	-9795.78	-21502	1910.04	0.08	0.21
Superior vena cava oxygen saturation	594.87	163.24	1026.50	0.02	0.08*
Pulmonary arterial oxygen saturation	938.32	324.21	1552.42	0.01	0.09*
Micro vein tortuosity					
Functional class	11.74	2.72	20.75	0.018	0.11*
Six-minute walk distance	-0.17	-0.43	0.08	0.16	0.29
Right atrial pressure	1.53	2.27	9.76	0.01	0.08*
Mean pulmonary artery pressure	22.40	1.61	43.20	0.03	0.08*
Cardiac output	-1.02	-3.22	1.17	0.28	0.39
Cardiac Index	0.55	-3.41	4.53	0.73	0.84
Pulmonary vascular resistance	183.17	-234.37	707.31	0.25	0.36
Superior vena cava oxygen saturation	48.54	-18.67	115.77	0.12	0.23
Pulmonary arterial oxygen saturation	19.67	-10.17	49.52	0.15	0.28

*Denotes significance given the FDR 0.20; functional class is in logit space.

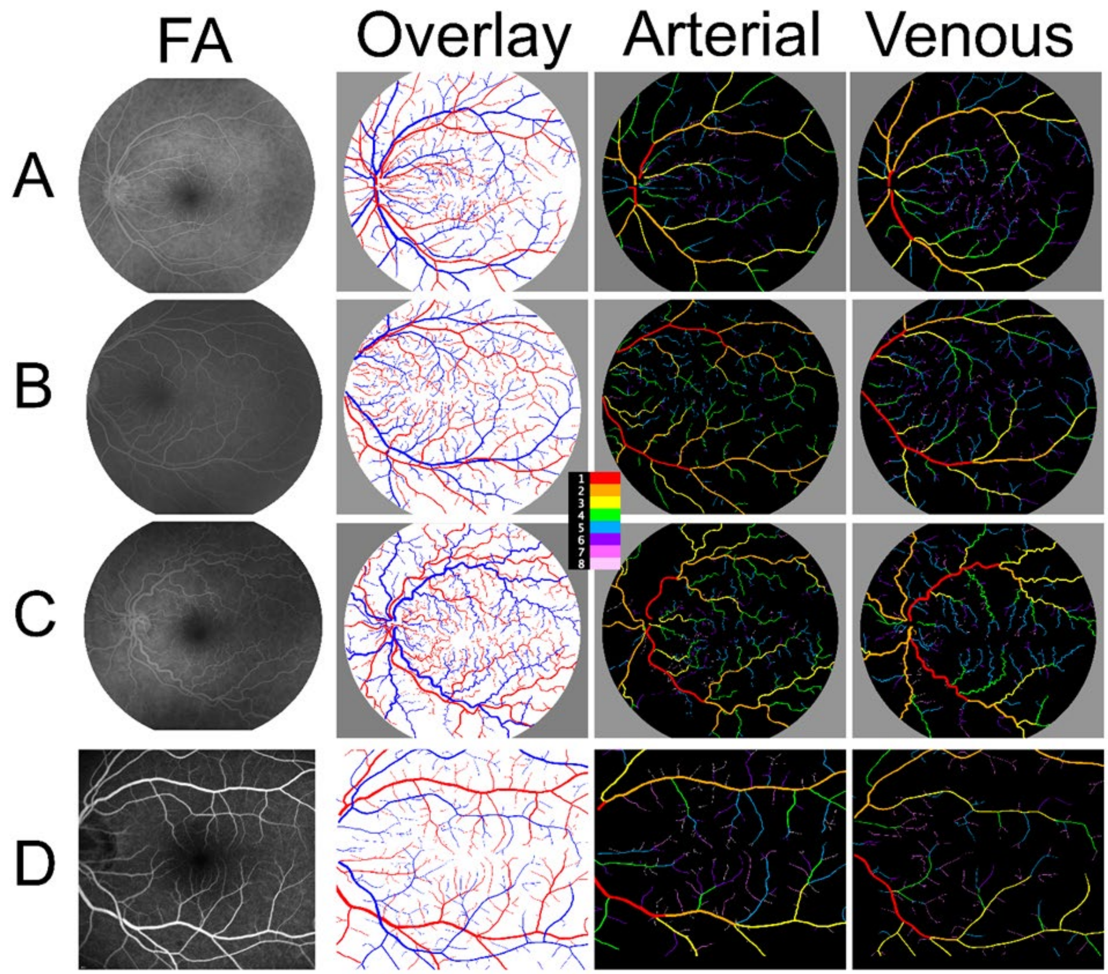

Figure 1: Illustrative retinal vascular changes in pulmonary arterial hypertension (PAH) subjects. Examples of vascular change during PAH illustrated by the complex retinal venous trees containing many vessels and branch points. (a) Retinal venous tree from right eye of 45-year-old female with mPAP of 47 mmHg, CO of 5.2 L/min, and PVR of 566 Dynes-s/cm−5. High Tv (1.22 pixel/pixel) and Av (0.13 pixel2/pixel2) illustrated in boxed area. (b) Retinal venous tree from right eye of 57-year-old female with mPAP of 25 mmHg, CO of 7.7 L/min, and PVR of 186 Dynes-s/cm−5 on PAH therapy. Mean Tv (1.20 pixel/pixel) and Av (0.08 pixel2/pixel2, boxed area). (c) Retinal venous tree from right eye of 72-year-old female with mPAP of 67 mmHg, CO of 5.5 L/min, and PVR of 775 Dynes-s/cm−5. Low Tv (1.18 pixel/pixel) and Av (0.07 pixel2/pixel2, boxed area)

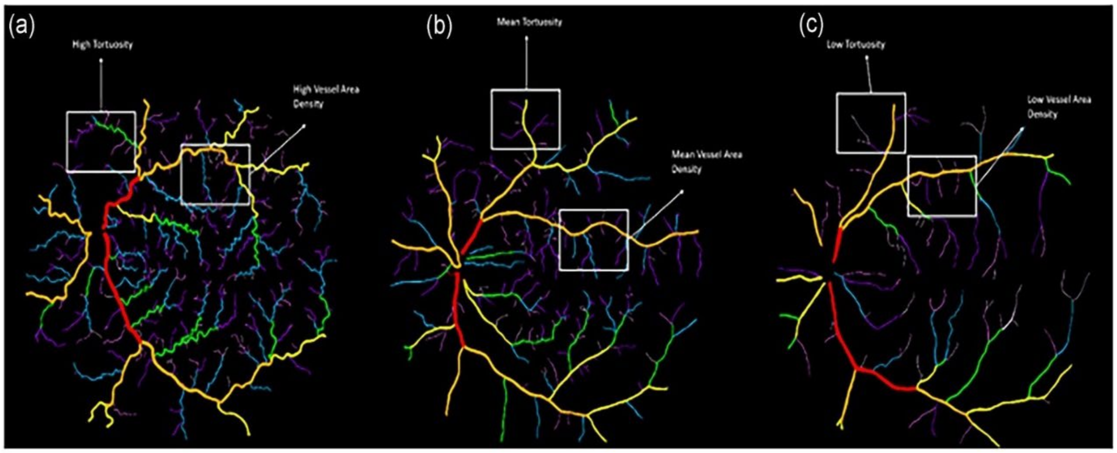

Figure 2: VESsel GENerational Analysis (VESGEN) characterization of retinal vascular phenotype in representative PAH patients and a control subject. Vascular images and VESGEN maps from the left retinas of (a) 57-year-old female PAH subject with mPAP of 25 mmHg, CO of 7.7 L/min and PVR of 186 Dynes-s/cm−5 on PAH therapy; (b) 59-year-old female PAH subject with mPAP of 43 mmHg, CO of 4.8 L/min and PVR of 567 Dynes-s/cm−5; and (c) 45-year-old female PAH subject with mPAP of 47 mmHg, CO of 5.2 L/min and PVR of 566 Dynes-s/cm−5. (d) Representative control retina from the left eye of a 46-year-old female with 35° imaging resolution. First column: Images generated by fluorescein angiography (FA). Second column: Overlap of arteries (red) and veins (blue). Third and fourth columns: Branching generation of arteries and veins, respectively, generated by VESGEN. Legend (center) identifies branching generations 1–8

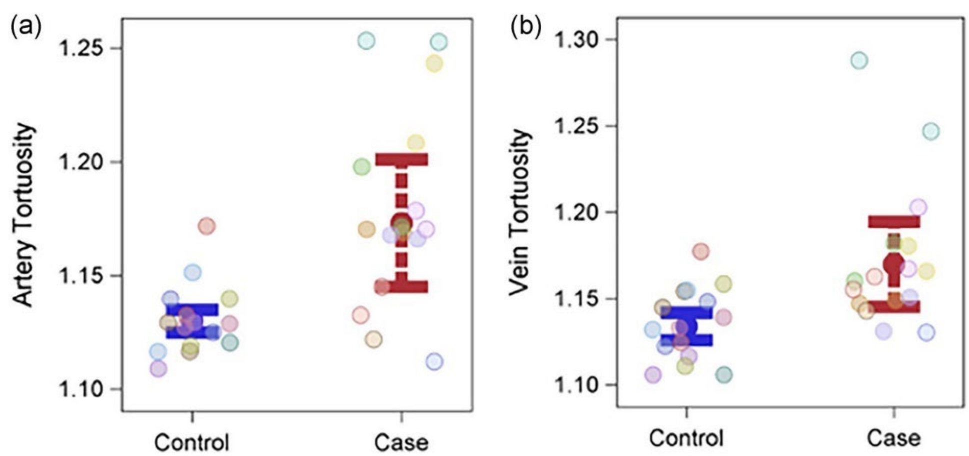

Figure 3: Retinas of pulmonary arterial hypertension (PAH) patients exhibit higher vessel tortuosity than controls. (a) Artery Tv between PAH (case; red) and controls (blue). (b) Vein Tv between PAH (case; red) and controls (blue). Individual observations are color-coded to denote the same patients (eyes)

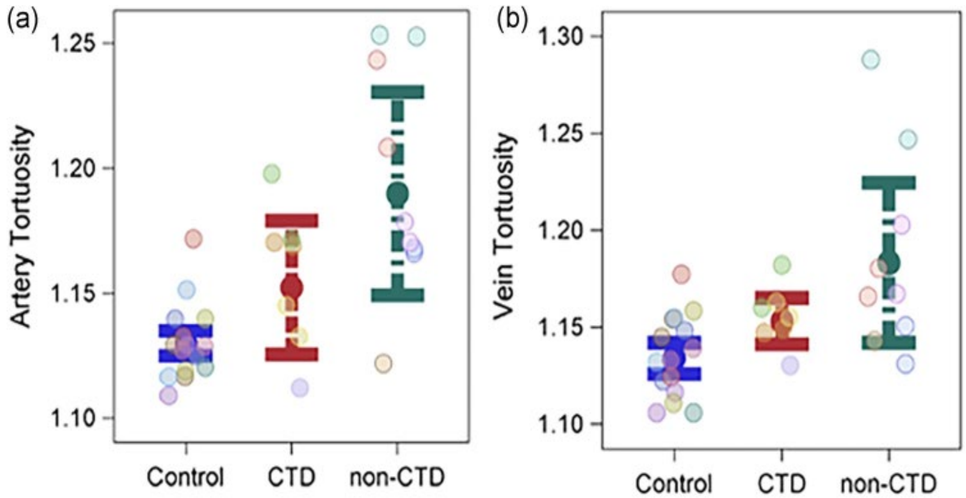

Figure 4: Retinas of pulmonary arterial hypertension (PAH) patients without connective tissue disease (CTD) exhibit higher vessel tortuosity than PAH patients with CTD and controls. (a) Artery Tv between PAH patients with CTD (red), PAH without CTD (green) and controls (blue). Y-axis is artery Tv, X-axis is disease group based on the presence of CTD. (b) Vein Tv between PAH patients with CTD (red), PAH without CTD (green) and controls (blue). Y-axis is vein Tv, and X-axis is disease group based on the presence of CTD. Individual observations are color-coded to denote the same patients (eyes)

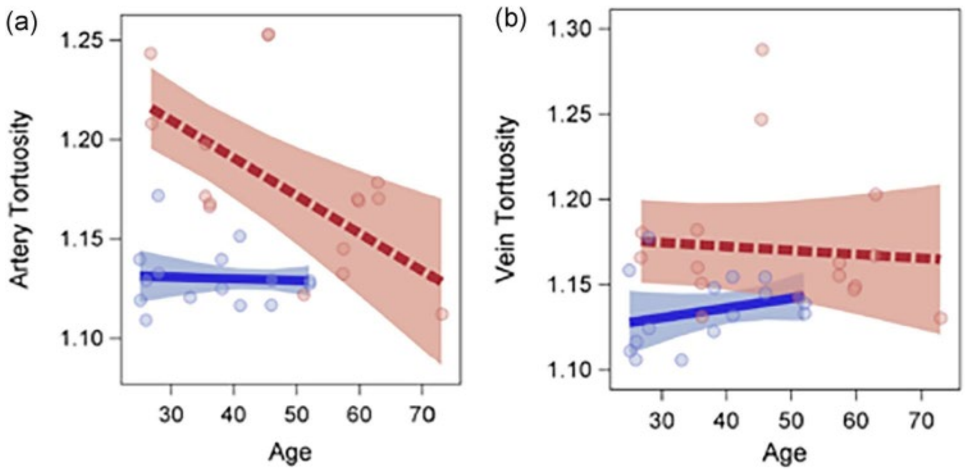

Figure 5: Age modifies the relationship with retinal artery tortuosity in pulmonary arterial hypertension (PAH), but not controls. (a) Arterial Tv decreases with age in PAH, but not controls. Y-axis is arterial Tv, X-axis is age in years. (b) There was no evidence of interaction by age in venous Tv. Y-axis is venous Tv, X-axis is age in years. In both panels, PAH cases are in red, controls are in blue. Red dashed (PAH cases) and dark blue lines (controls), effect estimate; Light red (PAH cases) and light blue (controls) bands, confidence bounds

OPTIMIZING RETINAL VASCULAR IMAGING FOR DETECTING CHANGES IN PULMONARY ARTERY HYPERTENSION

By

MARIANA DUPONT, JOHN HUNSICKER, SIMONA SHIRLEY, WARRINER WILLIAMS, ANNABELLE FRIEDMAN, REDDHYIA TAYLOR, MICHAEL DUPONT, MARK LAGATUZ , TAY YILMAZ, ANDREW FODERARO, GRAYSON L. BAIRD, TIM LAHM, COREY E. VENTETUOLO, MARIA B. GRANT

In preparation for *Translational Vision Science and Technology*

Format adapted for dissertation

ABSTRACT

Rationale: Retinal vascular imaging plays an important role in diagnosing and managing chronic diseases such as diabetic retinopathy, sickle cell retinopathy, and systemic hypertension. Previously, we have shown that individuals with pulmonary arterial hypertension (PAH) exhibit unique retinal vascular changes and that these changes correlate with pulmonary disease severity. In a previous study to visualize the retinal vasculature, we used fluorescein angiography (FA) which is an interventional study with inherent risk.

Objective: The goal of this study was to determine if color fundus (CF) imaging could be used to garner identical retinal information as FA in individuals with pulmonary artery hypertension.

Method: VESGEN, a computer software which assigns branching generation to vessels and details vascular patterns, was used to compare FA to CF imaging in PAH subjects (n=9) followed by deep learning processing output to increase the speed of analysis and facilitate clinical translation. Due to deep learning's inability to separate arterial and venous structures, only total vasculature was assessed.

Results: When FA and CF images were compared using VESGEN analysis, both showed identical tortuosity and vessel area density measures. This remained true, even when separating images based upon arterial trees. Deep learning only showed similarities when comparing FA and CF for structural differences (Df). When comparing CF imaging to deep learning imaging, similarities were lost for tortuosity or vessel area density.

Conclusion: CF, a non-invasive approach, can be used with VESGEN to provide an accurate and safer assessment of retinal vascular changes and provides additional clinical data to monitor disease progression in patients with PAH.

INTRODUCTION

The human eye offers a window into systemic diseases and disease progression [1–3]. As a result, imaging modalities of the retina that have the ability to detect changes in disease progression safely and effectively are in clinical demand[1,2,4]. Although widely used, fluorescein angiography (FA) is an invasive procedure involving the injection of sodium fluorescein to visualize the retinal vasculature. This imaging modality has been associated with an adverse event rate ranging from 1-22% [5]. Most commonly nausea, vomiting, gastrointestinal upset, and urticaria are reported. There have been reports of more severe complications, including anaphylaxis, cardiac events, tonicclonic seizures, and even death associated with FA [5–9]. According to a recent comprehensive literature review, there have been 11 reported deaths associated with FA amounting to an estimated 1:220,000 to 1:100,000 death rate [5]. Moreover, individuals with underlying systemic arterial hypertension, pulmonary artery hypertension, diabetes, sickle cell disease, or allergy history may be at increased risk of adverse events due to compromised kidney function. Importantly, retinal pathology has been associated with these systemic conditions[10].

Given these concerns, there is a need for non-invasive methods to detect retinal vascular changes without sacrificing image quality. Color fundus (CF) imaging typically is performed before FA. CF produces a colorized image using a fundus camera under the illumination of white light. Unlike the adverse events associated with FA imaging, there have been no known reports of photic injuries from standard fundus photography [11]. CF also offers a time-efficient and user-friendly technique typically completed in minutes during routine clinic visits. FA takes up to an hour to perform and also has greater associated cost [12]. This study aimed to provide evidence that CF can be used in individuals with PAH allowing for a safe, non-invasive method for detecting the vascular changes typically observed with FA.

METHODS

Clinical Study

The cohort of subjects for this study were individuals who have been confirmed to carry the diagnosis of World Health Organization (WHO) Group 1 PAH. In a previously published report, we compared these PAH subjects to controls and the relationship between retinal parameters obtained by FA and clinical measures of PAH severity (110). PAH subjects were recruited from the Rhode Island Hospital Pulmonary Hypertension Center. Each subject underwent both FA and CF on the same day.

The Institutional Review Boards approved this study at Indiana University, Rhode Island Hospital (Study #411516).

Image Acquisition and Processing

CF images of the subjects` retinas were performed by retinal photographers at Rhode Island Hospital in Providence, Rhode Island. Images were acquired with a 55-

degree field of view and resolution of 2392 by 2048 pixels, and processed, traced, and analyzed using 2019 and 2020 Photoshop Adobe Creative Cloud. To ensure uniformity among images, the final analysis of images was processed by a single individual, masked to the identity of the subjects and disease severity. Using the physiological vascular branching rules previously described, the CF image was used to define the difference between arteries and veins[14]. FA images of the same eye were acquired similarly. Due to the risk of inaccurate comparisons to CF images, three FA images were excluded from analysis due to poor image quality.

Vascular Quantification

The VESGEN software is a user-interactive JAVA-based computer interactive vascular analysis platform that is globally available from NASA (https://software.nasa.gov/search/software/vesgen) and operates as a complex plug-in to ImageJ software (National Institutes of Health, Bethesda, MD)[15]. Binary (black/white) images of the blood vessels were obtained from either manual preparation or via deep learning processing, The region of interest (ROI) was obtained by image processing. These images were imported into VESGEN, resulting in automatic mapping and quantification of various vascular parameters. Parameters of interest included the following: (1) Tortuosity (Tv; length of vessel divided by the distance between the two endpoints of the vessel), (2) fractural dimension (Df; a ratio for determining the complexity of the given measurement), and (3) vessel area density (Av; density of total vascular area, Av = vascular area/ROI). Macrovascular vessels were defined as generations 1 to 5. Microvascular vessels were defined as generation 6 and greater.

Deep Learning

The deep learning approach used was RVGAN, short for retinal vessel generative adversarial network (GAN), programmed in Python using Tensorflow. More details on model training and operation are available at https://github.com/SharifAmit/RVGAN. CF imaging models were pretrained on the STARE dataset[16,17] due to their higher specificity than other pre-trained models. Images in the STARE dataset had 18.5 pixels per degree of field of view (FOV), while the images used in this study had 40.9 pixels per FOV degree. Using linear interpolation, fundus images were scaled down to match the STARE dataset resolution for correct segmentation. Imaging dimensions were verified during output measurement of VESGEN. The output binary images were scaled up linearly to match the original input image sizes and for comparison with the traditional segmentation. Custom model evaluation code was written in Python to handle scaling and application of the pretrained model using libraries from the SciPy stack.

The resulting binary segmentation images were cleaned in MATLAB R2021a by removing small, connected components. The fundus photograph region of interest (ROI) masks were eroded by 3 pixels and applied to the binary images to trim artifacts caused by model edge effects. A border of 3 pixels around the edge of the binary images was removed to trim the remaining edge artifacts.

Statistical Analysis

The Bland–Altman plot (Difference plots) was used as it compares two measurements of the same variable. The X-axis represents the mean of two measurements, and the Y-axis represents the difference between the two measurements[18]. Plotting difference versus mean aids in the examination of any potential relationship between measurement inaccuracy and real value. A Bland-Altman plot provides information on the differences in measurements between two methods, and any relationship between the differences and true values. To compare the same eye with FA and CF imaging, the right and left eyes were analyzed separately. Agreement between biometrics was examined by eye (right vs. left) using Bland-Altman plots with 2 (red) and 3 (green) standard deviation reference bounds using SAS Software 9.4 (Cary, NC). Points scattered, above and below zero (mean black line) indicate that there is no persistent bias toward one imaging modality over the other[19]. In contrast if values increase/decrease, while the difference increases/decrease in a way that a slope could be fit, this indicates strong evidence that these measures are not concordant. Bland-Altman plots does not provide information on which method is better but simple suggest if they are similar. All data for Bland-Altman is provided as mean±SD.

RESULTS

Subject`s Characteristics

FA and CF images of 15 eyes from 9 individuals were compared. Detailed clinical characteristics have been previously described[13]. The mean age of the subjects was 50, with the youngest age being 26 and the oldest 72 years old. Eight of the nine subjects (89%) were females, seven of which were Caucasian (77%).

Color fundus imaging of retinal vascular phenotype in PAH

CF images (Figure 1; first column) with 55-degree field of view were processed, and binaries for VESGEN input were formulated to identify areas of interest. CF images were also used to identify arteries and veins, resulting in an overlapping image where red represented arteries and blue represented veins (Figure 1; second column). The generational summary was analyzed separately for arteries (Figure 1; third column) and veins (Figure 1; 4th column). Increasing severity is shown from column A to column C.

Manual Segmentation: CF vs. FA

To determine whether CF images could be used as a viable alternative to FA imaging using retinas from individuals with PAH. We compared total (artery and veins) vessels, and artery only, in both Tv and Av , in FA and CF images. Along with the micro vessels of total (arteries and veins) vessels. Tv and Av have previously been shown to indicate the progression of retinal pathology in diabetic retinopathy (14) and spaceflight associated neuro-ocular syndrome (SANS) (20,21). The right eye and left eye were separated for VESGEN analysis.

Manual processing of FA images (Figure 2A) and manual processing of CF images (Figure 2B) were compared to better understand if Tv, a known hypertension characterization, can be identified via CF similarly to FA. Tv total vessels (arteries and veins) and arteries only, the key component of the vasculature affected by PAH were examined. Tv output between CF and Tv showed an equal scattering of points both above and below the red solid line (mean), suggesting both imaging techniques (CF and FA) can produce similar levels of for the analysis of Tv in both higher and lower ranges (Figure 2C, 0.021 ± 0.28 vs. 0.013 ± 0.024). When comparing FA and CF with respect to arteries only, some points are scattered below and above the mean line (red solid line), suggesting both image methods result in similar Tv both below the mean and above (Figure 2D, -0.008±0.016 vs -0.007±0.028). These findings showed that manually segmented CF and FA fundus images contain similar levels of vessel tortuosity.

To identify angiogenesis and proliferation by vascular density via the ROI Vessel area density (Av) was examined using total vessels (arteries and veins). When comparing total Av in FA and CF images (Figure 3A), points were scattered below and above the mean (solid red line), suggesting good concordance was observed between FA and CF (-0.051±0.006 vs. -0.057±0.024). Next, arteries only were examined separately. When comparing FA and CF with respect to arteries, only Av points were equally scattered both above and below the solid red line (mean), also suggesting that both imaging techniques can produce similar levels of arterial Av in both the left and right eyes (Figure 3B), 0.012±0.005 vs. 0.002±0.0016). These findings support that manually segmented CF and FA fundus images contain similar vascular densities.

Microvessels are commonly affected in many systemic vascular diseases so we examined the number of total microvessels (G≥6) detectable in (artery and veins) . When first comparing total microvessels (Figure 4A), points were present above and below the mean. However, comparing the two imaging methods resulted in a linear slope suggesting poor concordance between FA and CF imaging. In the right eyes, an equal scatters of points both above and below the mean (red solid line) suggests better concordance between FA and CF in the right eye than in the left eye (193.42±234.85 vs. 98.22±214.29). When comparing to arteries, similarly total vessels resulted in a linear slope suggesting the two image method outputs were not similar between FA and CF imaging. However the right eye suggest better concordance between FA and CF compared to the left eye due to the linear slope seen in the left eye (62.57±77.71 vs. 46.56±77.69).

CF manual segmentation vs CF deep learning segmentation

Due to the extended preparation time required for inputting manual binary images, we sought to explore potential solutions to speed up image preparation. Manually processed images (Figure 5A) and deep learning processed (Figure 5B) images were compared. Due to deep learning's inability to separate arterial and venous structures, total vasculature was assessed, and arterials were manually separated for comparison between processed arterial (Figure 5C) and deep learning identification of arteries (Figure 5D). Total tortuosity and fractal dimension were compared to determine if deep learning processing could detect structural changes for these parameters. With respects to Tv the left eye resulted in more points below the mean when comparing manual binary images prepared in CF and deep learning processing output suggesting one provided lower Tv levels compared to the other image method. This was also true of the right eye, indicating that one of the imaging method outputs for Tv based on VESGEN resulted in lower tortuosity levels and did not result in similar measures compared to the other method (Figure 6A -0.008 ± 0.025 vs 0.0008 ± 0.019). When comparing arterials similar to total vessels a greater number of points were above the mean suggesting one image method was greater in Tv compared to the other and did not result in similar measurements between manually processed CF image and deep learning processed CF image (Figure

6B 0.007 ± 0.032 vs. 0.013 ± 0.034). When comparison of Tv between manual CF and CF deep learning segmentation using Bland-Altman plots showed a liner slope suggesting the failure of both image methods to provide similar Tv levels.

When comparing fractural dimension (Df) in both manual and deep learning, imaging processing showed scattering among the plot, with most points near the mean (solid red line) in the left and right eye. This suggests both imaging methods can detect Df changes among the entire image (Figure 6C,-0.0063 ± 0.021 vs. -0.0089 ± 0.036). Nevertheless, in respect to arteries many points were scattered suggesting some similarity between manually CF and deep learning. However, the left eye resulted in a linear slope suggesting poor concordance of the left eye better concordance between FA and CF in the right eye (Figure 6D -0.0098 ± 0.023 vs. -0.00084 ± 0.025).

Next, we compared to deep learning processing ability to compare density to manual binary imaging. These finding showed that manually segmented CF and CF deep learning segmentation contain similar vascular structures. Av showed an unfavorable comparison between the two imaging methods showing scattering with most points falling above the mean, suggesting the two imaging methods are not concordant. One method results in higher Av measurement than the other method (Figure 6E -0.0108 ± 0.017 vs -0.014 ± 0.031). This remained true for Av of the arterial, which also suggested the two image methods were not concordant (Figure 6F -0.0052 ± 0.0096 vs. -0.0021 ± 0.011) Last we compared deep learning's ability to identify the same number of vessels as manual preparation. Most points are gathered above the mean (red line), suggesting that one image method results in a higher number of vessels than the other image method suggesting the imaging method did not result in similar output data (Figure 6G,-769.4±581.91vs -674.66±453.41). Arterials showed a poor similarlity between manual and deep learning process using CF (Figure 6H -359.7 ± 225.6 vs. -352.9 ± 169.5). In the comparison of Av and number between manual CF and CF deep learning segmentation using Bland-Altman plots showed a linear slope suggesting the failure of the two image methods to provide similar density and number of vessel.

DISCUSSION

In this study, we provide further validation that a non-invasive technique may be useful for early detection or serial monitoring in PAH. Using VESGEN to analyze the images, CF images detect retinal vascular changes similar to FA in PAH subjects. We show that CF is able to detect retinal Tv and changes in total vascular area (Av = vascular area/ROI), two parameters that are associated with diseases serverity in PAH subjects[13].

Our results suggest that similar clinical information can be obtained from CF and has the added advantage of being safer for patients. While FA and CF were not concordant in identifying microvessels numbers, FA and CF resulted in similar T_v and A_v. Due to the inability in CF to substitute for FA in monitoring microvascular diseases, using CF for diseases such as diabetic retinopathy may not be feasible. The second main finding of this study is that we identify deep learning as an approach to reduce image preparation time. Image processing segmentation combines algorithms that identify, refine, and extract features of interest from CF images.

The difference between the left and right eyes outcome in similarity of image methods was an unexpected discovery. The left eye often resulted in poor concordance in various vascular patterns between image methods, whereas the right eye had good and superior concordance. Notably, a 2018(22) investigation in early-stage systemic hypertension alterations in the retina intended to investigate choriocapillaris vasculature ocular/systemic variables. The eyes of 361 healthy people and 206 people with systemic hypertension were investigated in this study. They discovered that the right eye's choriocapillaris vascular density was substantially higher than the left eye's. The cause of vascular asymmetry in the left and right eyes remains unknown.

One proposed theory is that the ophthalmic arteries differ somewhat between the left and right eyes because the ophthalmic artery arises from the internal carotids. Unlike the left common carotid, the right common carotid artery comes from the brachiocephalic trunk rather than directly off the aorta.

VESsel GENerational (VESGEN) analysis produces colorized image maps with over 30 different quantitative data points. VESGEN is a user-friendly software already studied with FA and colonic vasculature imaging studies [14,15,23-25]. It has been through several revisions and upgrades, and the latest version released in 2021(version 1.11) offers the most reliable and accurate output parameters. VESGEN generates parameters based on retinal vessel segmentation algorithms and physiological branching rules[26,27].

A drawback of VESGEN is that it requires hours of manual preparation preimage for analysis by the software. This meticulous process includes manually tracing retinal vessels, identifying arterial and venous characteristics, formatting images to appropriate input settings, along with implementing several checkpoints to ensure quality during the process. This time-consuming effort essentially precludes VESGEN as a feasible tool to be utilized in clinical practice and is currently limited to research only. This has resulted in the need for an automated software with an ability to perform accurate vessel segmentation avoiding the laborious manual preparation process. Moreover, color fundus vessel segmentation is a notoriously challenging image processing problem. Numerous papers have been published over four decades attempting to solve the problem with varying degrees of success[28-30].

Deep learning models are implicitly programmed, requiring training examples consisting of pairs of CF images and their manually segmented vessels. During training, the model learns what combination of features are needed to result in correct segmentation. Deep learning programming is expected to be more viable for clinical practice. We use a pre-trained, two-scale generative adversarial network (GAN)[31] trained on images from the STARE project.

Deep learning processing could offer the benefit to VESGEN analysis in that it eliminates the laborious manual preparation efforts required for VESGEN inputs. Deep learning programming provided evidence of potential use in combination with VESGEN to become a feasible and highly sensitive tool for the visualization of the retina and could potentially be incorporated into clinical practice. However, while the use of deep learning will speed up the process of image preparation, a major limitation is the inability to separate arteries and veins, which can quickly be done using manual processing. Deep learning also lacks the ability to assess tortuosity and vessel area density of both total and arterial compared to images processed using manual input. This is likely due to the lack of ability of deep learning to identify smaller vessels. Deep learning showed the ability to define similar structural changes in large vessels seen as fractal dimension (Df) across the retina compared to manual tracing of CF imaging.

While this proof-of-concept study provides insight into the potential use of CF imaging in future studies of pulmonary vascular diseases, our study has the limitations of including a small number of subjects. VESGEN in conjunction with deep learning processing, has great potential for speeding the preparation of images and potentially making this approach feasible for future clinical use, specifically aiding in earlier disease detection while providing clinicians the ability for easy longitudinal monitoring of retinal vascular changes that are both objective and comparable for each subject. This combination may also improve patient safety by eliminating invasive imaging techniques, improving diagnostic power, and faster and cost-efficient examinations.

CONCLUSION

Based on our results, we identified several key advantages of utilizing CF paired with VESGEN analysis as a retinal imaging modality over FA with manual input of images. CF is non-invasive imaging modality. It possesses the ability, alongside image processing segmentation, to provide valuable insight into vascular patterns of vessel generations 1-5 to understand systemic manifestations of PAH in the eye repeatedly and rapidly in the clinic setting.

ACKNOWLEDGMENTS

The authors acknowledge and thank the subjects that participated in this study and their families. Along with Alexander Decubellis and Kalah Ozimba for the help during the preparation of the images. The authors acknowledge the resources provided by the University of Alabama at Birmingham IT-Research Computing group for high-performance computing (HPC) support and compute time on the Cheaha cluster. The research was supported by the Department of Veterans Affairs Merit Review Award 1I01BX002042 (TL), NIH 1R01HL144727-01A1 (TL); NIH R01 HL141268 (CEV), P20 GM103652 (CEV), NASA Vascularized Tissue Centennial Challenge (ML), Space Radiation Program (ML), and the Human Research Program (ML).

REFERENCE

1. Wagner SK, Fu DJ, Faes L, et al. Insights into Systemic Disease through Retinal Imaging-Based Oculomics. Transl Vis Sci Technol. 2020;9(2):6. doi:10.1167/tvst.9.2.6

2. Schmitz-Valckenberg S, Holz FG, Bird AC, Spaide RF. Fundus autofluorescence imaging: review and perspectives. Retina (Philadelphia, Pa). 2008;28(3):385-409. doi:10.1097/IAE.0b013e318164a907

3. Besenczi R, Tóth J, Hajdu A. A review on automatic analysis techniques for color fundus photographs. Comput Struct Biotechnol J. 2016;14:371-384. doi:10.1016/j.csbj.2016.10.001

4. Salz DA, Witkin AJ. Imaging in diabetic retinopathy. Middle East Afr J Ophthalmol. 2015;22(2):145-150. doi:10.4103/0974-9233.151887

5. Kornblau IS, El-Annan JF. Adverse reactions to fluorescein angiography: A comprehensive review of the literature. Surv Ophthalmol. 2019;64(5):679-693. doi:10.1016/j.survophthal.2019.02.004

6. Xu K, Tzankova V, Li C, Sharma S. Intravenous fluorescein angiography-associated adverse reactions. Can J Ophthalmol. 2016;51(5):321-325. doi:10.1016/j.jcjo.2016.03.015

7. Yannuzzi LA, Rohrer KT, Tindel LJ, et al. Fluorescein angiography complication survey. Ophthalmology. 1986;93(5):611-617. doi:10.1016/s0161-6420(86)33697-2

8. Musa F, Muen WJ, Hancock R, Clark D. Adverse effects of fluorescein angiography in hypertensive and elderly patients. Acta Ophthalmol Scand. 2006;84(6):740-742. doi:10.1111/j.1600-0420.2006.00728.x

9. McAllister RG. Hypertensive crisis and myocardial infarction after fluorescein angiography. South Med J. 1981;74(4):508-509. doi:10.1097/00007611-198104000-00040

10. Lira RPC, Oliveira CL de A, Marques MVRB, Silva AR, Pessoa C de C. Adverse reactions of fluorescein angiography: a prospective study. Arq Bras Oftalmol. 2007;70(4):615-618. doi:10.1590/S0004-27492007000400011

11. Mainster MA, Turner PL. Retinal examination and photography are safe...is anyone surprised? Ophthalmology. 2010;117(2):197-198. doi:10.1016/j.ophtha.2009.11.046

12. Aronson JK. Meyler’s Side Effects Of Drugs. Elsevier; 2015:7674.

13. DuPont M, Lambert S, Rodriguez-Martin A, et al. Retinal vessel changes in pulmonary arterial hypertension. Pulm Circ. 2022;12(1):e12035. doi:10.1002/pul2.12035

14. Parsons-Wingerter P, Radhakrishnan K, Vickerman MB, Kaiser PK. Oscillation of angiogenesis with vascular dropout in diabetic retinopathy by VESsel GENeration analysis (VESGEN). Invest Ophthalmol Vis Sci. 2010;51(1):498-507. doi:10.1167/iovs.09-3968

15. Vickerman MB, Keith PA, McKay TL, et al. VESGEN 2D: automated, user-interactive software for quantification and mapping of angiogenic and lymphangiogenic trees and networks. Anat Rec (Hoboken). 2009;292(3):320-332. doi:10.1002/ar.20862

16. Hoover A, Kouznetsova V, Goldbaum M. Locating blood vessels in retinal images by piecewise threshold probing of a matched filter response. IEEE Trans Med Imaging. 2000;19(3):203-210. doi:10.1109/42.845178

17. Hoover A, Goldbaum M. Locating the optic nerve in a retinal image using the fuzzy convergence of the blood vessels. IEEE Trans Med Imaging. 2003;22(8):951-958. doi:10.1109/TMI.2003.815900

18. Giavarina D. Understanding Bland Altman analysis. Biochem Med (Zagreb). 2015;25(2):141-151. doi:10.11613/BM.2015.015

19. Kalra A. Decoding the Bland–Altman plot: Basic review. J Pract Cardiovasc Sci. 2017;3(1):36. doi:10.4103/jpcs.jpcs_11_17

20. Vyas RJ, Young M, Murray MC, et al. Decreased Vascular Patterning in the Retinas of Astronaut Crew Members as New Measure of Ocular Damage in Spaceflight-Associated Neuro-ocular Syndrome. Invest Ophthalmol Vis Sci. 2020;61(14):34. doi:10.1167/iovs.61.14.34

21. Taibbi G, Young M, Vyas RJ, et al. Opposite response of blood vessels in the retina to 6° head-down tilt and long-duration microgravity. NPJ Microgravity. 2021;7(1):38. doi:10.1038/s41526-021-00165-5

22. Takayama K, Kaneko H, Ito Y, Kataoka K, Iwase T, Yasuma T, et al. Novel Classification of Early-stage Systemic Hypertensive Changes in Human Retina Based on OCTA Measurement of Choriocapillaris. Sci Rep. 2018 Oct 11;8(1):15163

23. McKay TL, Gedeon DJ, Vickerman MB, et al. Selective inhibition of angiogenesis in small blood vessels and decrease in vessel diameter throughout the vascular tree by triamcinolone acetonide. Invest Ophthalmol Vis Sci. 2008;49(3):1184-1190. doi:10.1167/iovs.07-1329

24. Lagatuz M, Vyas RJ, Predovic M, et al. Vascular patterning as integrative readout of complex molecular and physiological signaling by vessel generation analysis. J Vasc Res. 2021;58(4):207-230. doi:10.1159/000514211

25. Parsons-Wingerter P, Reinecker H-C. For Application to Human Spaceflight and ISS Experiments: VESGEN Mapping of Microvascular Network Remodeling during Intestinal Inflammation. Gravit Space Biol Bull. 2012;26(2):2-12.

26. Teng T, Lefley M, Claremont D. Progress towards automated diabetic ocular screening: a review of image analysis and intelligent systems for diabetic retinopathy. Med Biol Eng Comput. 2002;40(1):2-13.

27. C haracterization of changes in blood vessel width and tortuosity in retinopathy of prematurity using image analysis.

28. Mookiah MRK, Hogg S, MacGillivray TJ, et al. A review of machine learning methods for retinal blood vessel segmentation and artery/vein classification. Med Image Anal. 2021;68:101905. doi:10.1016/j.media.2020.101905

29. Abdulsahib AA, Mahmoud MA, Mohammed MA. Comprehensive review of retinal blood vessel segmentation and classification techniques: Intelligent solutions for green computing in medical images, current …. … Modeling Analysis in …. 2021.

30. Chen C, Chuah JH, Raza A, Wang Y. Retinal Vessel Segmentation Using Deep Learning: A Review. IEEE Access. 2021.

31. Kamran SA, Hossain KF, Tavakkoli A, Zuckerbrod SL, Sanders KM, Baker SA. RV-GAN: Segmenting Retinal Vascular Structure in Fundus Photographs Using a Novel Multi-scale Generative Adversarial Network. In: de Bruijne M, Cattin PC, Cotin S, et al., eds. medical image computing and computer assisted intervention – MICCAI 2021: 24th international conference, strasbourg, france, september 27 – october 1, 2021, proceedings, part VIII. Vol 12908. Lecture notes in computer science. Cham: Springer International Publishing; 2021:34-44. doi:10.1007/978-3-030-87237-3_4

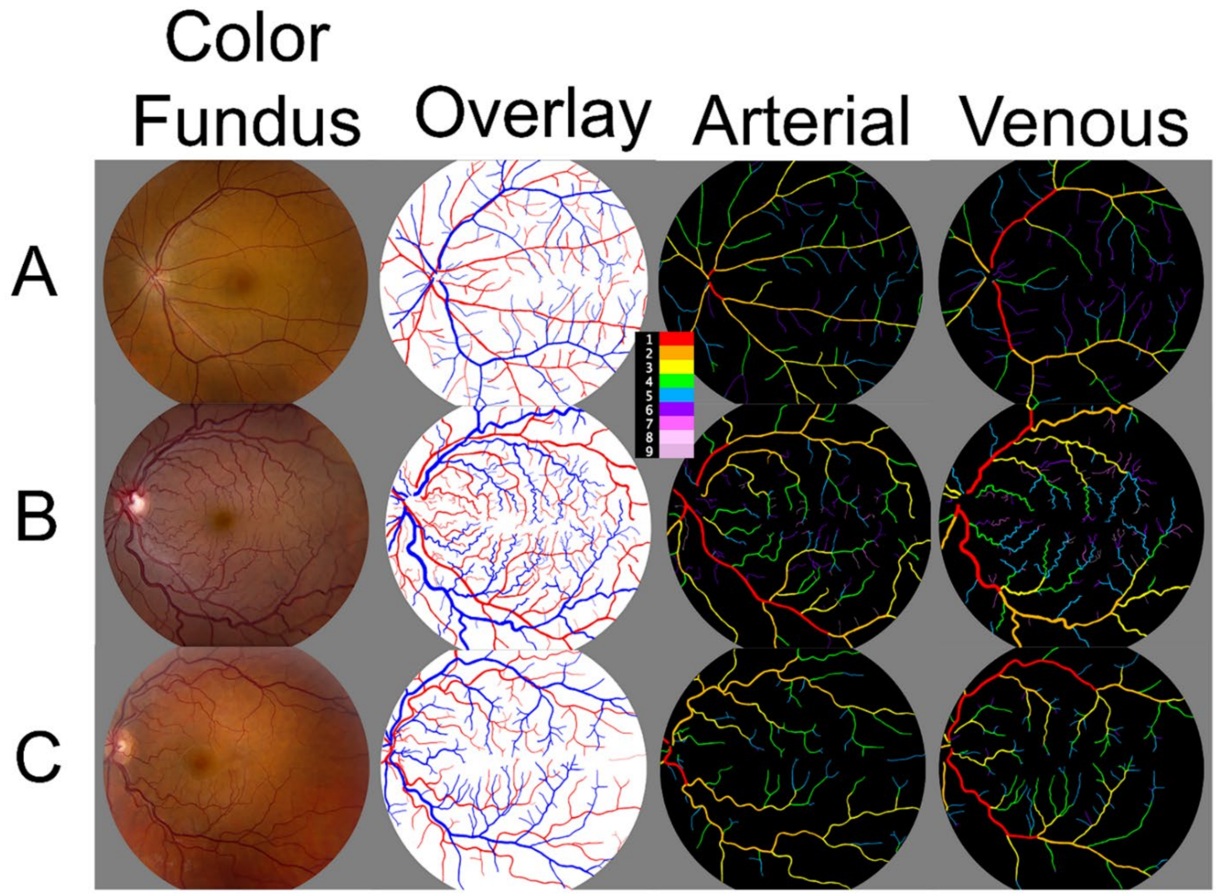

Figure 1: Representative output image of VESGEN analysis of the retinal vessels from PAH subjects. VESGEN imaging maps with a 55-degree imaging resolution of the right retina from a (A): 51year-old female PAH subject; (B) 36-year-old female PAH subject; (C) 72-year-old female PAH subject. First Column: Color fundus (CF) output image. Second column: Overlap of arteries (red) and veins (blue) generated manually. Third and fourth columns: Branching generation of arteries and veins, respectively, generated by VESGEN output. Legend (center) identifies branching generations 1-9.

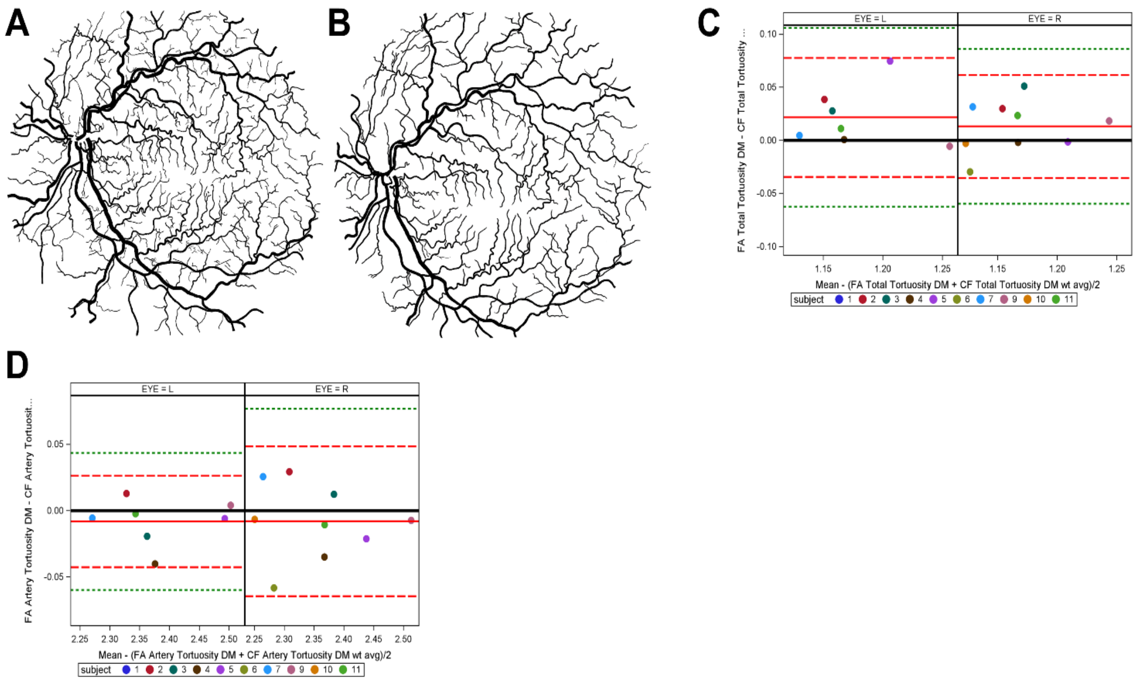

Figure 2: Fluorescein angiography and color fundus comparisons of vascular tortuosity

Fluorescein angiography (FA) binary images (A) and (B) color fundus (CF) prepared manually from the retina of a 45-year-old female with PAH. Right and left eyes were split on Bland-Altman plot where FA VESGEN output was compared to CF VESGEN output for total tortuosity, showing scatter of points suggesting similar results between imaging methods (C), and total artery tortuosity showing scatter of points suggesting similar results between image methods (D). The mean of the measures (x axis) and the difference of the measures (y axis). The reference line of no difference at 0 (solid black), a reference line at the mean of the difference in solid red (observed actual mean), a reference line at +/- 2SD of the mean of the difference in dashed red, and a reference line at +/-3SD of the mean of the differences in dashed green (C-D).

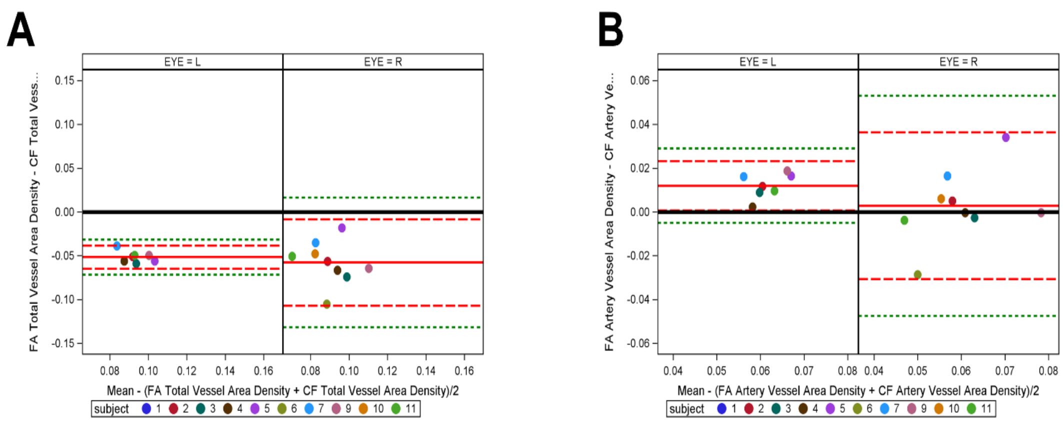

Figure 3: Fluorescein angiography and color fundus comparisons in vessel area density.

(A) Right and left eyes were split on Bland-Altman plot where fluorescein angiography (FA) VESGEN output was compared to color fundus (CF) VESGEN output for total vessel area density. Scattered points for both left and right eye data suggests no difference between imaging methods. (B) Total artery vessel area density with scattered points suggests no difference between imaging methods with points gather near mean. Plots show similarities between FA and CF imaging among total Av and total artery Av suggesting that CF can be used as a safer method for vascular change monitoring. The mean of the measures (x axis) by the difference of the measures (y axis). The reference line of no difference at 0 is the solid black, a reference line at the mean of the difference in solid red (observed actual mean), a reference line at +/- 2SD of the mean of the difference in dashed red, and a reference line at +/-3SD of the mean of the differences in dashed green.

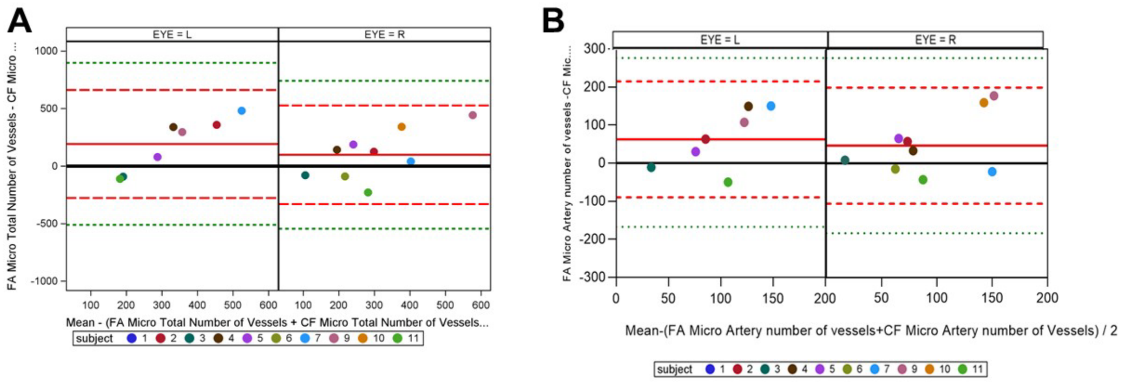

Figure 4: Fluorescein angiography and color fundus comparisons in microvessel number.

Right and left eyes were split on Bland-Altman plot where fluorescein angiography (FA) VESGEN output was compared color fundus (CF) VESGEN output for total number of microvessels (A) and total number of microvessels of the arteries(B). Plots show differences between FA and CF imaging in micro vessels of total vessels due to the linear scattering of the points. The mean of the measures (x axis) and the difference of the measures (y axis). The reference line of no difference at 0 (solid black), a reference line at the mean of the difference in solid red (observed actual mean), a reference line at +/- 2SD of the mean of the difference in dashed red, and a reference line at +/-3SD of the mean of the differences in dashed green.

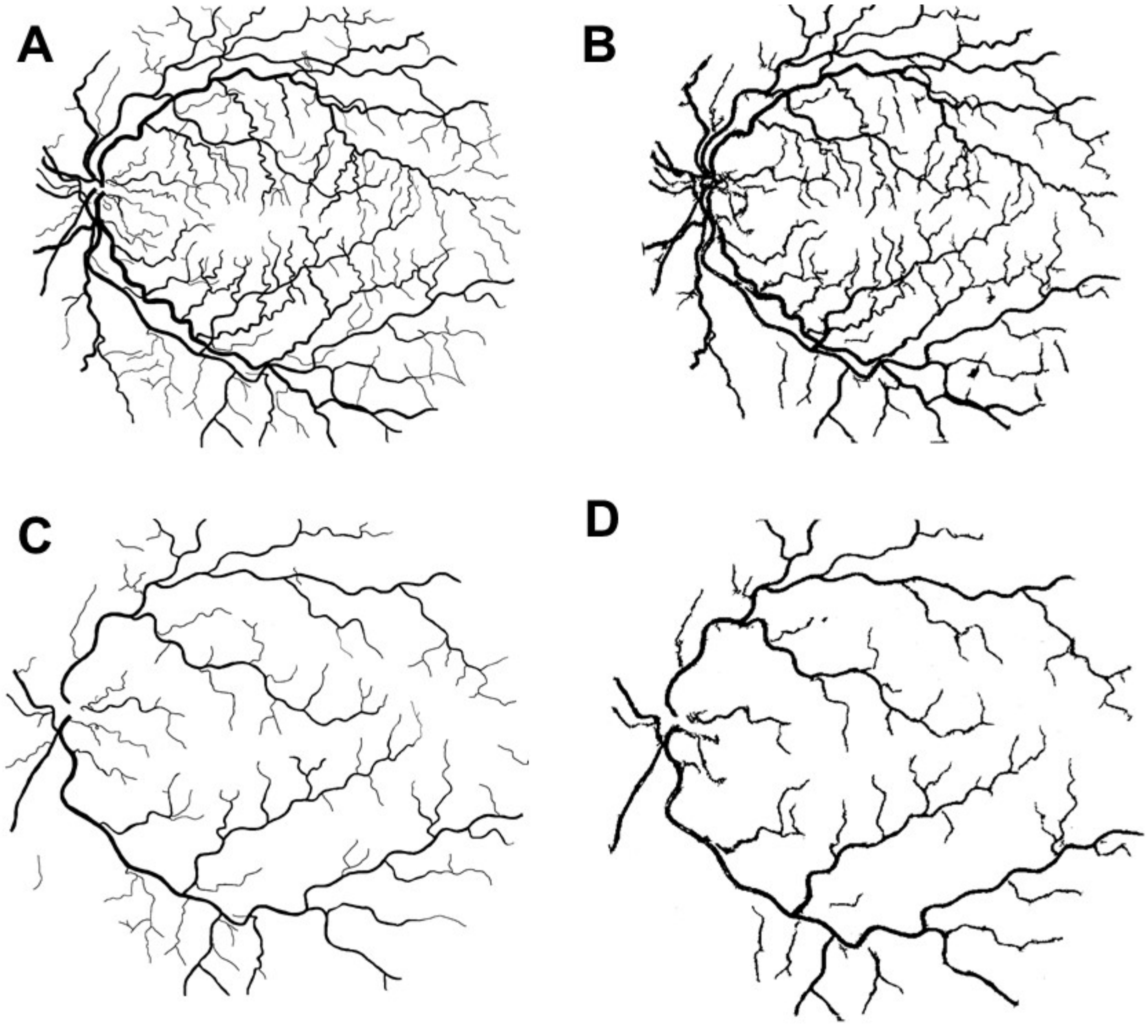

Figure 5: Binary images of manual and deep learning

CF binary images prepared (A) manually and by (B) deep processing using the retina of a 45-year-old female with PAH. CF binary images of the artery prepared (C) manually and by (D) deep processing using the retina of a 45-year-old female with PAH.

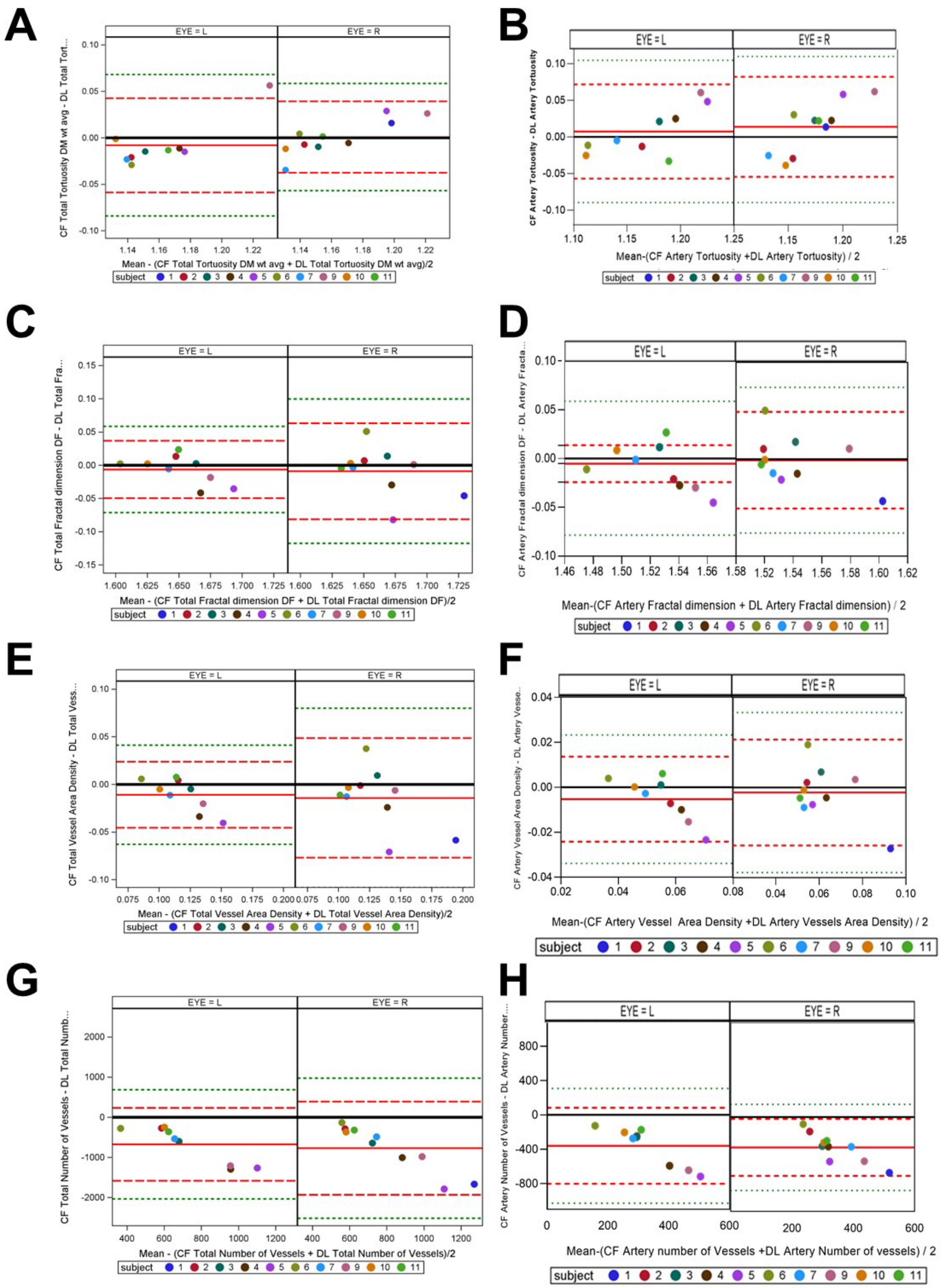
A
EYE = L
EYE = R
CF Total Tortuosity DM wt avg - DL Total Tort...
Mean - (CF Total Tortuosity DM wt avg + DL Total Tortuosity DM wt avg)/2
subject 1 2 3 4 5 6 7 9 10 11
B
EYE = L
EYE = R
CF Artery Tortuosity - DL Artery Tortuosity
Mean-(CF Artery Tortuosity +DL Artery Tortuosity) / 2
subject 1 2 3 4 5 6 7 9 10 11
C
EYE = L
EYE = R
CF Total Fractal dimension DF - DL Total Fra...
Mean - (CF Total Fractal dimension DF + DL Total Fractal dimension DF)/2
subject 1 2 3 4 5 6 7 9 10 11
D
EYE = L
EYE = R
CF Artery Fractal dimension DF - DL Artery Fracta...
Mean-(CF Artery Fractal dimension + DL Artery Fractal dimension) / 2
subject 1 2 3 4 5 6 7 9 10 11
E
EYE = L
EYE = R
CF Total Vessel Area Density - DL Total Vess...
Mean - (CF Total Vessel Area Density + DL Total Vessel Area Density)/2
subject 1 2 3 4 5 6 7 9 10 11
F
EYE = L
EYE = R
CF Artery Vessel Area Density - DL Artery Vesse...
Mean-(CF Artery Vessel Area Density +DL Artery Vessels Area Density) / 2
subject 1 2 3 4 5 6 7 9 10 11
G
EYE = L
EYE = R
CF Total Number of Vessels - DL Total Numb...
Mean - (CF Total Number of Vessels + DL Total Number of Vessels)/2
subject 1 2 3 4 5 6 7 9 10 11
H
EYE = L
EYE = R
CF Artery Number of Vessels - DL Artery Number...
Mean-(CF Artery number of Vessels +DL Artery Number of vessels) / 2
subject 1 2 3 4 5 6 7 9 10 11

Figure 6: Manuel and deep learning comparisons

Right and left eyes were split on Bland-Altman plot where color fundus (CF) VESGEN output was compared deep learning VESGEN output for total tortuosity (A), arterial tortuosity (B), total fractal dimension (C), arterial fractal dimension (D),total vessel area density (E), arterial vessel area density (F), total number of vessels (G) and arterial number of vessels (H). Plots show difference between FA and CF imaging among total vessels (Tv) (A), total tortuosity (C), and total number of vessels due to the liner scattering of the points. Plots show similarities between FA and CF imaging among total Df. This suggesting CF can be used as a safer method for vascular change monitoring. The mean of the measures (x axis) by the difference of the measures (y axis). The reference line of no difference at 0 is the solid black, a reference line at the mean of the difference in solid red (observed actual mean), a reference line at +/- 2SD of the mean of the difference in dashed red, and a reference line at +/-3SD of the mean of the differences in dashed green.

CHAPTER 4

DISCUSSION

Summary

Chapter 2- Associations between PAH and vasculature changes

In addition to the eye, significant morphological alterations occur in nailfold capillaries and sublingual vasculature have been reported (105,111). Nailfold capillaroscopy shows lower capillary density in individuals with IPAH and scleroderma PAH compared to healthy controls (102,105,111). In addition, individuals with PAH showed a lower sublingual blood flow index and increased tortuosity and curvature compared to healthy sex-matched control participants (106).

The key findings of this study show that, regardless of the PAH subtype, tortuosity increases in PAH participants compared to controls (CTD and non-CTD). This association varied by age, with younger PAH patients showing higher signs of vascular tortuosity. Retinal vascular adaptations during PAH showed increased retinal Tv and reduced Av. Use of images with a different magnification limited our comparison of vascular patterns to merely tortuosity, which is scale-invariant.

When compared to controls, PAH patients had more tortuosity in their retinal arteries and veins. Compared to controls, PAH patients without connective tissue disease exhibited the greatest degree of retinal tortuosity.

Changes in retinal vascular density have been identified as a potential biomarker in various disorders, including Alzheimer's disease, moderate cognitive impairment, and diabetes mellitus (29,112,113). Most of the population in this study had identical bilateral vascular alterations; however, there were several cases where OS and OD retinas had a different vascular pattern. Differences in Tv and vascular density between the eyes of the same person varied from 0.02 to 0.05 pixel/pixel and 0.01–0.03 $pixel^2/pixel^2$, respectively. The Tv of our control subjects varied from around 1.11 to 1.15 pixel/pixel. We take this observation to imply that prolonged increases in PVR may be the cause of retinal vascular remodeling, or that retinal vascular pathology occurs concurrently with pulmonary vascular disease. However, additional studies are needed to confirm our findings. PAH patients have aberrant retinal vasculature compared to controls, and retinal abnormalities may correspond with clinical outcome markers in PAH. These findings imply that PAH patients should be evaluated for increased vessel density and Tv ocular pathology.

In comparison, VESGEN has previously been used to examine vascular changes of both DR (14) and spaceflight-associated neuro-ocular syndrome (SANS)(114), resulting in different changes not seen in PAH retinas. In the first cross-sectional investigation, 15 eyes with DR were assessed using FA and graded using modified Early Treatment Diabetic Retinopathy Study criteria. This study aimed to examine branching patterns of the arterial and venous trees as diabetic retinopathy progressed. The main finding of this study was the oscillation (alternation) of increasing and decreasing density of tiny blood vessels, as mapped and measured by vessel length density and number density, in both arterial and venous trees during diabetic retinopathy from moderate to severe NPDR/early PDR. Throughout the evolution of diabetic retinopathy, the density of bigger vessels (G1-5) remained essentially constant, but the diameters of larger vessels (Dv1-5) grew slightly but continuously (14,115). During our examination of PAH, no changes in vessel length or number density were determined. The second study, which involved SANS (also known as visual impairment and intracranial pressure (VIIP) syndrome),found a combination of observations and symptoms observed in astronauts who have undergone long duration space flight (LDSF) missions in microgravity conditions.

SANS is characterized clinically by retinal folds unilateral or bilateral optic disc edema, globe flattening, choroidal, retinal folds, hyperopic refractive error changes, and nerve fiber layer infarcts. All of which are common results associated with structural alterations on ocular and orbital imaging examinations (116).

In this study, it was examined that prolonged headward fluid changes in SANS were mediated by retinal vascular remodeling, notably by smaller arteries. Only 11 of 16 retinas for arteries and veins show significant postflight declines in Df, Lv, and smaller vessels. The highest vascular reductions were observed in the single retina with clinical signs of SANS in the form of choroidal folds and optic disc edema. A unique vascular pathology index determined that declines in vascular density from Df and vessel length ranged from minor to significant in the remaining 15 retinas (114).

Neither of these studies correlated VESGEN parameters to known diagnostic measurement such as glycation hemoglobin (HbA1c) test (DR) or intracranial pressure (ICP; SANS). Damage to tiny blood vessels in the retina, kidney, and peripheral nerves is caused by glycation, where higher quantities of glucose expedite the process. This results in complications of diabetes, such as diabetic retinopathy, nephropathy, and neuropathy, as well as the avoidable outcomes of blindness, dialysis, and amputation (57). Unlike PAH, neither of these studies mentioned changes in Tv or Av of either the small or larger vessels, suggesting these changes may be unique to PAH and that each disease may have its own “eye print”.

Our PAH subjects showed changes in the larger vessel, which is a unique finding in PAH subjects that was not seen in either the DR or SANS studies. Arteries and other critical vascular irregularities, such as microaneurysms, are of the utmost importance for better longitudinal patient assessment (115). VESGEN allows minor detection changes that otherwise would be missed during a routine eye examination, allowing physicians an additional tool for monitoring the progression of diseases.

The first known study to show that ocular abnormalities preceded PAH exacerbation was in 2012. In this study, a 28-year-old female with PAH for three years exhibited impaired vision and metamorphopsia in the right eye, showing no prior ocular or medical history of the individual. FA and CF images revealed normal choroidal and retinal perfusion, scattered microaneurysms, and patches of minor capillary leakage in both eye. These results were consistent with higher systemic venous pressure and indicated PAH development. A 2017 study by Watanabe et. al. (103),(79) showed the presence of abnormal episcleral vessels in patients with familial PAH with bone morphogenetic protein receptor type II mutations, a genetic cause of PAH, and unaffected carriers before the development of PAH(103). Our results expand on these findings by revealing that retinal arterial Tv and density correlate with disease parameters in a well-characterized PAH population. Changes in ScVO2 or SvO2 may induce angiogenesis by activating hypoxia-inducible factors, resulting in increased retinal vascular density.

Thus, it was concluded that retinal abnormalities may correspond with established clinical outcome markers in PAH. These findings imply that PAH patients should be evaluated for ocular pathology and that retinal abnormalities may correlate with the severity of the pulmonary vascular disease.

Chapter 3- Manuel and deep learning imaging method

Systemic diseases such as diabetes, sickle cell, and systemic hypertension can benefit from retinal vascular imaging for diagnosis and management. Although commonly employed as a diagnostic and screening tool, FA is an invasive technique that has been linked to a 1-22 percent risk of adverse events. Often resulting in nausea, vomiting, gastrointestinal disturbance, and urticarial. Therefore, given these issues, non-invasive approaches for detecting retinal vascular alterations without losing picture quality is an unmet need. CF generates a colorized image with a fundus camera with no reports of photic injuries from normal fundus photography, in contrast to the adverse effects linked with FA imaging. CF also provides a user-friendly procedure normally accomplished in minutes in contrast to FA, which takes up to an hour to complete. Chapter 3 sought to demonstrate that CF utilized in people with PAH, in conjunction with VESGEN analysis as a retinal imaging modality, has advantages over FA with manual picture input.

This chapter identified a non-invasive approach for early detection or serial monitoring of PAH. The utilization of CF imaging in conjunction with VESGEN detected retinal vascular alterations in PAH patients similar to what was found with FA images. CF detected retinal Tv and changes in total vascular area (Av = vascular area/ROI), which have been shown to predict pulmonary function in PAH patients. These findings imply that CF can provide comparable clinical information while being safer. While FA and CF did not recognize comparable microvessel counts, they agreed on Tv and Av. However, bigger vessels heavily weigh the overall vessel area density. Because of this, CF cannot be used to replace FA in monitoring microvascular disorders such as diabetic retinopathy.

One unexpected finding was the difference between the left and right eye. In several vascular patterns, the left eye showed poor concordance, while the right eye resulted in good and better concordance. Interestingly, a 2018 (69) study in early-stage systemic hypertensive changes in the retina sought to explore ocular/systemic factors of the choriocapillaris vasculature. In this study, eyes from 361 controls and 206 individuals with systemic hypertension were examined. They found that choriocapillaris vessel density of the nasal area of the right eye was significantly larger than the left eye.

In contrast, vessel density in the temporal area of the left eyes was larger than right. Vessel length in the total area of the left eye was longer than the right eye (117). In addition, Ruiz-Medrano et al., showed an asymmetry in normative macular choroidal thickness, with right eyes having a thicker macular nasal choroid layer than left eyes (118). While the etiology of vascular asymmetry between the left and right eyes is unknown. One suggested theory is that the ophthalmic arteries may be slightly different between the left and right eyes, as the ophthalmic artery arises from the internal carotids, and these are different. The right internal carotid artery arises from the brachiocephalic trunk rather than coming directly from the aorta as does the left internal carotid.

One disadvantage in this study was the use of VESGEN manual preparation prior to analysis by the program. VESGEN is a NASA based software that maps and quantifies major vessel parameters such as the ones used in chapters 2 and 3 . The rigorous manual procedure entails tracing retinal veins, detecting arterial and venous features, formatting photos to acceptable input settings, and executing multiple quality checks. This time-consuming approach effectively eliminates VESGEN as a viable tool for clinical practice, and it is now restricted to research usage. This has led in the demand for automated software capable of performing precise vessel segmentation without the time-consuming human preparation procedure.

Previously VESGEN has been used in several studies (14,47–49), including a preliminary methodological study, where VESGEN 2D was used to investigate the progression of diabetic retinopathy (DR). The main finding of this study was the oscillation (alternation) of increasing and decreasing density of tiny blood vessels in both arterial and venous trees as diabetic retinopathy progressed from mild to extremely severe NPDR/early PDR. The smaller microvessel density improved from VRS1 to VRS2, reduced from VRS2 to VRS3, and increased again from VRS3 to VRS4, as assessed by VESGEN with high statistical confidence. Although the progressive change was consistently favorably associated between arterial and venous trees, arterial remodeling dominated the first two phases of increasing vascular density (VRS1 to VRS2 and VRS3 to VRS4) (14). In addition, the density of bigger vessels (G 1–5) remained largely constant during the evolution of diabetic retinopathy, whereas the diameters of larger vessels (D v1–5) grew slightly but regularly. Based on VESGEN finding the oscillation between angiogenesis and vascular dropout with diabetic retinopathy progression shows that the diabetic retina retains the ability to restore a normal vascular phenotype to some extent during the early stages of retinopathy (14).

The second significant outcome of this study is that deep learning reduces VESGEN picture preparation time compared to standard image processing. Image segmentation is the combination of algorithms that detect, refine, and extract aspects of interest from CF pictures. Deep learning processing may assist VESGEN analysis by eliminating the time-consuming manual preparation necessary for VESGEN inputs. Deep learning programming shown some promise for usage in conjunction with VESGEN to create a practical and extremely sensitive tool for retina imaging that may potentially be implemented into clinical practice. When compared to images processed with manual input, deep learning also lacks the capacity to detect tortuosity and vessel area density. Compared to the manual tracing of CF imaging, deep learning demonstrated the capacity to characterize identical structural changes in big vessels as a fractal dimension (Df) across the retina. This is most likely due to deep learning's inability to detect smaller vessels.

Based on our findings, we believe that using CF in conjunction with VESGEN analysis as a retinal imaging modality has advantages over FA with manual picture input. While CF is a safer, non-invasive imaging technique, it also can provide helpful insight into systemic manifestations of PAH in the eye when combined with image processing segmentation. Additional investigation is needed to fully understand CF imaging's potential and capabilities as a replacement for FA imaging in other systemic disorders.

LIMITATIONS

The studies in this dissertation have several limitations. First, a standard limitation among these chapters was the small population size. In Chapters 2 and 3, population size of the disease group was limited due to the rarity of pulmonary arterial hypertension, which only affects about 50 people per million each year. Due to this limitation, compiling a larger sample size becomes difficult. Inclusion of PH individuals as a whole regardless of subgroup (Group 2 and 3 PH) would have resulted in extra confounders such as age, smoking, obstructive sleep apnea, diabetes mellitus, and cardiovascular disease. Limiting our population group to those with PAH limited any factors associated with retinal abnormalities.

Ideally, 40 distinct patient specimens should be chosen to encompass the procedure's whole operating range and represent the disease spectrum (119). The total quantity of specimens tested is less essential than their quality. The quality of the experiment and the estimates of systematic errors will depend more on obtaining a diverse set of test results than a large number of test results. The key advantage of a large population is that it detects individual patient samples whose findings differ due to interferences in an individual sample matrix. This is of importance when the new approach employs a different chemical process or a different measuring mechanism (120).

Second, in Chapter 2, control images were acquired at a higher resolution than PAH images (Chapter 2, figure 1). We took a pragmatic approach in this chapter and leveraged images from another study cohort. Unfortunately, this did limit our examination of vascular patterns compared to control to only tortuosity, which is scale-invariant.

Third, one disadvantage of VESGEN is that it takes hours of manual preparation prior to picture processing by the program. This rigorous procedure entails manually tracing of retinal vessels, detecting arterial and venous features, formatting acceptable input settings, and executing multiple quality checks. This time-consuming process effectively eliminates VESGEN as a viable tool for clinical use. In addition, the lack of reproducibility while manually preparing an image can result in fluctuation of results, and CF imaging segments could not automatically separate arteries and veins.

In deep learning, also known as machine learning, reproducibility means running an algorithm on different datasets and getting the same (or similar) results on other projects (121). This has resulted in the requirement for an automated software capable of performing precise vessel segmentation without the time-consuming human preparation procedure. Reproducibility can have a variety of connotations, particularly when it comes to computational methodologies. Reproducibility, repeatability, and replicability are related concepts used in different circumstances, with slightly different meanings. The capacity to recreate results using the original researchers' data, tools and parameters is referred to as reproducibility. The capacity to get the same results with new data is referred to as replication (122). The capacity to replicate a published analytic procedure and obtain the same findings is referred to as repeatability. As machine learning continues to impact more healthcare choices, it becomes increasingly important to ensure that the basis on which these technologies are constructed are reproducibility, repeatability, and replicability. This means that computer intelligence is solely dependent mainly on the training material provided by the user. (123).

Fourth, the Bland-Altman plot used in Chapter 3 does not detail which method is better but only suggest if differences or similarities are found between the two methods. It measures the bias and provides a range of agreement that includes 95 percent of the discrepancies between one measurement and the other. This is because the line of equality is not inside the confidence interval of the mean difference. Nonetheless, only analytical, biological, or clinical aims can determine if the agreement interval is too large or too small for our specific purposes. The ideal purpose for using Bland-Altman plot would be to determine the boundaries of maximum tolerable discrepancies (anticipated limits of agreement), based on physiologically relevant criteria (124,125).

Bland –Altman plots, also known as difference plot is used when two techniques are supposed to agree one-to-one. These disparities should be distributed around the line of zero differences, with half above and half below. Any significant variances will stand out and bring attention to those specimens whose results require confirmation through repeat measurements (120,124). In contrast to comparison (similarity), plots which are used when the one-to-one agreement is not expected. As points are amassed, a visual line of best fit should be made to demonstrate the broad link between the approaches and aid in identifying discrepancies (120).

FUTURE DIRECTION

This work has established the ability of retinal imaging in FA and CF in combination with VESGEN as a valuable tool for monitoring ocular pathology and retinal vascular abnormalities of various diseases. This work has shown that larger vessel changes are unique to PAH, while microvessel changes appear more relevant to DR. The ideal next step in this experiment is to validation this study as a potential diagnostic tool for PAH. In order to achieve this, a validation cohort, or a set of patients also exhibiting PAH with a similar association and functional class should be examined. This cohort should be derived from a different location (different location/university), including a control group and different age groups and ethnicity. Each subject should be examining every 6 months for follow up examination to detect change. Each examination would include a retinal scan (126) and/or blood draw. This retina scan of a color fundus image may quickly be taken using a smart phone (126). Indirect ophthalmoscopy and the newest smartphone fundus photography both operate on the same principles. The flashlight on a smartphone is used as a light source or illumination system. After adjusting the filming distance, the smartphone camera focuses on an inverted image of the retina (126). A portable, cost-effective, affordable, and practical method for retinal imaging is smartphone fundus photography. The novice can become proficient in this method with practice and the use of smartphone camera applications made for this purpose. This images can then be applied to the newest VESGEN 1.11, which offers an automated segmentation of binary vascular patterns from grayscale photos using AI/machine learning and other computational breakthroughs (47,126,127). Ideally this entire process from acquiring images to binarizing images and finally generating analysis should result in completion in about two to three hours per image(47).

To compliment the retinal scans, systemic marker could be measured. These markers include keratinocyte growth factor (KGF) (128), Vascular endothelial growth factor (VEGF) (129), thrombospondin-1 (TSP-1) (130) and circulating angiogenic cells (CAC) (131) all of which are markers of angiogenesis or the growth of new vessels from pre-existing vessels. This can potentially provide information on new vessels forming in the retina, which in return can suggest changes in vessel area density.

KGF is a paracrine stimulator of proliferation and migration that uses FGF receptor isoforms in the epithelium, but not endothelium, and is produced throughout the body by mesenchymal cells, such fibroblasts (128). KGF was initially thought as a keratinocyte mitogen in wound healing, but it has since been shown to have cytoprotective properties including promoting repair and suppressing malignant epithelial phenotypes (128,132). A rupture in Bruch's membrane allows for the formation of aberrant new blood vessels, a key contributor to the pathogenesis of age related macular degeneration and vision loss as vessel enter from the underlying choroid and migrate into the subretinal pigment epithelium and into the photoreceptor layer. In one study, KGF significantly increased arterial tortuosity in an angiogenesis-related developmental model in the avian CAM, along with a minor rise in arterial density. In addition there were increases in tortuosity and vessel density of larger vessels (47,133). KGF, a vessel tortuosity regulator, may have boosted MMP activity in the chorionic epithelium, lowering tissue resistance to sinusoidal vascular patterning by pulsatile blood flow (47,133,134). In chapter 2, our study showed that individuals with PAH have increased Tv compared to controls. There was also a noticeable tortuosity of the larger retinal vessels which has not been previously seen in other retinal diseases. Elevations of KGF in the serum of PAH subjects may correlate with increased arterial Tv in the retina over time.

In terms of VEGF which is a secreted protein that is activated by hypoxia and interacts with its receptors VEGFR1 and VEGF R2 which are tyrosine kinases that promote angiogenesis (129). The most prevalent cardiovascular event associated with VEGF-signaling pathway inhibitors is hypertension. ET-1 is a crucial signaling mechanism that induces pulmonary vascular failure in PAH, and VEGF has been implicated in ET-1 expression. NO and prostanoid prostacyclin are downstream of VEGF signaling and have been shown to suppress ET-1 production. Thus, reducing these vasodilator products may elevate ET-1 levels, producing vasoconstriction, increased blood pressure, and promoting PAH (135–137).

An important endogenous angiogenesis inhibitor is TSP1. TSP1 blocks the development of new blood vessels in a variety of ways, including through interfering with pro-angiogenic proteins (130). Previous studies have shown high plasma levels of TSP-1 in PAH patients compared to controls(138–141). In one study TSP-1 levels in the plasma were shown to be higher and correlated with cutaneous disease severity in people with scleroderma, a vascular disease that is frequently worsened by the development of PAH. TSP-1 concentration was tested in the plasma of seven scleroderma patients before and after the onset of PAH. The two blood drawing were obtained on average 4.9 years apart. TSP-1 concentrations increased considerably following the development of PAH (141). Ideally, TSP-1 marker may be particularly useful in subjects expressing BMPR2, a gene commonly associated with PAH.

Lastly, CAC, which resemble monocytes, promote angiogenesis by secreting growth factors, including VEGF. Baseline blood levels of CACs and EPCs are low, which restricts their ability to reach ischemic regions and subsequently stimulates revascularization (131). One interesting study showed an increase in circulating $CD34^+CD133^+$ proangiogenic precursors of those with IPAH, suggesting evidence of vascular remodeling in the lungs of IPAH. In addition, it was suggested that these cells did not originate from the disease lung but in fact the lung's vascular microenvironment may stimulate their mobilization from the bone marrow and subsequent recruitment into lung vessels (142). Because of this, CAC cells may be used as a marker of worsening of the PAH or progression of lung damage to the lung.

Of interest, PAH is an umbrella disease to pulmonary hypertension. Examining groups two to five of pulmonary hypertensions would be interesting to determine if these vascular and blood/serum findings are unique to PAH and provided further evidence on a possible “eye print” for this disease. Using PH groups 2 to 5 would allow for large population size to due to their higher prevalence.

Second, these studies were limited to only three known imaging techniques. Other imaging, such as OCTA involving laser light instead of white light to illuminate the retina, should also be examined to determine the limitation of VESGEN`s ability to detect changes in the retina. Furthermore, addressing the unanswered questions in chapter 3, in terms of which image method results in better results. The Bland-Alman could only tell if the two methods were similar or if there was a threshold when the images no longer had similar methods. To address this question, ideally there must first be a standard or “ground truth” data to compare results. Since these methods are new, there is no true ground true image. Therefore, the simpler question is which method identifies more vessel numbers, in terms of both large and small vessels. In addition, if the two methods have significantly different Df and vessel length.

One possible way to address this, is by performing a simple standard student t-test. A student t-test is a ratio that measures the significance of the difference between the 'means' of two groups while accounting for variance or dispersion. Student's t-tests are classified into three types: (1) one-sample t-tests, (2) two-sample t-tests, and (3) two-sample paired t-tests. The one-sample t-test assesses a single list of numbers to test the hypothesis that a statistic of that set is equal to a certain value, such as testing the hypothesis that the set's mean is equal to zero. To capture the dependency of measures between the two groups, a paired two-sample t-test might be utilized. The one-sample t-test compares the statistic of a single set of numbers to a certain numeric value, whereas the two-sample t-test compares the values of a statistic between two groups. The dependence of the samples may be captured using a paired two-sample t-test (143). This would provide information on rather the mean of the two methods output results are similar or different which would provide information on which method identity more parameters.

Another option is a Passing and Bablock regression. Passing and Bablock regression is a statistical strategy that enables the useful estimation of the agreement between analytical procedures and any potential systematic bias between them. Passing-Bablok regression is a method comparison of a fitting a straight line to two-dimensional data where both variables, X and Y, are measured with error. It is helpful when comparing two devices that should provide the same measurements. This is done by generating a linear regression line and checking to see if the intercept and slope are both one. Regression using Passing and Bablok is a reliable and suitable model for analyzing the outcomes of method comparisons. Evaluating the proportional and constant bias between two approaches is simple, and obtained parameters enable corrective actions (144).

Additionally, CF's inability to substitute for FA in monitoring microvascular diseases such as diabetic retinopathy is not feasible. Therefore, the need to identify ideal imaging techniques for different systemic diseases could improve retinal disease diagnostics and reduce costs due to unnecessary imaging. In this dissertation, VESGEN was only used in the human eye but has the capability to be utilized in non-human research. Of interest, examining retinal vasculature changes in known animal models of diabetic retinopathy, PAH would provide insight into an ideal animal model for examining vascular changes.

Last, addressing the major drawback of VESGEN which, requires many hours of manual preparation pre-image. This meticulous process results in a time-consuming effort, which precludes VESGEN as a feasible tool for clinical practice. This has resulted in the need for automated software with the ability to perform accurate vessel segmentation. Unfortunately, the deep learning process failed to provide similar output imaging (Chapter 3) but demonstrated great potential. One possibility is to compare current data with newest VESGEN version 1.11 which offers an automated segmentation of binary vascular patterns from grayscale photos using AI/machine learning and other computational breakthroughs. A DR dataset was used for extensive AI research, which included 34 example cases of clinical retinal images in grayscale and binary (black/white) images of the vascular pattern that skilled vascular analysts retrieved. The methods of artificial intelligence and machine learning can generalize and do reasonably well on previously undiscovered images. However there has been no published worked using these prototypes (47). The need to further train the deep learning process and explore other means of automated vessel segmentation is of great need for the future success of this study.

GENERAL REFERENCE

1. Kiel JW. The ocular circulation. Colloquium series on integrated systems physiology …. 2011;

2. Kolb H. Facts and figures concerning the human retina. In: Kolb H, Fernandez E, Nelson R, editors. Webvision: the organization of the retina and visual system. Salt Lake City (UT): University of Utah Health Sciences Center; 1995.

3. Mahabadi N, Al Khalili Y. Neuroanatomy, Retina. StatPearls. Treasure Island (FL): StatPearls Publishing; 2022.

4. Tucker WD, Arora Y, Mahajan K. Anatomy, Blood Vessels. StatPearls. Treasure Island (FL): StatPearls Publishing; 2022.

5. Blood Vessels and Endothelial Cells - Molecular Biology of the Cell - NCBI Bookshelf [Internet]. [cited 2022 Jul 8]. Available from: https://www.ncbi.nlm.nih.gov/books/NBK26848/#:~:text=The%20largest%20blood%20vessels%20are,layers%20by%20a%20basal%20lamina.

6. Sumpio BE, Riley JT, Dardik A. Cells in focus: endothelial cell. Int J Biochem Cell Biol. 2002 Dec;34(12):1508–1512.

7. Rahman M, Siddik AB. Anatomy, Arterioles. StatPearls. Treasure Island (FL): StatPearls Publishing; 2022.

8. White HJ, Borger J. Anatomy, abdomen and pelvis, aorta. StatPearls. Treasure Island (FL): StatPearls Publishing; 2019.

9. Majesky MW, Dong XR, Hoglund V, Mahoney WM, Daum G. The adventitia: a dynamic interface containing resident progenitor cells. Arterioscler Thromb Vasc Biol. 2011 Jul;31(7):1530–1539.

10. Taylor AM, Bordoni B. Histology, blood vascular system. StatPearls. Treasure Island (FL): StatPearls Publishing; 2022.

11. Pournaras CJ, Rungger-Brändle E, Riva CE, Hardarson SH, Stefansson E. Regulation of retinal blood flow in health and disease. Prog Retin Eye Res. 2008 May;27(3):284–330.

12. Kolb H. Simple anatomy of the retina. In: Kolb H, Fernandez E, Nelson R, editors. Webvision: the organization of the retina and visual system. Salt Lake City (UT): University of Utah Health Sciences Center; 1995.

13. Anatomy - The Ocular Circulation - NCBI Bookshelf [Internet]. [cited 2022 May 10]. Available from: https://www.ncbi.nlm.nih.gov/books/NBK53329/

14. Parsons-Wingerter P, Radhakrishnan K, Vickerman MB, Kaiser PK. Oscillation of angiogenesis with vascular dropout in diabetic retinopathy by VESsel GENeration analysis (VESGEN). Invest Ophthalmol Vis Sci. 2010 Jan;51(1):498–507.

15. Oluleye ST, Olusanya BA, Adeoye AM. Retinal vascular changes in hypertensive patients in Ibadan, Sub-Saharan Africa. Int J Gen Med. 2016 Aug 4;9:285–290.

16. Modi P, Arsiwalla T. Hypertensive Retinopathy. StatPearls. Treasure Island (FL): StatPearls Publishing; 2020.

17. Shin ES, Sorenson CM, Sheibani N. Diabetes and retinal vascular dysfunction. J Ophthalmic Vis Res. 2014 Sep;9(3):362–373.

18. Ciurică S, Lopez-Sublet M, Loeys BL, Radhouani I, Natarajan N, Vikkula M, et al. Arterial Tortuosity. Hypertension. 2019 May;73(5):951–960.

19. Keele KD, Roberts J. Leonardo da Vinci: anatomical drawings from the Royal library, Windsor Castle. books.google.com; 1983.

20. Weibel J, Fields WS. Tortuosity, coiling, and kinking of the internal carotid artery. ii. relationship of morphological variation to cerebrovascular insufficiency. Neurology. 1965 May;15:462–468.

21. Eleid MF, Guddeti RR, Tweet MS, Lerman A, Singh M, Best PJ, et al. Coronary artery tortuosity in spontaneous coronary artery dissection: angiographic characteristics and clinical implications. Circ Cardiovasc Interv. 2014 Oct;7(5):656–662.

22. Cheung CY-L, Zheng Y, Hsu W, Lee ML, Lau QP, Mitchell P, et al. Retinal vascular tortuosity, blood pressure, and cardiovascular risk factors. Ophthalmology. 2011 May;118(5):812–818.

23. Del Corso L, Moruzzo D, Conte B, Agelli M, Romanelli AM, Pastine F, et al. Tortuosity, kinking, and coiling of the carotid artery: expression of atherosclerosis or aging? Angiology. 1998 May;49(5):361–371.

24. Sun Z, Jiang D, Liu P, Muccio M, Li C, Cao Y, et al. Age-Related Tortuosity of Carotid and Vertebral Arteries: Quantitative Evaluation With MR Angiography. Front Neurol. 2022 Apr 29;13:858805.

25. Sasongko MB, Wong TY, Nguyen TT, Cheung CY, Shaw JE, Wang JJ. Retinal vascular tortuosity in persons with diabetes and diabetic retinopathy. Diabetologia. 2011 Sep 1;54(9):2409–2416.

26. Lewczuk N, Zdebik A, Bogusławska J, Turno-Kręcicka A, Misiuk-Hojło M. Ocular manifestations of pulmonary hypertension. Surv Ophthalmol. 2019 Mar 6;64(5):694–699.

27. Karamysheva AF. Mechanisms of angiogenesis. Biochemistry (Mosc). 2008 Jul;73(7):751–762.

28. Agabiti-Rosei E, Rizzoni D. Microvascular structure as a prognostically relevant endpoint. J Hypertens. 2017 May;35(5):914–921.

29. Saif PS, Salman AE-RG, Omran NAH, Farweez YAT. Assessment of diabetic retinopathy vascular density maps. Clin Ophthalmol. 2020 Nov 17;14:3941–3953.

30. Chua J, Chin CWL, Hong J, Chee ML, Le T-T, Ting DSW, et al. Impact of hypertension on retinal capillary microvasculature using optical coherence tomographic angiography. J Hypertens. 2019 Mar;37(3):572–580.

31. Greene AS, Rieder MJ. Measurement of vascular density. Methods Mol Med. 2001;51:489–496.

32. Stanley HE, Amaral LAN, Buldyrev SV. Scaling and universality in living systems. … Journal on the …. 1996;

33. Masters BR. Fractal analysis of the vascular tree in the human retina. Annu Rev Biomed Eng. 2004;6:427–452.

34. Wong TY, Klein R, Klein BE, Tielsch JM, Hubbard L, Nieto FJ. Retinal microvascular abnormalities and their relationship with hypertension, cardiovascular disease, and mortality. Surv Ophthalmol. 2001 Aug;46(1):59–80.

35. Smith TG, Marks WB, Lange GD, Sheriff WH, Neale EA. A fractal analysis of cell images. J Neurosci Methods. 1989 Mar 1;27(2):173–180.

36. Keeler CR. 150 years since Babbage's ophthalmoscope. Arch Ophthalmol. 1997 Nov;115(11):1456–1457.

37. Helmholtz H. Beschreibung des Augenspiegels. Beschreibung Eines Augen-Spiegels. Berlin, Heidelberg: Springer Berlin Heidelberg; 1851. p. 28–34.

38. Abràmoff MD, Garvin MK, Sonka M. Retinal imaging and image analysis. IEEE Rev Biomed Eng. 2010;3:169–208.

39. Jackman WT, Webster JD. On photographing the retina of the living human eye. Philadelphia photographer. 1886;

40. Brown AC, Nwanyanwu K. Retinopathy Of Prematurity. StatPearls. Treasure Island (FL): StatPearls Publishing; 2021.

41. Wong TY, Mitchell P. The eye in hypertension. Lancet. 2007 Feb 3;369(9559):425–435.

42. Baumal CR. Imaging in diabetic retinopathy. Current management of diabetic retinopathy. Elsevier; 2018. p. 25–36.

43. Bennett TJ, Quillen DA, Coronica R. Fundamentals of fluorescein angiography. Insight. 2016;41(1):5–11.

44. Tsang SH, Sharma T. Fluorescein Angiography. Adv Exp Med Biol. 2018;1085:7–10.

45. Pothen A-G, Parmar M. Fluorescein. StatPearls. Treasure Island (FL): StatPearls Publishing; 2022.

46. Kornblau IS, El-Annan JF. Adverse reactions to fluorescein angiography: A comprehensive review of the literature. Surv Ophthalmol. 2019 Feb 14;64(5):679–693.

47. Lagatuz M, Vyas RJ, Predovic M, Lim S, Jacobs N, Martinho M, et al. Vascular patterning as integrative readout of complex molecular and physiological signaling by vessel generation analysis. J Vasc Res. 2021 Apr 9;58(4):207–230.

48. Vickerman MB, Keith PA, McKay TL, Gedeon DJ, Watanabe M, Montano M, et al. VESGEN 2D: automated, user-interactive software for quantification and mapping of angiogenic and lymphangiogenic trees and networks. Anat Rec (Hoboken). 2009 Mar;292(3):320–332.

49. Parsons-Wingerter P, Reinecker H-C. For Application to Human Spaceflight and ISS Experiments: VESGEN Mapping of Microvascular Network Remodeling during Intestinal Inflammation. Gravit Space Biol Bull. 2012 Oct 1;26(2):2–12.

50. Parsons-Wingerter PA, Vickerman MB, Keith PA. VESGEN Software for Mapping and Quantification of Vascular Regulators. 2012;

51. LeCun Y, Bengio Y, Hinton G. Deep learning. Nature. 2015 May 28;521(7553):436–444.

52. Hoover A, Kouznetsova V, Goldbaum M. Locating blood vessels in retinal images by piecewise threshold probing of a matched filter response. IEEE Trans Med Imaging. 2000 Mar;19(3):203–210.

53. Kamran SA, Hossain KF, Tavakkoli A, Zuckerbrod SL, Sanders KM, Baker SA. RV-GAN: Segmenting Retinal Vascular Structure in Fundus Photographs Using a Novel Multi-scale Generative Adversarial Network. In: de Bruijne M, Cattin PC, Cotin S, Padoy N, Speidel S, Zheng Y, et al., editors. Medical image computing and computer assisted intervention – MICCAI 2021: 24th international conference, strasbourg, france, september 27 – october 1, 2021, proceedings, part VIII. Cham: Springer International Publishing; 2021. p. 34–44.

54. Witt N, Wong TY, Hughes AD, Chaturvedi N, Klein BE, Evans R, et al. Abnormalities of retinal microvascular structure and risk of mortality from ischemic heart disease and stroke. Hypertension. 2006 May;47(5):975–981.

55. McClintic BR, McClintic JI, Bisognano JD, Block RC. The relationship between retinal microvascular abnormalities and coronary heart disease: a review. Am J Med. 2010 Apr;123(4):374.e1–7.

56. Kim DH, Chaves PHM, Newman AB, Klein R, Sarnak MJ, Newton E, et al. Retinal microvascular signs and disability in the Cardiovascular Health Study. Arch Ophthalmol. 2012 Mar;130(3):350–356.

57. Sapra A, Bhandari P. Diabetes Mellitus. StatPearls. Treasure Island (FL): StatPearls Publishing; 2022.

58. Saeedi P, Petersohn I, Salpea P, Malanda B, Karuranga S, Unwin N, et al. Global and regional diabetes prevalence estimates for 2019 and projections for 2030 and 2045: Results from the International Diabetes Federation Diabetes Atlas, 9th edition. Diabetes Res Clin Pract. 2019 Nov;157:107843.

59. American Diabetes Association. Diagnosis and classification of diabetes mellitus. Diabetes Care. 2004 Jan;27 Suppl 1:S5–S10.

60. GBD 2019 Blindness and Vision Impairment Collaborators, Vision Loss Expert Group of the Global Burden of Disease Study. Causes of blindness and vision impairment in 2020 and trends over 30 years, and prevalence of avoidable blindness in relation to VISION 2020: the Right to Sight: an analysis for the Global Burden of Disease Study. Lancet Glob Health. 2021 Feb;9(2):e144–e160.

61. Shukla UV, Tripathy K. Diabetic Retinopathy. StatPearls. Treasure Island (FL): StatPearls Publishing; 2022.

62. Nguyen TT, Wong TY. Retinal vascular changes and diabetic retinopathy. Curr Diab Rep. 2009 Aug;9(4):277–283.

63. Duh EJ, Sun JK, Stitt AW. Diabetic retinopathy: current understanding, mechanisms, and treatment strategies. JCI Insight. 2017 Jul 20;2(14).

64. Alghadyan AA. Diabetic retinopathy - An update. Saudi J Ophthalmol. 2011 Apr;25(2):99–111.

65. Simonneau G, Montani D, Celermajer DS, Denton CP, Gatzoulis MA, Krowka M, et al. Haemodynamic definitions and updated clinical classification of pulmonary hypertension. Eur Respir J. 2019 Jan 24;53(1).

66. Lai Y-C, Potoka KC, Champion HC, Mora AL, Gladwin MT. Pulmonary arterial hypertension: the clinical syndrome. Circ Res. 2014 Jun 20;115(1):115–130.

67. Hoeper MM, Simon R Gibbs J. The changing landscape of pulmonary arterial hypertension and implications for patient care. Eur Respir Rev. 2014 Dec 1;23(134):450–457.

68. Levine DJ. Pulmonary arterial hypertension: updates in epidemiology and evaluation of patients. Am J Manag Care. 2021 Mar;27(3 Suppl):S35–S41.

69. Rosenkranz S, Preston IR. Right heart catheterisation: best practice and pitfalls in pulmonary hypertension. Eur Respir Rev. 2015 Dec;24(138):642–652.

70. Farina S, Correale M, Bruno N, Paolillo S, Salvioni E, Badagliacca R, et al. The role of cardiopulmonary exercise tests in pulmonary arterial hypertension. Eur Respir Rev. 2018 Jun 30;27(148).

71. Laveneziana P, Weatherald J. Pulmonary vascular disease and cardiopulmonary exercise testing. Front Physiol. 2020 Aug 5;11:964.

72. Southgate L, Machado RD, Gräf S, Morrell NW. Molecular genetic framework underlying pulmonary arterial hypertension. Nat Rev Cardiol. 2020 Feb;17(2):85–95.

73. Koehler R, Grünig E, Pauciulo MW, Hoeper MM, Olschewski H, Wilkens H, et al. Low frequency of BMPR2 mutations in a German cohort of patients with sporadic idiopathic pulmonary arterial hypertension. J Med Genet. 2004 Dec 1;41(12):e127.

74. Evans JDW, Girerd B, Montani D, Wang X-J, Galiè N, Austin ED, et al. BMPR2 mutations and survival in pulmonary arterial hypertension: an individual participant data meta-analysis. Lancet Respir Med. 2016 Feb;4(2):129–137.

75. Koudstaal T, Boomars KA, Kool M. Pulmonary arterial hypertension and chronic thromboembolic pulmonary hypertension: an immunological perspective. J Clin Med. 2020 Feb 19;9(2).

76. Naeije R, Manes A. The right ventricle in pulmonary arterial hypertension. Eur Respir Rev. 2014 Dec 1;23(134):476–487.

77. Sinan ÜY, Demir R, Canbolat İP, Palabıyık M, Kaya A, Küçükoğlu MS. Pulmonary hypertension experience in an expert university hospital. Anatol J Cardiol. 2018 Jul;20(1):35–40.

78. Brown LM, Chen H, Halpern S, Taichman D, McGoon MD, Farber HW, et al. Delay in recognition of pulmonary arterial hypertension: factors identified from the REVEAL Registry. Chest. 2011 Jul 1;140(1):19–26.

79. Nickel NP, Yuan K, Dorfmuller P, Provencher S, Lai Y-C, Bonnet S, et al. Beyond the lungs: systemic manifestations of pulmonary arterial hypertension. Am J Respir Crit Care Med. 2020 Jan 15;201(2):148–157.

80. Tuder RM, Abman SH, Braun T, Capron F, Stevens T, Thistlethwaite PA, et al. Development and pathology of pulmonary hypertension. J Am Coll Cardiol. 2009 Jun 30;54(1 Suppl):S3–9.

81. Fourie PR, Coetzee AR, Bolliger CT. Pulmonary artery compliance: its role in right ventricular-arterial coupling. Cardiovasc Res. 1992 Sep 1;26(9):839–844.

82. Sysol JR, Machado RF. Classification and pathophysiology of pulmonary hypertension. Cont Cardiol Educ. 2018 Jun;4(1):2–12.

83. Jain S, Ventura H, deBoisblanc B. Pathophysiology of pulmonary arterial hypertension. Semin Cardiothorac Vasc Anesth. 2007 Jun;11(2):104–109.

84. Ranchoux B, Harvey LD, Ayon RJ, Babicheva A, Bonnet S, Chan SY, et al. Endothelial dysfunction in pulmonary arterial hypertension: an evolving landscape (2017 Grover Conference Series). Pulm Circ. 2018 Mar;8(1):2045893217752912.

85. Siobal MS. Pulmonary vasodilators. Respir Care. 2007 Jul;52(7):885–899.

86. Lan NSH, Massam BD, Kulkarni SS, Lang CC. Pulmonary arterial hypertension: pathophysiology and treatment. Diseases. 2018 May 16;6(2).

87. Mehta S, Stewart DJ, Langleben D, Levy RD. Short-term pulmonary vasodilation with L-arginine in pulmonary hypertension. Circulation. 1995 Sep 15;92(6):1539–1545.

88. Zuckerbraun BS, Shiva S, Ifedigbo E, Mathier MA, Mollen KP, Rao J, et al. Nitrite potently inhibits hypoxic and inflammatory pulmonary arterial hypertension and smooth muscle proliferation via xanthine oxidoreductase-dependent nitric oxide generation. Circulation. 2010 Jan 5;121(1):98–109.

89. Hunter CJ, Dejam A, Blood AB, Shields H, Kim-Shapiro DB, Machado RF, et al. Inhaled nebulized nitrite is a hypoxia-sensitive NO-dependent selective pulmonary vasodilator. Nat Med. 2004 Oct;10(10):1122–1127.

90. Baliga RS, Milsom AB, Ghosh SM, Trinder SL, Macallister RJ, Ahluwalia A, et al. Dietary nitrate ameliorates pulmonary hypertension: cytoprotective role for endothelial nitric oxide synthase and xanthine oxidoreductase. Circulation. 2012 Jun 12;125(23):2922–2932.

91. Christman BW, McPherson CD, Newman JH, King GA, Bernard GR, Groves BM, et al. An imbalance between the excretion of thromboxane and prostacyclin metabolites in pulmonary hypertension. N Engl J Med. 1992 Jul 9;327(2):70–75.

92. Blaise G, Langleben D, Hubert B. Pulmonary arterial hypertension: pathophysiology and anesthetic approach. The Journal of the American …. 2003;

93. Tabima DM, Frizzell S, Gladwin MT. Reactive oxygen and nitrogen species in pulmonary hypertension. Free Radic Biol Med. 2012 May 1;52(9):1970–1986.

94. Giaid A, Yanagisawa M, Langleben D, Michel RP, Levy R, Shennib H, et al. Expression of endothelin-1 in the lungs of patients with pulmonary hypertension. N Engl J Med. 1993 Jun 17;328(24):1732–1739.

95. Osman MN, Dunlap ME. Management of heart failure with pulmonary hypertension. Curr Cardiol Rep. 2005 May;7(3):196–203.

96. Kenaan M, Eagle K. Heart Failure. The Saint-Chopra Guide to Inpatient Medicine. Oxford University Press; 2018. p. 95–102.

97. Flammer AJ, Anderson T, Celermajer DS, Creager MA, Deanfield J, Ganz P, et al. The assessment of endothelial function: from research into clinical practice. Circulation. 2012 Aug 7;126(6):753–767.

98. Flammer J, Konieczka K, Bruno RM, Virdis A, Flammer AJ, Taddei S. The eye and the heart. Eur Heart J. 2013 May 1;34(17):1270–1278.

99. Kotliar KE, Mücke B, Vilser W, Schilling R, Lanzl IM. Effect of aging on retinal artery blood column diameter measured along the vessel axis. Invest Ophthalmol Vis Sci. 2008 May;49(5):2094–2102.

100. Dorner GT, Garhofer G, Kiss B, Polska E, Polak K, Riva CE, et al. Nitric oxide regulates retinal vascular tone in humans. Am J Physiol Heart Circ Physiol. 2003 Aug 1;285(2):H631–6.

101. Skondra D, Chang GC, Farber HW, Eliott D. Ophthalmologic diagnosis of exacerbation of idiopathic pulmonary arterial hypertension. Arch Ophthalmol. 2012 Dec 1;130(12):1619–1621.

102. Riccieri V, Vasile M, Iannace N, Stefanantoni K, Sciarra I, Vizza CD, et al. Systemic sclerosis patients with and without pulmonary arterial hypertension: a nailfold capillaroscopy study. Rheumatology. 2013 Aug;52(8):1525–1528.

103. Watanabe M, Makino S, Obata H. Bilaterally dilated episcleral vessels in patients with heritable pulmonary arterial hypertension. J Gen Fam Med. 2017 Dec;18(6):464–465.

104. Rudra O, Baisya S, Mallick S, Chatterjee G. Nailfold Capillaroscopic Changes as a Marker of Interstitial Lung Disease in Systemic Sclerosis: A Cross-Sectional Study in a Tertiary Care Hospital in Eastern India. Indian Dermatol Online J. 2022 Apr;13(2):216–220.

105. Hofstee HMA, Vonk Noordegraaf A, Voskuyl AE, Dijkmans BAC, Postmus PE, Smulders YM, et al. Nailfold capillary density is associated with the presence and severity of pulmonary arterial hypertension in systemic sclerosis. Ann Rheum Dis. 2009 Feb;68(2):191–195.

106. Dababneh L, Cikach F, Alkukhun L, Dweik RA, Tonelli AR. Sublingual microcirculation in pulmonary arterial hypertension. Annals of the American Thoracic Society. 2014 May;11(4):504–512.

107. Nickel NP, Shamskhou EA, Razeen MA, Condon DF, Messentier Louro LA, Dubra A, et al. Anatomic, genetic and functional properties of the retinal circulation in pulmonary hypertension. Pulm Circ. 2020 Jun;10(2):2045894020905508.

108. Wagner SK, Fu DJ, Faes L, Liu X, Huemer J, Khalid H, et al. Insights into Systemic Disease through Retinal Imaging-Based Oculomics. Transl Vis Sci Technol. 2020 Feb 12;9(2):6.

109. Selvam S, Kumar T, Fruttiger M. Retinal vasculature development in health and disease. Prog Retin Eye Res. 2018 Mar;63:1–19.

110. DuPont M, Lambert S, Rodriguez-Martin A, Hernandez O, Lagatuz M, Yilmaz T, et al. Retinal vessel changes in pulmonary arterial hypertension. Pulm Circ. 2022 Jan;12(1):e12035.

111. Corrado A, Correale M, Mansueto N, Monaco I, Carriero A, Mele A, et al. Nailfold capillaroscopic changes in patients with idiopathic pulmonary arterial hypertension and systemic sclerosis-related pulmonary arterial hypertension. Microvasc Res. 2017 Nov;114:46–51.

112. Wang X, Zhao Q, Tao R, Lu H, Xiao Z, Zheng L, et al. Decreased retinal vascular density in alzheimer’s disease (AD) and mild cognitive impairment (MCI): an optical coherence tomography angiography (OCTA) study. Front Aging Neurosci. 2020;12:572484.

113. Cennamo G, Montorio D, Santoro C, Cocozza S, Spinelli L, Di Risi T, et al. The retinal vessel density as a new vascular biomarker in multisystem involvement in

fabry disease: an optical coherence tomography angiography study. J Clin Med. 2020 Dec 18;9(12).

114. Vyas RJ, Young M, Murray MC, Predovic M, Lim S, Jacobs NM, et al. Decreased Vascular Patterning in the Retinas of Astronaut Crew Members as New Measure of Ocular Damage in Spaceflight-Associated Neuro-ocular Syndrome. Invest Ophthalmol Vis Sci. 2020 Dec 1;61(14):34.

115. Vickerman MB, Keith PA, McKay TL. VESGEN 2D: Automated, user-interactive software for quantification and mapping of angiogenic and lymphangiogenic trees and networks. … Record: Advances in …. 2009;

116. Lee AG, Mader TH, Gibson CR, Brunstetter TJ, Tarver WJ. Space flight-associated neuro-ocular syndrome (SANS). Eye (Lond). 2018 Mar 12;32(7):1164–1167.

117. Takayama K, Kaneko H, Ito Y, Kataoka K, Iwase T, Yasuma T, et al. Novel Classification of Early-stage Systemic Hypertensive Changes in Human Retina Based on OCTA Measurement of Choriocapillaris. Sci Rep. 2018 Oct 11;8(1):15163.

118. Ruiz-Medrano J, Flores-Moreno I, Peña-García P, Montero JA, Duker JS, Ruiz-Moreno JM. Asymmetry in macular choroidal thickness profile between both eyes in a healthy population measured by swept-source optical coherence tomography. Retina (Philadelphia, Pa). 2015 Oct;35(10):2067–2073.

119. Fu H, Yan S, Wang Y, Gu D, Li X, Yang G, et al. Methods comparison and bias estimation of three distinct biochemistry analytical systems in one clinical laboratory using patient samples. Clin Lab. 2016;62(01+02/2016).

120. Westgard JO. Basic Method Validation and Verfication. 4th ed. Madison, Wisconsin: Westgard Qc; 2020.

121. Beam AL, Manrai AK, Ghassemi M. Challenges to the reproducibility of machine learning models in health care. JAMA. 2020 Jan 28;323(4):305–306.

122. Hartley M, Olsson TSG. dtoolAI: Reproducibility for Deep Learning. Patterns. 2020 Aug;1(5):100073.

123. Badillo S, Banfai B, Birzele F, Davydov II, Hutchinson L, Kam-Thong T, et al. An introduction to machine learning. Clin Pharmacol Ther. 2020 Apr;107(4):871–885.

124. Ranganathan P, Pramesh CS, Aggarwal R. Common pitfalls in statistical analysis: Measures of agreement. Perspect Clin Res. 2017 Dec;8(4):187–191.

125. Giavarina D. Understanding Bland Altman analysis. Biochem Med (Zagreb). 2015 Jun 5;25(2):141–151.

126. Iqbal U. Smartphone fundus photography: a narrative review. Int J Retina Vitreous. 2021 Jun 8;7(1):44.

127. Jansen LG, Schultz T, Holz FG, Finger RP, Wintergerst MWM. [Smartphone-based fundus imaging: applications and adapters]. Ophthalmologe. 2021 Dec 16;

128. Finch PW, Rubin JS. Keratinocyte growth factor/fibroblast growth factor 7, a homeostatic factor with therapeutic potential for epithelial protection and repair. Adv Cancer Res. 2004;91:69–136.

129. Jin K, Zhu Y, Sun Y, Mao XO, Xie L, Greenberg DA. Vascular endothelial growth factor (VEGF) stimulates neurogenesis in vitro and in vivo. Proc Natl Acad Sci USA. 2002 Sep 3;99(18):11946–11950.

130. Rohrs JA, Sulistio CD, Finley SD. Predictive model of thrombospondin-1 and vascular endothelial growth factor in breast tumor tissue. NPJ Syst Biol Appl. 2016 Oct 20;2.

131. Shepherd RM, Capoccia BJ, Devine SM, Dipersio J, Trinkaus KM, Ingram D, et al. Angiogenic cells can be rapidly mobilized and efficiently harvested from the blood following treatment with AMD3100. Blood. 2006 Dec 1;108(12):3662–3667.

132. Toriseva M, Ala-aho R, Peltonen S, Peltonen J, Grénman R, Kähäri V-M. Keratinocyte growth factor induces gene expression signature associated with suppression of malignant phenotype of cutaneous squamous carcinoma cells. PLoS One. 2012 Mar 12;7(3):e33041.

133. Zhang C, Han M, Wu S. Silencing fibroblast growth factor 7 inhibits krypton laser-induced choroidal neovascularization in a rat model. J Cell Biochem. 2019;

134. Chang Z, Niu J, Peng B, Xia Q, Lu W, Huang P. Keratinocyte growth factor/fibroblast growth factor-7-regulated cell migration and invasion through activation of NF-kappaB transcription factors. Cancer Res. 2008;

135. Kelly LK, Wedgwood S, Steinhorn RH, Black SM. Nitric oxide decreases endothelin-1 secretion through the activation of soluble guanylate cyclase. Am J Physiol Lung Cell Mol Physiol. 2004 May;286(5):L984–91.

136. Prins BA, Hu RM, Nazario B, Pedram A, Frank HJ, Weber MA, et al. Prostaglandin E2 and prostacyclin inhibit the production and secretion of endothelin from cultured endothelial cells. J Biol Chem. 1994 Apr 22;269(16):11938–11944.

137. Kappers MHW, Smedts FMM, Horn T, van Esch JHM, Sleijfer S, Leijten F, et al. The vascular endothelial growth factor receptor inhibitor sunitinib causes a preeclampsia-like syndrome with activation of the endothelin system. Hypertension. 2011 Aug 1;58(2):295–302.

138. Kuebler WM. What mediates the effects of thrombospondin-1 in pulmonary hypertension? New evidence for a dual-pronged role of CD47. Cardiovasc Res. 2017 Jan;113(1):3–5.

139. Kumar R, Mickael C, Kassa B, Gebreab L, Robinson JC, Koyanagi DE, et al. TGF-β activation by bone marrow-derived thrombospondin-1 causes Schistosoma- and hypoxia-induced pulmonary hypertension. Nat Commun. 2017 May 30;8:15494.

140. Rice LM, Ziemek J, Stratton EA, McLaughlin SR, Padilla CM, Mathes AL, et al. A longitudinal biomarker for the extent of skin disease in patients with diffuse cutaneous systemic sclerosis. Arthritis Rheumatol. 2015 Nov;67(11):3004–3015.

141. Kaiser R, Frantz C, Bals R, Wilkens H. The role of circulating thrombospondin-1 in patients with precapillary pulmonary hypertension. Respir Res. 2016 Jul 30;17(1):96.

142. Asosingh K, Aldred MA, Vasanji A, Drazba J, Sharp J, Farver C, et al. Circulating angiogenic precursors in idiopathic pulmonary arterial hypertension. Am J Pathol. 2008 Mar;172(3):615–627.

143. Wadhwa RR, Marappa-Ganeshan R. T Test. StatPearls. Treasure Island (FL): StatPearls Publishing; 2021.

144. Bilic-Zulle L. Comparison of methods: Passing and Bablok regression. Biochemia medica. 2011;

APPENDIX A

INSTITUTIONAL REVIEW BOARD FOR HUMAN USE APPROVAL LETTERS

THE UNIVERSITY OF
ALABAMA AT BIRMINGHAM
Office of the Institutional Review Board for Human Use

470 Administration Building
701 20th Street South
Birmingham, AL 35294-0104
205.934.3789 | Fax 205.934.1301 |
irb@uab.edu

APPROVAL LETTER

TO: Grant, Maria Bartolomeo

FROM: University of Alabama at Birmingham Institutional Review Board
Federalwide Assurance # FWA00005960
IORG Registration # IRB00000196 (IRB 01)
IORG Registration # IRB00000726 (IRB 02)
IORG Registration # IRB00012550 (IRB 03)

DATE: 23-Jun-2021

RE: IRB-300000068
IRB-300000068-006
LXR as a Novel Therapeutic Target in Diabetic Retinopathy

The IRB reviewed and approved the Continuing Review submitted on 14-Jun-2021 for the above referenced project. The review was conducted in accordance with UAB's Assurance of Compliance approved by the Department of Health and Human Services.

Type of Review: Expedited
Expedited Categories: 2, 5,
Determination: Approved
Approval Date: 23-Jun-2021
Approval Period: One Year
Expiration Date: 22-Jun-2022

The following apply to this project related to informed consent and/or assent:

- Waiver of 24 Hour Waiting Period
- Waiver (Partial) of HIPAA

Documents Included in Review:

- CONTINUING REVIEW EFORM

To access stamped consent/assent forms (full and expedited protocols only) and/or other approved documents:
1. Open your protocol in IRAP.

2. On the Submissions page, open the submission corresponding to this approval letter. NOTE: The Determination for the submission will be “Approved.”
3. In the list of documents, select and download the desired approved documents. The stamped consent/assent form(s) will be listed with a category of Consent/Assent Document (CF, AF, Info Sheet, Phone Script, etc.)

THE UNIVERSITY OF ALABAMA AT BIRMINGHAM
Office of the Institutional Review Board for Human Use

470 Administration Building
701 20th Street South
Birmingham, AL 35294-0104
205.934.3789 | Fax 205.934.1301 |
irb@uab.edu

APPROVAL LETTER

TO: Grant, Maria Bartolomeo

FROM: University of Alabama at Birmingham Institutional Review Board
Federalwide Assurance # FWA00005960
IORG Registration # IRB00000196 (IRB 01)
IORG Registration # IRB00000726 (IRB 02)
IORG Registration # IRB00012550 (IRB 03)

DATE: 29-Apr-2022

RE: IRB-300000188
IRB-300000188-015
Dyslipidemia and Diabetic Retinopathy

The IRB reviewed and approved the Continuing Review submitted on 12-Apr-2022 for the above referenced project. The review was conducted in accordance with UAB's Assurance of Compliance approved by the Department of Health and Human Services.

Type of Review: Expedited
Expedited Categories: 2, 4, 5,
Determination: Approved
Approval Date: 28-Apr-2022
Approval Period: One Year
Expiration Date: 27-Apr-2023

Linked Records:

- 000517950

The following apply to this project related to informed consent and/or assent:

- Waiver (Partial) of HIPAA

Documents Included in Review:

- CONTINUING REVIEW EFORM

To access stamped consent/assent forms (full and expedited protocols only) and/or other approved documents:
1. Open your protocol in IRAP.
2. On the Submissions page, open the submission corresponding to this approval letter. NOTE: The Determination for the submission will be “Approved.”
3. In the list of documents, select and download the desired approved documents. The stamped consent/assent form(s) will be listed with a category of Consent/Assent Document (CF, AF, Info Sheet, Phone Script, etc.)

THE UNIVERSITY OF ALABAMA AT BIRMINGHAM
Office of the Institutional Review Board for Human Use

470 Administration Building
701 20th Street South
Birmingham, AL 35294-0104
205.934.3789 | Fax 205.934.1301 | irb@uab.edu

APPROVAL LETTER

TO: Grant, Maria Bartolomeo

FROM: University of Alabama at Birmingham Institutional Review Board
Federalwide Assurance # FWA00005960
IORG Registration # IRB00000196 (IRB 01)
IORG Registration # IRB00000726 (IRB 02)
IORG Registration # IRB00012550 (IRB 03)

DATE: 25-Jun-2021

RE: IRB-300000173
IRB-300000173-007
Human iPSC for Repair of Vasodegenerative Vessels in Diabetic Retinopathy

---

The IRB reviewed and approved the Continuing Review submitted on 14-Jun-2021 for the above referenced project. The review was conducted in accordance with UAB's Assurance of Compliance approved by the Department of Health and Human Services.

Type of Review:	Expedited
Expedited Categories:	2, 5,
Determination:	Approved
Approval Date:	25-Jun-2021
Approval Period:	One Year
Expiration Date:	24-Jun-2022

The following apply to this project related to informed consent and/or assent:

- Waiver of 24 Hour Waiting Period
- Waiver (Partial) of HIPAA

Documents Included in Review:

- CONTINUING REVIEW EFORM

To access stamped consent/assent forms (full and expedited protocols only) and/or other approved documents:
1. Open your protocol in IRAP.

INTEGRATED RESEARCH
ADMINISTRATION PORTAL

IRB Personnel eForm

GENERAL INFORMATION

PROJECT OVERVIEW

Project Title Dyslipidemia and Diabetic Retinopathy

IRB Project Number IRB-300000188

Investigator Assurance

- All key personnel listed on the protocol have completed initial IRB training and have or will complete continuing IRB training as required, and
- All personnel are qualified and licensed/credentialed for the procedures they will be performing, if applicable.

PERSONNEL

Click here to add new key personnel. See the Key Personnel Flowchart.

To remove personnel, enter an end date into the personnel record below.

See the Other Personnel section of this form for how to add UAB, Children's of Alabama, Lakeshore, or BVAMC staff members not in the picklist. All other non-affiliated personnel should be added via Project Revision/Amendment Form.

FDA: For studies involving investigational drugs, list all investigators who will be listed on FDA Form 1572 and include a copy of the 1572. Send the IRB a copy of Form 1572 any time you update the form with the FDA.

Name
Aluri, Akshay K

Email	akshay9@uab.edu
Department	Graduate School Dean's Office

Principal Investigator ☐ | Start Date 25-Feb-2020 | End Date | * Role Other Personnel

Certifications

Certification	Begin	End
IRB Initial Training - CITI	10-Nov-2019	10-Nov-2022
Financial Conflict of Interest	09-Mar-2020	09-Mar-2024

Degree medical student

Training certificates

Indicate the following activities in which this individual will be involved. If this individual is not involved in any of these activities, he/she should not be listed as key personnel on the IRB submission:

- ☐ Involved in the design of the human subjects research
- ☑ Obtaining informed consent*
- ☑ Interacting/intervening with participants for research purposes
- ☑ Obtaining private identifiable data or identifiable specimens
- ☐ Administering investigational (non-FDA-approved) product (e.g., drug, device, or biologic)
- ☐ Named on the FDA 1572 or device agreement*
- ☐ Required to complete sponsor's conflict of interest form*

Yes Is the individual named above "responsible" for the design, conduct, or reporting of the research?

Yes Will the individual named above be involved in explaining the study, risk-benefit, and/or alternatives to potential participants?

No Does this individual have a financial interest in this project (see below for definition)?

Please note: Individuals in a role of PI, Co-PI, and/or Faculty Advisor, as well as anyone who is involved in an activity marked with an asterisk, or answers yes to one of the additional questions related to responsible personnel above must file a disclosure of financial interests and complete training requirements of the UAB CIRB .

Name
Boulton, Michael E

Email	mboulton@uab.edu
Department	Ophthalmology

Principal Investigator ☐ | Start Date 21-Jul-2017 | End Date | * Role Subinvestigator

Certifications

Certification	Begin	End
IRB Initial Training - CITI	27-Jun-2017	27-Jun-2020
Financial Conflict of Interest	08-Sep-2017	08-Sep-2021
IRB CITI 2018 Refresher Training	04-Jun-2020	04-Jun-2023
Financial Conflict of Interest in Research - 4th Yr Refresher	03-Aug-2020	03-Aug-2024

Degree PhD

Training certificates

Indicate the following activities in which this individual will be involved. If this individual is not involved in any of these activities, he/she should not be listed as key personnel on the IRB submission:

- ☑ Involved in the design of the human subjects research
- ☐ Obtaining informed consent*
- ☐ Interacting/intervening with participants for research purposes
- ☑ Obtaining private identifiable data or identifiable specimens
- ☐ Administering investigational (non-FDA-approved) product (e.g., drug, device, or biologic)

☐ Named on the FDA 1572 or device agreement*

☐ Required to complete sponsor's conflict of interest form*

Yes Is the individual named above "responsible" for the design, conduct, or reporting of the research?

No Will the individual named above be involved in explaining the study, risk-benefit, and/or alternatives to potential participants?

No Does this individual have a financial interest in this project (see below for definition)?

Please note: Individuals in a role of PI, Co-PI, and/or Faculty Advisor, as well as anyone who is involved in an activity marked with an asterisk, or answers yes to one of the additional questions related to responsible personnel above must file a disclosure of financial interests and complete training requirements of the UAB CIRB .

Name
Dorin, Natalie A

Email	nadorin@uab.edu
Department	Graduate School Dean's Office

Principal Investigator ☐

Start Date 30-Aug-2021

End Date

* Role Other Personnel

Certifications

Certification	Begin	End
IRB Initial Training - CITI	25-Aug-2021	25-Aug-2024
Financial Conflict of Interest	27-Aug-2021	27-Aug-2025

Degree student

Training certificates

Indicate the following activities in which this individual will be involved. If this individual is not involved in any of these activities, he/she should not be listed as key personnel on the IRB submission:

☐ Involved in the design of the human subjects research

☑ Obtaining informed consent*

☑ Interacting/intervening with participants for research purposes

☑ Obtaining private identifiable data or identifiable specimens

☐ Administering investigational (non-FDA-approved) product (e.g., drug, device, or biologic)

☐ Named on the FDA 1572 or device agreement*

☐ Required to complete sponsor's conflict of interest form*

No Is the individual named above "responsible" for the design, conduct, or reporting of the research?

Yes Will the individual named above be involved in explaining the study, risk-benefit, and/or alternatives to potential participants?

No Does this individual have a financial interest in this project (see below for definition)?

Please note: Individuals in a role of PI, Co-PI, and/or Faculty Advisor, as well as anyone who is involved in an activity marked with an asterisk, or answers yes to one of the additional questions related to responsible personnel above must file a disclosure of financial interests and complete training requirements of the UAB CIRB .

Name
DuPont, Mariana

Email	mdupont@uab.edu
Department	Vision Science Graduate PGM

Principal Investigator ☐

Start Date 16-May-2018

End Date

* Role Other Personnel

Certifications

Certification	Begin	End
IRB Initial Training - NIH	06-Feb-2015	06-Feb-2018
IRB Continuing Training (CITI Refresher Course)	07-Mar-2018	07-Mar-2021
Financial Conflict of Interest	18-May-2018	18-May-2022
Financial Conflict of Interest in Research - 4th Yr Refresher	27-Aug-2020	27-Aug-2024
IRB CITI 2018 Refresher Training	17-May-2021	17-May-2024
IRB ICH-GCP	18-May-2021	18-May-2024

Degree grad student

Training certificates

Indicate the following activities in which this individual will be involved. If this individual is not involved in any of these activities, he/she should not be listed as key personnel on the IRB submission:

☐ Involved in the design of the human subjects research

☑ Obtaining informed consent*

☑ Interacting/intervening with participants for research purposes

☑ Obtaining private identifiable data or identifiable specimens

☐ Administering investigational (non-FDA-approved) product (e.g., drug, device, or biologic)

☐ Named on the FDA 1572 or device agreement*

☐ Required to complete sponsor's conflict of interest form*

Yes Is the individual named above "responsible" for the design, conduct, or reporting of the research?

Yes Will the individual named above be involved in explaining the study, risk-benefit, and/or alternatives to potential participants?

No Does this individual have a financial interest in this project (see below for definition)?

Please note: Individuals in a role of PI, Co-PI, and/or Faculty Advisor, as well as anyone who is involved in an activity marked with an asterisk, or answers yes to one of the additional questions related to responsible personnel above must file a disclosure of financial interests and complete training requirements of the UAB CIRB .

Name

Grant, Maria Bartolomeo

Email	mabgrant@uab.edu
Department	Ophthalmology

Principal Investigator ☑ | Start Date 19-Jul-2017 | End Date | * Role PI

Certifications

Certification	Begin	End
IRB Initial Training - CITI	27-Jun-2017	27-Jun-2020
Financial Conflict of Interest	08-Sep-2017	08-Sep-2021
IRB CITI 2018 Refresher Training	08-Jun-2020	08-Jun-2023
Financial Conflict of Interest in Research - 4th Yr Refresher	11-Aug-2021	11-Aug-2025

Degree MD

Training certificates

Indicate the following activities in which this individual will be involved. If this individual is not involved in any of these activities, he/she should not be listed as key personnel on the IRB submission:

- ☑ Involved in the design of the human subjects research
- ☑ Obtaining informed consent*
- ☑ Interacting/intervening with participants for research purposes
- ☑ Obtaining private identifiable data or identifiable specimens
- ☐ Administering investigational (non-FDA-approved) product (e.g., drug, device, or biologic)
- ☐ Named on the FDA 1572 or device agreement*
- ☐ Required to complete sponsor's conflict of interest form*

Yes Is the individual named above "responsible" for the design, conduct, or reporting of the research?

Yes Will the individual named above be involved in explaining the study, risk-benefit, and/or alternatives to potential participants?

No Does this individual have a financial interest in this project (see below for definition)?

Please note: Individuals in a role of PI, Co-PI, and/or Faculty Advisor, as well as anyone who is involved in an activity marked with an asterisk, or answers yes to one of the additional questions related to responsible personnel above must file a disclosure of financial interests and complete training requirements of the UAB CIRB .

Name
Harbour, Angela

Email	harboura@uab.edu
Department	Ophthalmology

Principal Investigator ☐ | Start Date 30-Aug-2021 | End Date | * Role Other Personnel

Certifications

Certification	Begin	End
IRB Initial Training - CITI	20-Aug-2021	20-Aug-2024
Financial Conflict of Interest	20-Aug-2021	20-Aug-2025
IRB ICH-GCP	24-Aug-2021	24-Aug-2024

Degree student

Training certificates

Indicate the following activities in which this individual will be involved. If this individual is not involved in any of these activities, he/she should not be listed as key personnel on the IRB submission:

- ☐ Involved in the design of the human subjects research
- ☑ Obtaining informed consent*
- ☑ Interacting/intervening with participants for research purposes
- ☑ Obtaining private identifiable data or identifiable specimens
- ☐ Administering investigational (non-FDA-approved) product (e.g., drug, device, or biologic)
- ☐ Named on the FDA 1572 or device agreement*
- ☐ Required to complete sponsor's conflict of interest form*

No Is the individual named above "responsible" for the design, conduct, or reporting of the research?

Yes Will the individual named above be involved in explaining the study, risk-benefit, and/or alternatives to potential participants?

No Does this individual have a financial interest in this project (see below for definition)?

Please note: Individuals in a role of PI, Co-PI, and/or Faculty Advisor, as well as anyone who is involved in an activity marked with an asterisk, or answers yes to one of the additional questions related to responsible personnel above must file a disclosure of financial interests and complete training requirements of the UAB CIRB .

Name
Kichler, Kara

Email	kkichler@uab.edu
Department	Physician Scientist Development OFC

Principal Investigator ☐ | Start Date 11-Jun-2021 | End Date | * Role Other Personnel

Certifications

Certification	Begin	End
IRB Initial Training - CITI	07-Mar-2019	07-Mar-2022
IRB ICH-GCP	08-Apr-2019	08-Apr-2022
Financial Conflict of Interest	05-Jun-2021	05-Jun-2025

Degree medical student

Training certificates

Indicate the following activities in which this individual will be involved. If this individual is not involved in any of these activities, he/she should not be listed as key personnel on the IRB submission:

- [ ] Involved in the design of the human subjects research
- [x] Obtaining informed consent*
- [x] Interacting/intervening with participants for research purposes
- [x] Obtaining private identifiable data or identifiable specimens
- [ ] Administering investigational (non-FDA-approved) product (e.g., drug, device, or biologic)
- [ ] Named on the FDA 1572 or device agreement*
- [ ] Required to complete sponsor's conflict of interest form*

No Is the individual named above "responsible" for the design, conduct, or reporting of the research?

Yes Will the individual named above be involved in explaining the study, risk-benefit, and/or alternatives to potential participants?

No Does this individual have a financial interest in this project (see below for definition)?

Please note: Individuals in a role of PI, Co-PI, and/or Faculty Advisor, as well as anyone who is involved in an activity marked with an asterisk, or answers yes to one of the additional questions related to responsible personnel above must file a disclosure of financial interests and complete training requirements of the UAB CIRB .

Name
Moorer, Jennifer M

Email	jmoorer@uab.edu
Department	Ophthalmology

Principal Investigator
- [ ]

Start Date
18-Oct-2017

End Date

* Role
Other Personnel

Certifications

Certification	Begin	End
IRB Initial Training - CITI	26-Apr-2007	26-Apr-2010
Financial Conflict of Interest	13-Sep-2013	13-Sep-2017
IRB Investigator 101 Initial Training	15-Sep-2013	15-Sep-2016
IRB Continuing Training (CITI Refresher Course)	15-Oct-2015	15-Oct-2018
IRB CITI Good Clinical Practice Refresher	13-Jan-2017	13-Jan-2020
IRB ICH-GCP	17-Oct-2017	17-Oct-2020
IRB CITI 2018 Refresher Training	19-Sep-2018	19-Sep-2021
Good Clinical Practices (GCP) Refresher Course	03-May-2020	03-May-2023
Financial Conflict of Interest in Research - 4th Yr Refresher	10-Jul-2020	10-Jul-2024

Degree HS

Training certificates

Indicate the following activities in which this individual will be involved. If this individual is not involved in any of these activities, he/she should not be listed as key personnel on the IRB submission:

- [ ] Involved in the design of the human subjects research
- [x] Obtaining informed consent*
- [x] Interacting/intervening with participants for research purposes
- [x] Obtaining private identifiable data or identifiable specimens
- [ ] Administering investigational (non-FDA-approved) product (e.g., drug, device, or biologic)
- [ ] Named on the FDA 1572 or device agreement*
- [ ] Required to complete sponsor's conflict of interest form*

Yes Is the individual named above "responsible" for the design, conduct, or reporting of the research?

Yes Will the individual named above be involved in explaining the study, risk-benefit, and/or alternatives to potential participants?

No Does this individual have a financial interest in this project (see below for definition)?

Please note: Individuals in a role of PI, Co-PI, and/or Faculty Advisor, as well as anyone who is involved in an activity marked with an asterisk, or answers yes to one of the additional questions related to responsible personnel above must file a disclosure of financial interests and complete training requirements of the UAB CIRB .

Name
Shirley, Simona

Email	sns2022@uab.edu
Department	Undergraduate Admissions

Principal Investigator
- [ ]

Start Date
04-Mar-2020

End Date

* Role
Other Personnel

Certifications

Certification	Begin	End
IRB ICH-GCP	02-Jun-2019	02-Jun-2022
IRB Initial Training - CITI	03-Jun-2019	03-Jun-2022
Financial Conflict of Interest	08-Mar-2020	08-Mar-2024

Degree student

Training certificates

Indicate the following activities in which this individual will be involved. If this individual is not involved in any of these activities, he/she should not be listed as key personnel on the IRB submission:

- [ ] Involved in the design of the human subjects research
- [x] Obtaining informed consent*
- [x] Interacting/intervening with participants for research purposes
- [x] Obtaining private identifiable data or identifiable specimens
- [ ] Administering investigational (non-FDA-approved) product (e.g., drug, device, or biologic)
- [ ] Named on the FDA 1572 or device agreement*

☐ Required to complete sponsor's conflict of interest form*

No Is the individual named above "responsible" for the design, conduct, or reporting of the research?

Yes Will the individual named above be involved in explaining the study, risk-benefit, and/or alternatives to potential participants?

No Does this individual have a financial interest in this project (see below for definition)?

Please note: Individuals in a role of PI, Co-PI, and/or Faculty Advisor, as well as anyone who is involved in an activity marked with an asterisk, or answers yes to one of the additional questions related to responsible personnel above must file a disclosure of financial interests and complete training requirements of the UAB CIRB .

Financial Interest – for each individual listed above, answer Yes or No as to whether the individual or an immediate family member has any of the following:

- An ownership interest, stock options, or other equity interest related to the investigator's institutional responsibilities of any value.
- Compensation greater than $5,000 in the previous two years when aggregated for the immediate family
- Proprietary interest including, but not limited to, a patent, trademark, copyright, or licensing agreement.
- Board of executive relationship, regardless of compensation.
- Any other Financial Interest as defined by the UAB CIRB.

UAB Personnel : If the individual or his/her spouse or dependent child has a Financial Interest, a disclosure has to be made to the UAB CIRB. A completed CIRB evaluation has to be available before the IRB can complete its review.

OTHER PERSONNEL

Affiliated Personnel

☐ Yes ☑ No Do you have any UAB, Children's of Alabama, Lakeshore, or BVAMC personnel that need to be added who are not listed in the picklist?

Updated By: Karen Baldus Searcey @ 30-Aug-2021 02:01:42 PM

University of Alabama at Birmingham

Office of the IRB

Phone: 205-934-3789 | Fax: 205-934-1301

www.uab.edu/irb

Questions?

Form Version: 1.0 | Date: 07/30/2019

Appendix 1

EForm Name: IRB PERSONNEL EFORM
Page: PERSONNEL
Section: Personnel - Review
Question: Training certificates
File Name: FCOI_training_General Certificate_AluriAkshay.pdf

Project Revision/Amendment Form

Form version: June 26, 2012

In MS Word, click in the white boxes and type your text; double-click checkboxes to check/uncheck.

- **Federal regulations require IRB approval before implementing proposed changes. See Section 14 of the IRB Guidebook for Investigators for additional information.**
- **Change means any change, in content or form, to the protocol, consent form, or any supportive materials (such as the Investigator's Brochure, questionnaires, surveys, advertisements, etc.). See Item 4 for more examples.**

1. Today's Date	3/8/2018

2. Principal Investigator (PI)			
Name (with degree)	Maria Grant, MD	**Blazer ID**	mabgrant
Department	Ophthalmology	**Division (if applicable)**	
Office Address	VH390D	**Office Phone**	205-996-8660
E-mail	mabgrant@uab.edu	**Fax Number**	205-934-3425
Contact person who should receive copies of IRB correspondence (Optional)			
Name	Karen Searcey	**E-Mail**	karensearcey@uabmc.edu
Phone	325-8310	**Fax Number**	205-325-8692

Office Address (if different from PI)	EFH609

3. UAB IRB Protocol Identification					
3.a. Protocol Number	IRB-300000068				
3.b. Protocol Title	LXR as a novel therapeutic target in diabetic retinopathy				
3.c. Current Status of Protocol—Check ONE box at left; provide numbers and dates where applicable					
☐	**Study has not yet begun**		**No participants, data, or specimens have been entered.**		
☒	**In progress, open to accrual**		**Number of participants, data, or specimens entered:**	13	
☐	**Enrollment temporarily suspended by sponsor**				
☐	**Closed to accrual, but procedures continue as defined in the protocol (therapy, intervention, follow-up visits, etc.)**				
	Date closed:		**Number of participants receiving interventions:**		
			Number of participants in long-term follow-up only:		
☐	**Closed to accrual, and only data analysis continues**				
	Date closed:		**Total number of participants entered:**		

4. Types of Change

Check all types of change that apply, and describe the changes in Item 5.c. or 5.d. as applicable. To help avoid delay in IRB review, please ensure that you provide the required materials and/or information for each type of change checked.

☒ **Protocol revision (change in the IRB-approved protocol)**

In Item 5.c., if applicable, provide sponsor's protocol version number, amendment number, update number, etc.

☐ **Protocol amendment (addition to the IRB-approved protocol)**

In Item 5.c., if applicable, provide funding application document from sponsor, as well as sponsor's protocol version number, amendment number, update number, etc.

☒ **Add or remove personnel**

In Item 5.c., include name, title/degree, department/division, institutional affiliation, and role(s) in research, and address whether new personnel have any conflict of interest. See "Change in Principal Investigator" in the IRB Guidebook if the principal investigator is being changed.

☐ **Add graduate student(s) or postdoctoral fellow(s) working toward thesis, dissertation, or publication**

In Item 5.c., (a) identify these individuals by name; (b) provide the working title of the thesis, dissertation, or publication; and (c) indicate whether or not the student's analysis differs in any way from the purpose of the research described in the IRB-approved HSP (e.g., a secondary analysis of data obtained under this HSP).

☐	**Change in source of funding; change or add funding** In Item 5.c., describe the change or addition in detail, include the applicable OSP proposal number(s), and provide a copy of the application as funded (or as submitted to the sponsor if pending). Note that some changes in funding may require a new IRB application.
☐	**Add or remove performance sites** In Item 5.c., identify the site and location, and describe the research-related procedures performed there. If adding site(s), attach notification of permission or IRB approval to perform research there. Also include copy of subcontract, if applicable. If this protocol includes acting as the Coordinating Center for a study, attach IRB approval from any non-UAB site added.
☐	**Add or change a genetic component or storage of samples and/or data component—this could include data submissions for Genome-Wide Association Studies (GWAS)** To assist you in revising or preparing your submission, please see the IRB Guidebook for Investigators or call the IRB office at 934-3789.
☐	**Suspend, re-open, or permanently close protocol to accrual of individuals, data, or samples (IRB approval to remain active)** In Item 5.c., indicate the action, provide applicable dates and reasons for action; attach supporting documentation.
☐	**Report being forwarded to IRB (e.g., DSMB, sponsor or other monitor)** In Item 5.c., include date and source of report, summarize findings, and indicate any recommendations.

☒	**Revise or amend consent, assent form(s)** Complete Item 5.d.
☐	**Addendum (new) consent form** Complete Item 5.d.
☐	**Add or revise recruitment materials** Complete Item 5.d.
☒	**Other (e.g., investigator brochure)** Indicate the type of change in the space below, and provide details in Item 5.c. or 5.d. as applicable. Include a copy of all affected documents, with revisions highlighted as applicable. ▶ report consent form issue

5. Description and Rationale **In Item 5.a. and 5.b, check** Yes **or** No **and see instructions for** Yes **responses.** **In Item 5.c. and 5.d, describe—and explain the reason for—the change(s) noted in Item 4.**	
☒ Yes ☐No	**5.a. Are any of the participants enrolled as normal, healthy controls?** If yes, describe in detail in Item 5.c. how this change will affect those participants.

☒ Yes ☐No	**5.b. Does the change affect subject participation, such as procedures, risks, costs, location of services, etc.?** If yes, FAP-designated units complete a FAP submission and send to fap@uab.edu. Identify the FAP-designated unit in Item 5.c. For more details on the UAB FAP, see www.uab.edu/cto.

5.c. Protocol Changes: In the space below, briefly describe—and explain the reason for—all change(s) to the protocol.

- ► We would like to increase the participant payments from $20 to $50. We have discovered that this payment is lower than most other protocols in the department and we would like to increase so that is in line with other study payments.
- ► It was discovered today that the ***Controls Non-Diabetic Participants Consent form*** contained a typo in the consent form version date. A PRAF was submitted on 10/13/2017 that revised the type of payment from a gift card to a check. The language in the payment section of the ICF was changed from a ***gift card*** to the standard language of ***Ask your study staff about the method of payment***. The version date that was submitted on the revised consent form indicated the version date was 10/13/2013. This was a typo. It should have been 10/13/2017. The version date on the Diabetic consent form had the correct date of 10/13/2017. Due to the fact we are increasing the participant payment, the version date will be revised.
- ► In going through the consent forms today, we found that the coordinator had failed to use the new consent forms that were approved on 11/02/2017 (version date 10/13/2017) with 12 of the 13 participants enrolled in the study. The only change in this version of the consent form was the method of payment. The originally approved consent form indicated participants would receive a gift card whereas the payment section on the 10/13/2017 version of the consent form indicated the new language was changed from a gift card to the standard language of *Ask your*

study staff about the method of payment. All participants received a check as indicated in the PRAF that was approved 11/02/2017.

►Of note is that the UAB Clinical Trials Admin Office has identified our department as one of the first departments to use the Greenphire/Clincard for participant payments. This week we began using the Greenphire system and participants will be receiving clincards and not checks.

CORRECTIVE ACTION PLAN: I met with the coordinator of this study and discussed how this happened. It appears that the coordinator was using her hard copy consent to make copies of the consent form which was the original approved consent. Although she was emailed the revised consent on 11/2/2017 and was informed that the new consent was in a shared drive on the computer in a folder labelled "Current Consent Forms", she inadvertently used the old consent forms that she had made copies of. Going forward, once she receives an email of a revised consent, she will print it immediately as a reference as to the Current Consent version date. Additionally, she will no longer make copies of the consent form in advance, rather she will go to the Current Consent folder on the computer and print the consent form from that folder.

►We would like to add Mariana Dupont to the protocol. Mariana is a 1st year Vision Science graduate student and will assist with data collection, analysis and presentation. She has no conflict of interest and has current IRB training.

5.d. Consent and Recruitment Changes: In the space below, **(a) describe all changes to IRB-approved forms or recruitment materials and the reasons for them;** **(b) describe the reasons for the addition of any materials (e.g., addendum consent, recruitment); and** **(c) indicate either how and when you will reconsent enrolled participants or why reconsenting is not necessary (not applicable for recruitment materials).** **Also, indicate the number of forms changed or added. For new forms, provide 1 copy. For revised documents, provide 3 copies:** **• a copy of the currently approved document (showing the IRB approval stamp, if applicable)** **• a revised copy highlighting all proposed changes with "tracked" changes** **• a revised copy for the IRB approval stamp.**
► The version date that was submitted on the revised Control consent form indicated the version date was 10/13/2013 (they Diabetic consent form had the correct date of 10/13/2017). This was a typo. It should have been 10/13/2017 but because we are increasing the participant payment from \$20 to \$50, we will be revising the version date to today's date.

Signature of Principal Investigator____

______________ Date___03/08/2018___________

FOR IRB USE ONLY

☐ Received & Noted ☐ Approved Expedited* ☐ To Convened IRB

____ _________________

Signature (Chair, Vice-Chair, Designee) Date

DOLA ___________________

Change to Expedited Category **Y / N / NA**

*No change to IRB's previous determination of approval criteria at 45 CFR 46.111 or 21 CFR 56.111

Project Revision/Amendment Form

Form version: June 26, 2012

In MS Word, click in the white boxes and type your text; double-click checkboxes to check/uncheck.

- **Federal regulations require IRB approval before implementing proposed changes. See Section 14 of the IRB Guidebook for Investigators for additional information.**
- **Change means any change, in content or form, to the protocol, consent form, or any supportive materials (such as the Investigator's Brochure, questionnaires, surveys, advertisements, etc.). See Item 4 for more examples.**

1. Today's Date	3/6/2018

2. Principal Investigator (PI)			
Name (with degree)	Maria Grant, MD	**Blazer ID**	mabgrant
Department	Ophthalmology	**Division (if applicable)**	
Office Address	VH390D	**Office Phone**	205-996-8660
E-mail	mabgrant@uab.edu	**Fax Number**	205-934-3425
Contact person who should receive copies of IRB correspondence (Optional)			
Name	Karen Searcey	**E-Mail**	karensearcey@uabmc.edu
Phone	325-8310	**Fax Number**	205-325-8692

Office Address (if different from PI)	EFH609

3. UAB IRB Protocol Identification					
3.a. Protocol Number	IRB-300000173				
3.b. Protocol Title	Human iPSC for Repair of Vasodegenerative Vessels in Diabetic Retinopathy				
3.c. Current Status of Protocol—Check ONE box at left; provide numbers and dates where applicable					
☐	Study has not yet begun		No participants, data, or specimens have been entered.		
☒	In progress, open to accrual			Number of participants, data, or specimens entered:	8
☐	Enrollment temporarily suspended by sponsor				
☐	Closed to accrual, but procedures continue as defined in the protocol (therapy, intervention, follow-up visits, etc.)				
	Date closed:			Number of participants receiving interventions:	
				Number of participants in long-term follow-up only:	
☐	Closed to accrual, and only data analysis continues				
	Date closed:			Total number of participants entered:	

4. Types of Change

Check all types of change that apply, and describe the changes in Item 5.c. or 5.d. as applicable. To help avoid delay in IRB review, please ensure that you provide the required materials and/or information for each type of change checked.

☒ **Protocol revision (change in the IRB-approved protocol)**

In Item 5.c., if applicable, provide sponsor's protocol version number, amendment number, update number, etc.

☐ **Protocol amendment (addition to the IRB-approved protocol)**

In Item 5.c., if applicable, provide funding application document from sponsor, as well as sponsor's protocol version number, amendment number, update number, etc.

☒ **Add or remove personnel**

In Item 5.c., include name, title/degree, department/division, institutional affiliation, and role(s) in research, and address whether new personnel have any conflict of interest. See "Change in Principal Investigator" in the IRB Guidebook if the principal investigator is being changed.

☐ **Add graduate student(s) or postdoctoral fellow(s) working toward thesis, dissertation, or publication**

In Item 5.c., (a) identify these individuals by name; (b) provide the working title of the thesis, dissertation, or publication; and (c) indicate whether or not the student's analysis differs in any way from the purpose of the research described in the IRB-approved HSP (e.g., a secondary analysis of data obtained under this HSP).

☐	**Change in source of funding; change or add funding** In Item 5.c., describe the change or addition in detail, include the applicable OSP proposal number(s), and provide a copy of the application as funded (or as submitted to the sponsor if pending). Note that some changes in funding may require a new IRB application.
☐	**Add or remove performance sites** In Item 5.c., identify the site and location, and describe the research-related procedures performed there. If adding site(s), attach notification of permission or IRB approval to perform research there. Also include copy of subcontract, if applicable. If this protocol includes acting as the Coordinating Center for a study, attach IRB approval from any non-UAB site added.
☐	**Add or change a genetic component or storage of samples and/or data component—this could include data submissions for Genome-Wide Association Studies (GWAS)** To assist you in revising or preparing your submission, please see the IRB Guidebook for Investigators or call the IRB office at 934-3789.
☐	**Suspend, re-open, or permanently close protocol to accrual of individuals, data, or samples (IRB approval to remain active)** In Item 5.c., indicate the action, provide applicable dates and reasons for action; attach supporting documentation.
☐	**Report being forwarded to IRB (e.g., DSMB, sponsor or other monitor)** In Item 5.c., include date and source of report, summarize findings, and indicate any recommendations.

☐	**Revise or amend consent, assent form(s)** Complete Item 5.d.
☐	**Addendum (new) consent form** Complete Item 5.d.
☐	**Add or revise recruitment materials** Complete Item 5.d.
☒	**Other (e.g., investigator brochure)** Indicate the type of change in the space below, and provide details in Item 5.c. or 5.d. as applicable. Include a copy of all affected documents, with revisions highlighted as applicable. ▶ Report consent form issue

5. Description and Rationale **In Item 5.a. and 5.b, check** Yes **or** No **and see instructions for** Yes **responses.** **In Item 5.c. and 5.d, describe—and explain the reason for—the change(s) noted in Item 4.**	
☒ Yes ☐No	**5.a. Are any of the participants enrolled as normal, healthy controls?** If yes, describe in detail in Item 5.c. how this change will affect those participants.

☐ Yes ☒No	**5.b. Does the change affect subject participation, such as procedures, risks, costs, location of services, etc.?** If yes, FAP-designated units complete a FAP submission and send to fap@uab.edu. Identify the FAP-designated unit in Item 5.c. For more details on the UAB FAP, see www.uab.edu/cto.

5.c. Protocol Changes: In the space below, briefly describe—and explain the reason for—all change(s) to the protocol.

- ▶In going through the consent forms today, we found that the coordinator had failed to use the new consent forms that were approved on 12/12/2017 (version date 11/20/2017) with 6 of the 8 participants enrolled in the study. The only change in this version of the consent form was the method of payment. The original approved consent form indicated participants would receive a gift card whereas the payment section on the 11/20/2017 version of the consent form indicated the new language was changed from a gift card to the standard language of *Ask your study staff about the method of payment*. All participants received a check as indicated in the PRAF that was approved 12/12/2017.
- ▶Of note is that the UAB Clinical Trials Admin Office has identified our department as one of the first departments to use the Greenphire/Clincard for participant payments. This week we began using the Greenphire system and participants will be receiving clincards.

- ▶**CORRECTIVE ACTION PLAN:** I met with the coordinator of this study and discussed how this happened. It appears that the coordinator was using her hard copy consent to make copies of the consent form which was the original approved consent. Although she was emailed the revised consent on 12/12/2017 and was informed that the new consent was in a shared drive on the computer in a folder labelled "Current Consent Forms", she inadvertently used the old consent forms that she had made copies of. Going forward, once she receives an email of a revised consent, she will print it immediately as a reference as to the Current Consent version date. Additionally, she will no longer make copies of the consent form in advance, rather she will go to the Current Consent folder on the computer and print the consent form from that folder.

► We would like to add Mariana Dupont to the protocol. Mariana is a 1st year Vision Science graduate student and will assist with data collection, analysis and presentation. She has no conflict of interest and has current IRB training.

5.d. Consent and Recruitment Changes: In the space below,

(a) describe all changes to IRB-approved forms or recruitment materials and the reasons for them;

(b) describe the reasons for the addition of any materials (e.g., addendum consent, recruitment); and

(c) indicate either how and when you will reconsent enrolled participants or why reconsenting is not necessary (not applicable for recruitment materials).

Also, indicate the number of forms changed or added. For new forms, provide 1 copy. For revised documents, provide 3 copies:

- **a copy of the currently approved document (showing the IRB approval stamp, if applicable)**
- **a revised copy highlighting all proposed changes with "tracked" changes**
- **a revised copy for the IRB approval stamp.**

►**n/a**

Signature of Principal Investigator____

____________________ Date___3/6/2018____________

FOR IRB USE ONLY

☐ Received & Noted ☐ Approved Expedited* ☐ To Convened IRB

____ ________________

Signature (Chair, Vice-Chair, Designee) Date

DOLA ___________________

Change to Expedited Category **Y / N / NA**

*No change to IRB's previous determination of approval criteria at 45 CFR 46.111 or 21 CFR 56.111